1-1-2000

# Model polypeptides and molecular recognition at a monolayer interface.

Susan L. Dawson
*University of Massachusetts Amherst*

# MODEL POLYPEPTIDES AND MOLECULAR RECOGNITION AT A MONOLAYER INTERFACE

A Dissertation Presented

by

SUSAN L. DAWSON

Submitted to the Graduate School of the
University of Massachusetts Amherst in partial fulfillment
of the requirements for the degree of

DOCTOR OF PHILOSOPHY

September 2000

Department of Polymer Science and Engineering

# MODEL POLYPEPTIDES AND MOLECULAR RECOGNITION AT A MONOLAYER INTERFACE

A Dissertation Presented

by

SUSAN L. DAWSON

Approved as to style and content by:

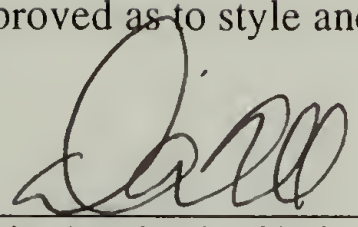

David A. Tirrell, Chair

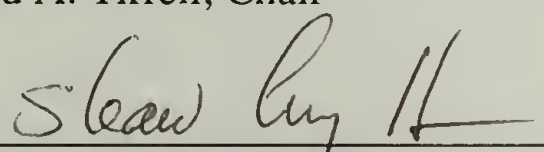

Shaw-Ling Hsu, Member

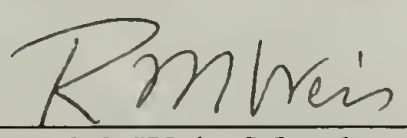

Robert M. Weis, Member

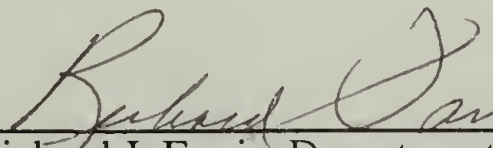

Richard J. Farris, Department Head
Polymer Science and Engineering

# ACKNOWLEDGMENTS

There are many people that contribute both directly and indirectly to ones development as a scientist. I extend my gratitude to them all and especially to Professor David Tirrell. As mentor and scientist he has taught me much. He has offered good council, sound leadership, encouragement and friendship. I thank him not only for his coaching, but also for providing a rich environment of curious scientists and engineers who challenged me and made science fun.

I wish to express my sincere gratitude to my committee members Professors Shaw-Ling Hsu, Robert Weis and Scott Barton for their interest in my work and their insight and suggestions as well as their friendship. I will always appreciate the support of Professors Muthukumar and Farris, their encouragement and their ability to teach an old dog some new tricks during her first year in Amherst. I am also grateful to Dr. Dean Sadat-Aalaee who introduced me to peptide synthesis.

This thesis work required sharing instruments in other laboratories, departments and Universities. Within the PSE Department I have learned XPS from Jacob Hirsch, contact angle and XPS from the McCarthy group and ellipsometry from Professor Hoagland and his colleagues. I spent many hours in the Hsu laboratory gathering data and I thank them for their knowledge, support and equipment time. I wish to thank Dr. Charlie Dickinson for his assistance with NMR experiments and Dr. Alan Waddon for his help with X-ray measurements. Chuck Musante assisted in the ECE clean room. I thank him for his support and for coating silicon wafers with gold. Paul Fentor collected the x-ray reflectivity data at Princeton and Brookhaven and Brenda Rosenau assisted with the model preparation on Silicon Graphics Iris work station. I am grateful for their assistance.

At Eastman Kodak Company as a visiting scientist investigating molecular recognition I learned about surface science from Avi Ulman and his colleges, Bill

McKenna, Doug Margevich, Jim Elman and Dominic Motyl. I am grateful for their time and instruction and their continued support as fellow Eastman Kodak scientists.

I wish to thank Linda Stregowski for her assistance with manuscript preparation and her friendship throughout my graduate training. Eileen Beese endeavored to keep me on track throughout my graduate career and for that and her friendship, I will be forever grateful.

The network of friends at Amherst sustained me in my absence from my family. Their friendship, stimulating conversation and the kindness extended to my family will always be treasured. I am grateful to Geni Dessipri, Katherine and Kirill Bakeev, Jim Thomas, Marianne Yarmey and Scott Joslin and consider their continued friendship a wonderful gift. To the many Tirrell coworkers, Mark (and Amy) Krejchi, Lynore Abbott, Laurie Gower, Ajay Parkhe, Seenu Kothakota, Kean Hock Yeap, Howard Creel, Wendy Petka, Howard Bowman, Carisa Soto, I extend by gratitude.

Without the encouragement from my family I never could have come to Amherst and pursued a degree. Their love and support has been the sole motivator. Perspective is best acquired with the passage of time. It his my fervent hope that what I perceive to have been our experience, that sacrifice was balanced with gain, continues to be true in the future. My utmost gratitude to Noah, Aaron and Jay. Thank you.

ABSTRACT

MODEL POLYPEPTIDES AND MOLECULAR RECOGNITION AT A MONOLAYER INTERFACE

SEPTEMBER 2000

SUSAN L. DAWSON, B.S., UNIVERSITY OF CONNECTICUT

M.S., UNIVERSITY OF CONNECTICUT

Ph.D., UNIVERSITY OF MASSACHUSETTS AMHERST

Directed by: Professor David A. Tirrell

The enormous interest in organic thin films during the last fifteen years has been driven by the prospect of utilizing these films in applications, particularly in the areas of nonlinear optics, pyroelectric materials, sensors and protective layers. The ease of formation and monolayer stability of self-assembled films, has been responsible, in part, for this renaissance. In fact, these self-assembled monolayers are now widely used to study more complex systems. Presented herein, is an example of a self-assembling process, wherein a relatively weak hydrogen bonding interaction (molecular recognition) leads to the formation of bilayers. The molecular recognition at a 2,4-diaminopyrimidine terminated monolayer (host) by a succinimide derivative (guest) has resulted in the formation of bilayers. The bilayer structures and the hydrogen bonding interactions were analyzed by external-reflection Fourier transform infrared spectroscopy, ellipsometry, and X-ray photoelectron spectroscopy.

The lateral stability of self-assembled monolayers is limited by the strength of the van der Waal interaction, although, the stability is improved over Langmuir-Blodgett systems. We propose to improve these systems further. We have been exploring the self-assembly of artificial proteins on metals. The hydrogen bonding

capacity of protein monolayers would be expected to provide enhanced stability for these films due to the multiplicity of hydrogen bonds. Polymers of sequence $[-(AlaGly)_3CysGly(AlaGly)_3GluGly-]_n$ have been designed to adopt β-sheet structures on metallic and oxide surfaces. To better understand and control polypeptide adsorption, we have focused on the self-assembly of model compounds which capture the substrate and lateral interactions.

Results are reported for the synthesis of layered arrays of N-stearoyl L-cysteine methyl ester ($CH_3(CH_2)_{16}COCysOMe$) on the surface of gold. This compound serves as a simple model of the related polypeptide and enable us to probe the cysteine-substrate interaction. We describe the preparation of monolayers and characterization of these layers via ellipsometry, vibrational spectroscopy and x-ray photoelectron spectroscopy. The results are most consistent with a disordered array of the alkyl chains, in which close packing is frustrated by a mismatch in the cross-sectional areas of the cysteinyl ester headgroup and the stearoyl chains of the thiol. Despite the disorder, the alkyl chains form a hydrophobic surface layer, with an advancing contact angle for water comparable to that observed for octadecanethiol on gold.

The assembly of N-Acetyl-L-alanylglycyl-L-alanylglycyl-L-alanylglycyl-L-cysteine methyl ester ($CH_3O(AlaGly)_3CysOCH_3$) on the surface of gold is reported herein. We describe the synthesis of the oligopeptide, preparation of monolayers assembled under different solution conditions, and characterization of these layers via ellipsometry, x-ray reflectivity, vibrational spectroscopy and x-ray photoelectron spectroscopy. The oligopeptide chemisorbs to gold via the cysteine thiol and forms monolayers. The infrared data demonstrates that the oligopeptide tertiary structure in monolayer **2** is different than what is typically seen in peptide structures. The implication is that the gold (111) surface forces an uncharacteristic peptide packing.

TABLE OF CONTENTS

LIST OF TABLES

LIST OF FIGURES

Figure

Page

# LIST OF SCHEMES

Scheme

Page

# CHAPTER 1

# INTRODUCTION

## 1.1 Thin Films

The enormous interest in organic thin films during the last fifteen years has been driven by the prospect of utilizing these films in applications, particularly in the areas of nonlinear optics, pyroelectric materials, sensors (acoustic, chemical and bio) and protective layers[1]. The interest in monolayer and multilayer films can be traced to the work of Langmuir[2] and Blodgett[3]. While Langmuir-Blodgett (LB) films have been useful as model systems, they are often limited by the lack of mechanical, thermal, and chemical stability. This stability can be attributed, to a large extent, to weak intermolecular interactions, which fail to maintain the integrity of the film.

One approach to solve stability problems has been to introduce polymer materials into LB films. This can be accomplished by ordering monomers on the trough and transferring the monomer (which is subsequently polymerized) or transferring the polymer (polymerized in situ) to the substrate. An alternative mechanism involves the ordering and transfer of preformed polymers and copolymers. Although there has been improvement in the thermal stability of these polymer films with the introduction of main chain hydrophilic spacers in polymers[4] or the use of polyimides[5], technological applications for these films are not immediately apparent.

The development of self-assembled systems (Figure 1.1), a new method for the formation of monolayers[6,7], led to the construction of more stable films[8]. In these self-organizing systems the adsorbate diffuses through solution to the substrate, chemisorbs to the surface and packs to form a well ordered material[9]. The strong

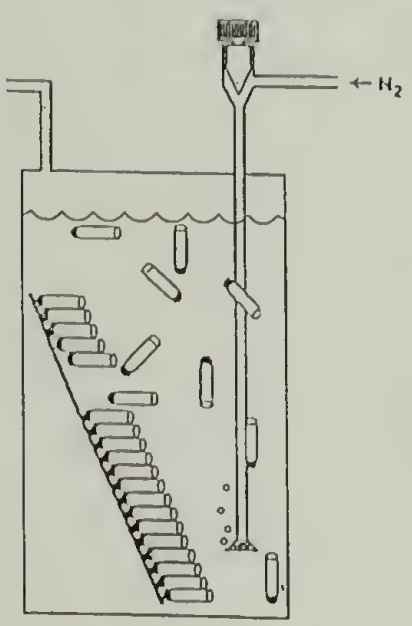


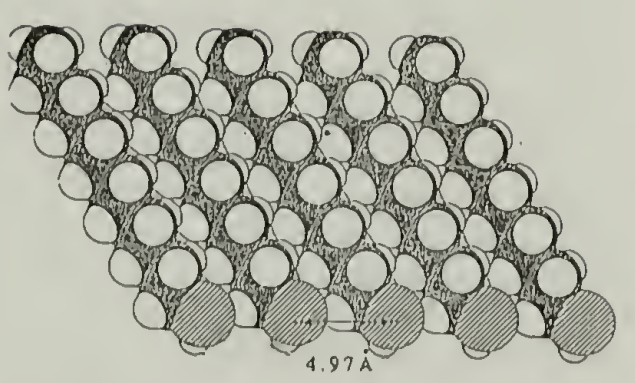


*A. Ulman, An Introduction to Ultrathin Organic Films: From Langmuir-Blodgett to Self-Assembly; copyright © 1991 by Academic Press, reproduced by permission of the publisher.*

Figure 1.1 Self-assembled monolayers. Monolayer formation (a) and an alkyl thiolate monolayer (b).

binding of the head group to the surface confers increased stability to the film[10]. With this new approach Netzer and Sagiv[11] fabricated multilayer films with bifunctional silane building blocks. Development of self-assembled systems has expanded beyond organosilicon monolayers on hydroxylated or oxide surfaces ($SiO_2$/Si, $Al_2O_3$/Al, and glass) to include a variety of adsorbates and substrates; alkane thiols on metals (Au, Ag, and Cu)[12-17]; alkyl sulfides[18] and dialkylsulfides[19-23] on Au; amines on platinum[24]; and carboxylic acids metals and oxides (Ag and $Al_2O_3$)[25,26].

Alkyl thiols adsorbed on gold constitute one of the most frequently studied monolayer systems. There are good reasons for this combination. Gold is inert and does not readily oxidize, making it easier to use in ambient environments. Additionally, thiols are one of the few functional groups to react with gold. The stability of these monolayers originates from the strong bonding between the gold and the thiolate adsorbate (~44 Kcal/mole) and for monolayers with longer alkyl chains, from interchain van der Waal interactions. The alkyl chains cant ~30° to maximize this interaction. The chemisorption of alkyl thiols proceeds rapidly from solution, but the second stage ordering of the monolayer can take days[14].

Methyl terminated, bifunctional, and mixed monolayers have been useful as model systems for the elucidation of wetting[27], friction, biological adhesion[28], molecular recognition[29,30], and protein adsorption behavior[31], and in facilitating AFM and STM[32] study of proteins. Self-assembled materials are receiving considerable attention with respect to future applications. They have already been shown to perform effectively as nanoresists[33].

Polymer thin films fabricated by self-assembly methods have also attracted attention. The polymer chemisorbs to the metal via pendant functionalities, typically dialkyldisulfide or sulfide, as in the adsorption of acrylate polymers containing dithioalkyl chains[34], disulfide functionalized amphiphilic copolymers[35], siloxane-based graft copolymers[36], and poly(styrene-propylene sulfide) block copolymers[37]. Formation of polymer thin films with pendant functionalities has been accomplished by electropolymerizing pyrrole on a pyrrole terminated monolayer to form electrically conducting films[38,39] or by the selective electropolymerization of aniline on a photopatterned SAM[33].

Polymers can also be tethered to a metal surface through chain termini. Enriquez et. al.[40] have formed self-assembled monolayers on gold with terminally functionalized (lipoic acid) poly (γ-benzyl-L-glutamate). Their attempts to form well

ordered monolayers have not yet been realized. A novel approach was reported by Whitesell and Chang[41] to form a helical polypeptide monolayers aligned perpendicular to the surface. They initiated in situ polymerization of alanine N-carboxyanhydride from an amine terminated trithiol platform. The area of the platform adsorbed on Au (100) is somewhat larger than the dimensions of the polypeptide $\alpha$ helix.

## 1.2 Theme

The literature, as described earlier, is replete with examples of self-assembled monolayers developed to study structure and function. In this thesis, self-assembled monolayers are employed to study interfacial molecular recognition and the assembly of model structures which mimic certain aspects of the assembly of polypeptides, specifically [-(AlaGly)3CysGly(AlaGly)3GluGly-]n (**1**), to form ordered polypeptide films exhibiting enhanced stability.

## 1.3 Molecular Recognition

There is a growing interest in applying the principles of biological recognition to the construction of new synthetic materials; although the issues that govern the interaction of large biological molecules do not always apply, in a simple way, to recognition events in small molecules. It has been demonstrated that "self-assembly on templates is an important synthetic strategy" for developing complex architectures[42,43] which may be exploited for device and sensor applications. Toward that end, self-assembled monolayers can probe specific interactions to answer fundamental questions concerning host guest pairings in molecular recognition events. In Chapter 2, a self-assembled monolayer containing an interfacial recognition site was fabricated to

study molecular recognition at a 2,4-diamiopyrimidine terminated monolayer by a succinimide guest.

## 1.4 Interfacial Self-Assembly of Model Polypeptides

The lateral stability of self-assembled monolayers is limited by the strength of the van der Waals interaction, although, the stability is improved over Langmuir-Blodgett systems. We propose to improve these systems further. We have been exploring the self-assembly of materials, specifically artificial proteins, which are characterized by stronger lateral interactions[44]. The hydrogen bonding capacity of protein monolayers would be expected to provide enhanced stability for these films[45]. Polymers of sequence $[-(AlaGly)_3CysGly(AlaGly)_3GluGly-]_n$ have been designed to adopt folded β sheet structures on metallic and oxide surfaces. In Figure 1.2, the metal surface directs the orientation of the polymer through its interaction with the periodically spaced functional groups (Y) of the chain. Novel interfaces can then be engineered further through the elaboration of the "outer surface" functionality (X). In the design strategy for these polypeptides we relied on clues from nature, selecting amino acids alanine and glycine because they are associated with β sheet structures. The number of these alanylglycine dyads incorporated into the repeating unit defines the lamellar thickness. Amino acids with bulky side chains, here cysteine and glutamic acid, were selected to create reverse turns. In artificial proteins of this kind, the side chain functionality is expected to direct the assembly of the chain on metal surfaces.

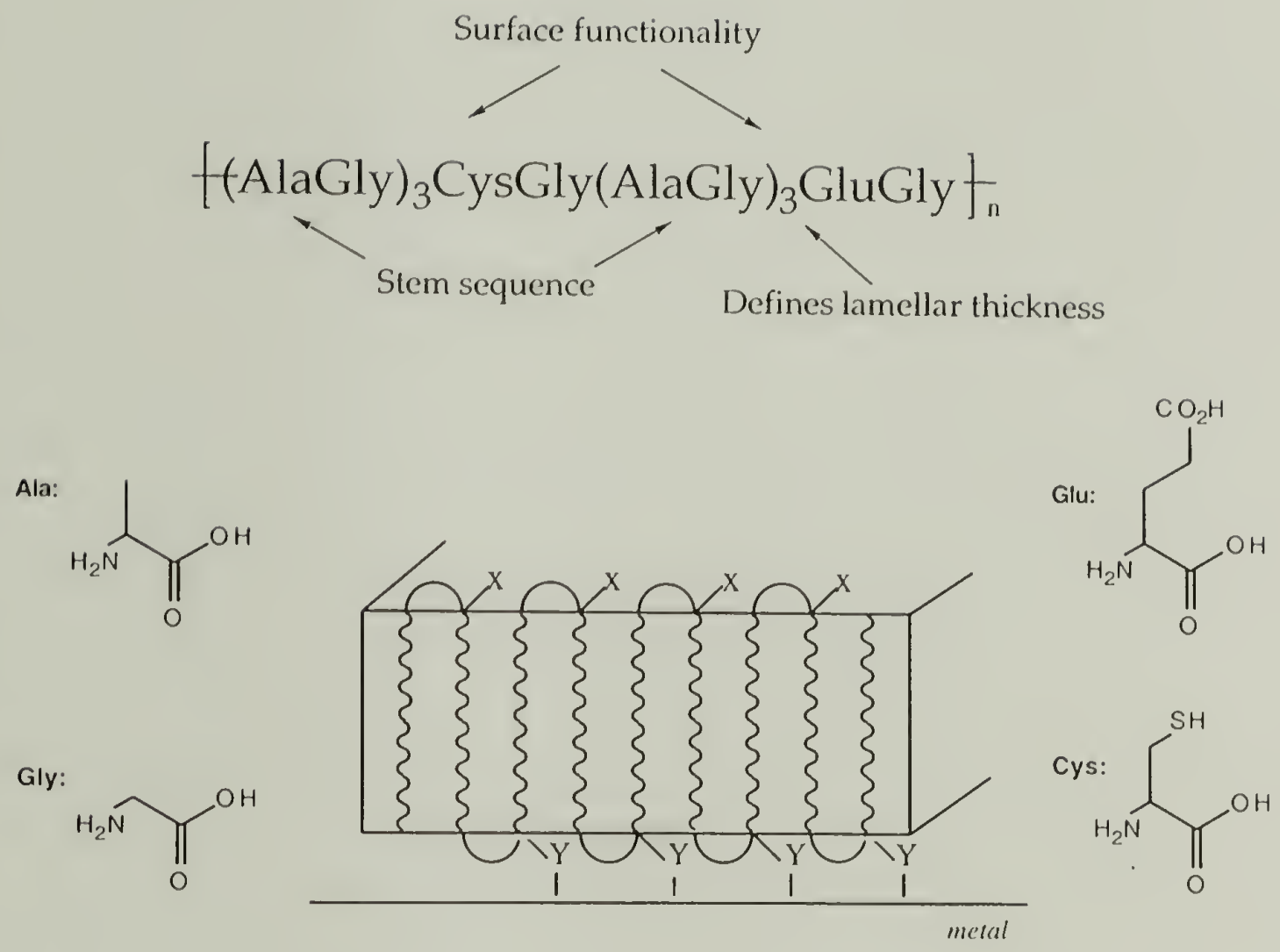


Figure 1.2 Design strategy for folded polypeptide and idealized adsorption on metal surfaces.

The polymer **1** was designed to provide a structure with chemically distinct surface functionality. Solution self-assembly of **1** on metals by chemisorption would form novel monolayers with lamellar structure. The strong interaction between Y andthe metal provides an additional driving force for this polymer to fold into a lamellar structure. The orientation of the polypeptide **1** can be controlled by the choice of metal. The cysteine thiol (X=$CO_2H$, Y=S) of **1** should chemisorb onto gold substrates. The

| Metal | X | Y |
|---|---|---|
| Au | $CO_2H$ | S |
| $Al_2O_3$ | SH | $CO_2$ |
| Ag | $CO_2R$ | S |

strong affinity of the γ-carboxylic acid of glutamic acid should reverse the orientation of **1** (X=SH, Y=$CO_2$) on an aluminum oxide substrate[25,46]. We anticipate that the orientation of the functional groups will be specific on both metals based on the work of Laibinis and coworkers[47]. These workers found that functionally terminated alkanethiols and alkane carboxylic acids specifically adsorbed on gold and aluminum oxide surfaces respectively. The cysteine thiol of the γ-carboxylic acid protected polypeptide **1** (X=$CO_2R$, Y=S) should chemisorb on a silver surface to form the lamellar structure in Figure 1.2.

The structures of such monolayers will be governed by interactions of the side chain functionality with the substrate, by intermolecular hydrogen bonding interactions, and by chain connectivity. The solution conditions for forming regular, well-ordered lamellar crystals with no loops or switchbacks become enormously important for polypeptides. In order to simplify the problem, our initial efforts have focused on the

self-assembly of two model compounds which capture the substrate and lateral interactions, but defer the complications associated with chain connectivity.

In chapter 3, the interaction of the side chain functionality with the substrate is reported with a simple model compound, the methyl ester of stearoyl cysteine ($C_{17}H_{35}COCysOCH_3$, **2** ). Studies of **2** enable us to probe the effect of the size of the interacting cysteine methyl ester, which affects the packing density of these monolayers. The compound $CH_3CO(AlaGly)_3CysOCH_3$ (**3**), a strand of the β sheet architecture represented in Figure 2, serves as a model of the polypeptide **1**. The self-assembly of **3** on gold is described in chapter 4. Molecular models of the monolayers **2** and **3** were constructed using the Molecular Simulations Biograf Program, running on a Silicon Graphics Iris work station and are shown in Figures 1.3 and 1.4.

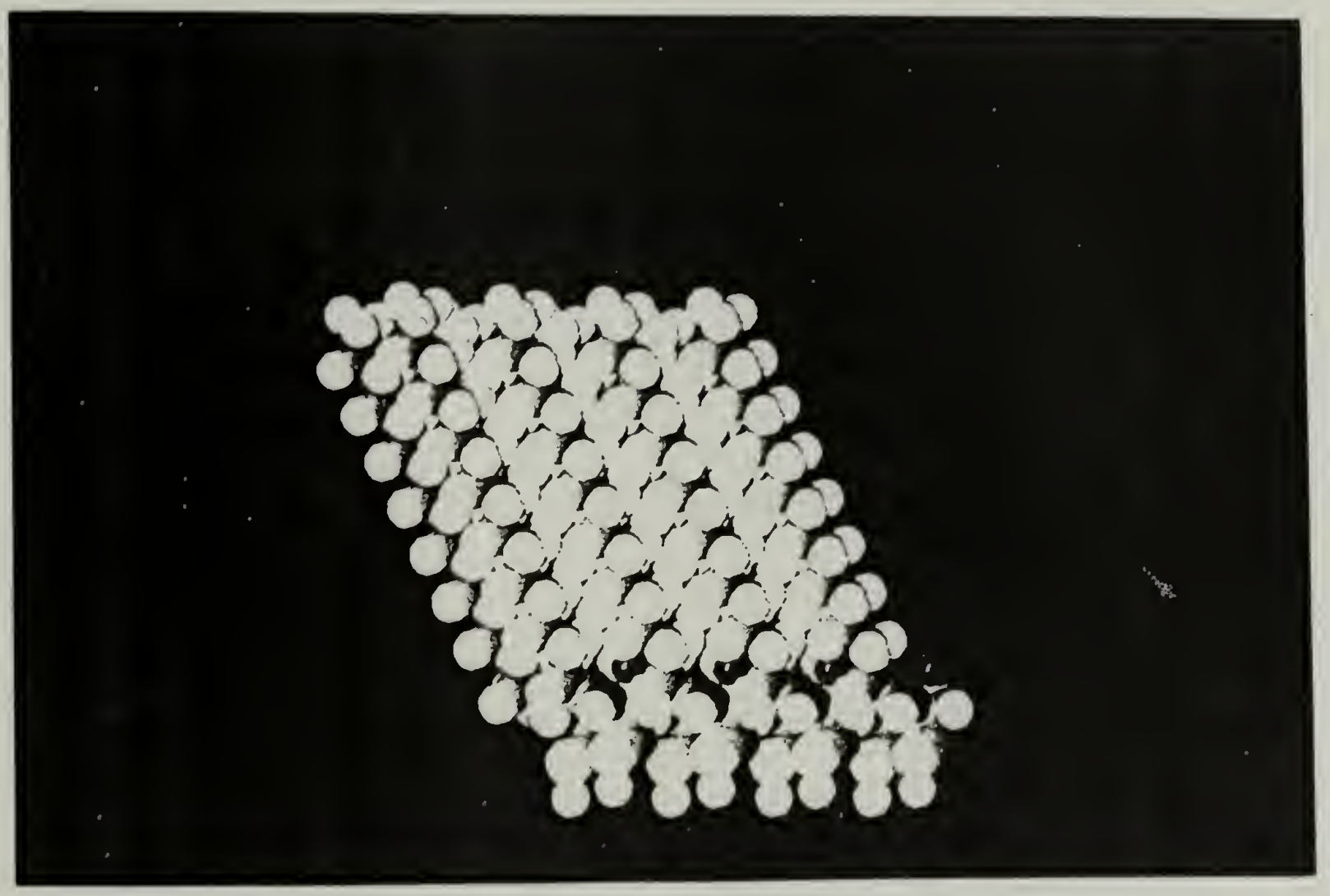

Figure 1.3 Hypothetical monolayer of $C_{17}H_{35}COCysOCH_3$ on gold.

Figure 1.4 Hypothetical monolayer of $CH_3CO(AlaGly)_3CysOCH_3$ on gold.

## 1.5 References


(1) Swalen, J. D.; Allara, D. L.; Andrade, J. D.; Chandross, E. A.; Garoff, S.; Israelachvili, J.; McCarthy, T. J.; Murray, R.; Pease, R. F.; J, F. R.; Wynne, K. J.; Yu, H. *Langmuir* **1987**, 3, 932.

(2) Langmuir, I. *J. Am. Chem. Soc.* **1917**, 39, 1848.

(3) Blodgett, K. A. *J. Am. Chem. Soc.* **1935**, 57, 1007.

(4) Elbert, R.; Laschewsky, A.; Ringsdorf, H. *J. Am. Chem. Soc.* **1985**, 107, 4134.

(5) Angle, A. K.; Yoden, T.; Sanui, K.; Ogata, N. *J. Am.Chem. Soc.* **1985**, 107, 8308.

(6) Bigelow, W. C.; Pickett, D. L.; Zisman, W. A. *J. Colloid Interface Sci.* **1946**, 1, 513.

(7) Sagiv, J. *J. Am. Chem. Soc.* **1980**, 102, 92.

(8) Netzer, L.; Sagiv, J. *J. Am. Chem. Soc.* **1983**, 105, 674.

(9) Ulman, A. *An Introduction to Ultrathin Films: from Langmuir-Blodgett to Self-Assembly*; Academic Press: Boston, **1991**; p. 280.

(10) Nuzzo, R. G.; Dubois, L. H.; Allara, D. A. *J. Am. Chem. Soc.* **1990**, 112, 558.

(11) Netzer, L.; Iscovici, R.; Sagiv, J. *Thin Solid Films* **1983**, 99, 235.

(12) Porter, M. D.; Bright, T. B.; Allara, D.; Chidsey, C. E. D. *J. Am. Chem. Soc.* **1987**, 109, 3559.

(13) Bain, C. D.; Troughton, E. B.; Toa, Y.-T.; Evall, J.; Whitesides, G. M. *J. Am. Chem. Soc* **1989**, 111, 321.

(14) Dubois, L. H.; Nuzzo, R. G. *Annu. Rev. Phys. Chem.* **1992**, 43, 437.

(15) Walczak, M. M.; Chung, C.; Stole, S. M.; Widrig, C. A.; Porter, M. D. *J. Am. Chem. Soc.* **1991**, 113, 2370.

(16) Bryant, M. A.; Pemberton, J. E. *J. Am. Chem. Soc.* **1991**, 113, 3629.

(17) Labinis, P. E.; Whitesides, G. M.; Allara, D. L.; Tao, Y.-T.; Parikh, A. N.; Nuzzo, R. G. *J. Am. Chem. Soc.* **1991**, 113, 7152.

(18) Troughton, E. B.; Bain, C. D.; Whitesides, G. M.; Nuzzo, R. G.; Allara, D.; Porter, M. D. *Langmuir* **1988**, 4, 365.

(19) Nuzzo, R. G.; Allara, D. L. *J. Am. Chem. Soc.* **1983**, 105, 4481.

(20) Li, T. T.-T.; Weaver, M. J. *J. Am. Chem. Soc.* **1980**, 106, 6107.

(21) Nuzzo, R. G.; Zegarski, B. R.; Dubois, L. H. *J. Am. Chem. Soc.* **1987**, 109, 733.

(22) Nuzzo, R. G.; Fusco, F. A.; Allara, D. L. *J. Am. Chem. Soc.* **1987**, 109, 2358.

(23) Bain, C. D.; Biebuyck, H. A.; Whitesides, G. M. *Langmuir* **1989**, 5, 723.

(24) Bartell, L. S.; Betts, J. *J. Phys. Chem.* **1960**, 64, 1075.

(25) Allara, D. L.; Nuzzo, R. G. *Langmuir* **1985**, 1, 45.

(26) Allara, D. L.; Nuzzo, R. G. *Langmuir* **1985**, 1, 52.

(27) Dubois, L. H.; Zegarski, B. R.; Nuzzo, R. G. *J. Am. Chem. Soc.* **1990**, 112, 570.

(28) Lopez, G. P.; Albers, M. W.; Schreiber, S. I.; Carroll, R.; Peralta, R.; Whitesides, G. M. *J. Am. Chem. Soc.* **1993**, 115, 5877.

(29) Motesharei, G.; Myles, D. C. *J. Am. Chem. Soc.* **1994**, 116, 7413.

(30) Spinke, J.; Liley, M.; Schmitt, F.-J.; Guder, H.-J.; Angermaier, L.; Knoll, W. *J. Chem. Phys.* **1993**, 99, 7012.

(31) Lopez, G. P,; Biebuyck, H. A.; Kumar, R. H.; Whitesides, G. M. *J. Am. Chem. Soc.* 1993, 115, 10774.

(32) Leggett, G. J.; Roberts, C. J.; Williams, P. M.; C.Davies, M.; Jackson, D. E.; Tendler, S. J. B. *Langmuir* **1993**, 9, 2356.

(33) Kumar, A.; Abbott, N. L.; Kim, E.; Biebuyck, H. A.; Whitesides, G. M. *Acc. Chem. Res.* **1995**, 28, 219.

(34) Sun, F.; Grainger, D. W.; Castner, D. G. *J. Vac. Sci. Technol A.* **1994**, 12, 2499.

(35) Erdelen, C.; Haussling, L.; Naumann, R.; Ringsdorf, H.; Wolf, H.; Yang, J.; Liley, M.; Spinke, J.; Knoll, W. *Langmuir* **1994**, 10, 11246.

(36) Sun, F.; Mao, G.; W.Granger, D.; Castner, D. G. *Thin Solid Films* **1994**, 242, 106.

(37) Waldman, D. A.; Kolb, B. U.; McCarthy, T. J.; Hsu, S. L. *Polym. Mater. Sci. Eng.* **1988**, 59, 326.

(38) Collard, D. M.; Sayre, C. N. *J. Electroannal. Chem.* **1994**, 375, 367.

(39) Willicut, R. J.; McCarley, R. L. *J. Am. Chem. Soc.* **1994**, 116, 10823.

(40) Enriquez, E. P.; Gray, K. H.; Guarisco, V. F.; Linton, R. W.; Mar, K. D.; Samulski, E. T. *J. Vac. Sci Technol. A* **1992**, 10, 2775.

(41) Whitesell, J. K.; Chang, H. K. *Science* **1993**, 261, 73.

(42) Holzwarth, J. F.; Whitesides, G. M. *Current Opionion in Colloid & Interface Science* **1996**, 1, 61.

(43) Bishop, A. R.; Nuzzo, R. G. *Curr. Opion. Colloid & Interface Sci***1996**, 1, 127.

(44) Krejchi, M. T.; Atkins, E. D. T.; Waddon, A. J.; Fournier, M. J.; Mason, T. L.; Tirrell, D. A. *Science* **1994**, 265, 1427.

(45) Dawson, S. L.; Fournier, M. J.; Mason, T. L.; Tirrell, D. A. *Polymer Preprints* **1994**, 35, 413.

(46) Allara, D. L.; Nuzzo, R. G. *Langmuir* **1985**, 1, 52.

(47) Labinis, P. E.; Hickman, J. J.; Wrighton, M. S.; Whitesides, G. M. *Science* **1989**, 245, 845.

# CHAPTER 2

## MOLECULAR RECOGNITION AT A MONOLAYER INTERFACE: 2,4-DIAMINOPYRIMIDINE-SUCCINIMIDE HOST-GUEST PARTNERS

### 2.1 Abstract

Molecular recognition at a 2,4-diaminopyrimidine terminated monolayer **1** (host) by a succinimide derivative (guest) has resulted in the formation of bilayers. The bilayers were prepared either from solution or by transfer from the air-water interface to the monolayer substrate. The preorganized 2,4-diaminopyrimidine is oriented for recognition with a molecule of complementary hydrogen bonding ability, succinimide **2**. The resultant bilayer **3** is stabilized by the formation of three hydrogen bonds per host-guest pair. We present an example of a self-assembling process, wherein a relatively weak hydrogen bonding interaction (molecular recognition) leads to the formation of bilayers. The bilayer structures and the hydrogen bonding interactions were analyzed by external-reflection Fourier transform infrared spectroscopy (FTIR), ellipsometry, and X-ray photoelectron spectroscopy (XPS).

### 2.2 Introduction

Molecular recognition, the selection and non-covalent binding of a guest molecule by a host[1,2], is ubiquitous in nature. Specific recognition processes, e.g.

between antibody and antigen, enzyme and substrate (or inhibitor), or hormone and receptor, play important roles in mediating a variety of biological processes.

There is growing interest in applying the principles of biological recognition to the construction of new synthetic materials[3,4]. The issues that govern the interaction of large biological molecules do not always apply in a simple way to recognition events in smaller molecules[5]; however, we can adopt two key elements -complementarity and specificity[5,6] - to the design of molecular recognition sites in synthetic systems. Complementary molecules have geometries that allow binding through multiple, non-covalent intermolecular interactions; e.g., hydrogen bonding, van der Waals forces, and electrostatic interactions[7]. The weak interaction energies associated with these forces result in modest enthalpic contributions to the Gibbs free energy of binding, and binding is easily prohibited by comparable, unfavorable entropic contributions[8]. One approach to the minimization of the unfavorable entropic contribution of host-guest pairing is to preorganize the host[9] with rigid elements or through the formation of clefts and cavities. For example, preorganization of cyanuric acid and melamine derivatives by tethering them to central hubs permits assembly of rosettes or linear tape[10].

Although molecular recognition events have been investigated most thoroughly in solution, a recent approach has been to incorporate artificial receptors at monolayer interfaces. Studies at the air-water interface have involved chiral recognition[11-13], and amino acid or nucleic acid base complexation[14]. Monolayers self-assembled on substrates have been utilized to probe interfacial recognition of a variety of host-guest partners; including dioctadecyldithiocarbamate and $Cu^{2+}$ [15], thiolated β-cyclodextrin and ferrocene[16], a biotinylated polythiophene copolymer with streptavidin and a biotinylated photoactive protein[17], and 4-hydroxythiophenol with $Ru(NH_3)_6^{3+}$ [18], with proposed technological applications ranging from chemical and biosensors to opto-electronic signal transducers.

The recognition of streptavidin by biotin-terminated monolayers has been extensively studied[19,20]. The binding interaction of this host-guest pair ($K_a$= $10^{15}$ $M^{-1}$)[21] is so strong that it is essentially irreversible. In nature recognition is predominantly a reversible interaction and strong binding can result in inhibition of the process of interest[22]. A weaker binding interaction can lead to reversible recognition and the construction of semi-permanent structures. The relatively weak hydrogen bonding interactions ($K_a$=$10^2$ to $10^4$ $M^{-1}$ in $CDCl_3$)[23,24] of imides with 2,4-diamidoazines and 2,4-diaminoazines has provided a basis for the self-assembly of synthetic replicators[25,26], supramolecular strands[27,28], and supramolecular complexes[10]. In aqueous systems the binding of nucleic acid bases to diaminotriazines has a comparable binding constant ($10^2$ $M^{-1}$)[29]. Thus, binding energies such as those in the biotin-streptavidin system are not necessary to assemble supramolecules[30,31] and nanostructures[8]. In this report we present preliminary results on a self-assembly process, wherein relatively weak hydrogen bonding interactions lead to the formation of bilayers.

## 2.3 Results and Discussion

### 2.3.1 Bilayer Formation

We have engineered recognition sites into a self-assembled alkanethiolate monolayer (**1**) on a gold substrate. The preorganized 2,4-diaminopyrimidine terminal groups are oriented for recognition of molecules with complementary arrangements of acidic protons and electron pairs. This preorganization reduces the often substantial entropic barrier to recognition. Recognition of the monolayer **1** (host) by the succinimide derivative (**2**) (guest) results in the formation of a bilayer **3** (Figure 2.1),

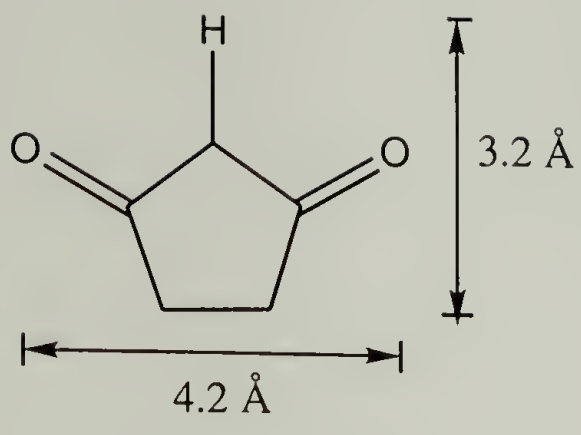


Guest

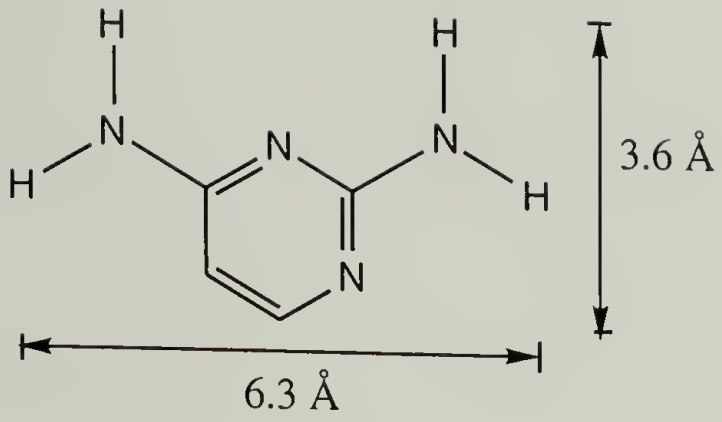


Host

which is stabilized by formation of three hydrogen bonds per host-guest pair. The monolayer is easily prepared by solution self-assembly of the pyrimidine derivative on gold[32,33]. Ellipsometry measurements of film thickness are in good agreement with the calculated maximum thickness for an all-trans alkyl chain (22 Å).

2.3.2 Langmuir-Blodgett Bilayer.

A monolayer of **2** was first compressed at the air-water interface (Figure 2.2) and then transferred onto monolayer **1**. The resultant bilayer is comprised of host-guest molecules positioned at the interface. Figure 2.3A presents the external-reflection Fourier transform infrared (FTIR) spectrum for the monolayer **1**. The 2- and 4- amino ($NH_2$) scissoring vibrations appear at 1638 and 1665 $cm^{-1}$, respectively. The $NH_2$ scissoring vibration of the 2-amino group (2-aminopyrimidine) always appears at a higher frequency than that of the 4-amino group (4-aminopyrimidine)[34,35]. We assume the same assignment in 1,4-diaminopyrimidine. One of the four ring stretching modes, $\nu_8$ ($C_S$, A'), appears at 1576 $cm^{-1}$ (1563 $cm^{-1}$ in KBr). The frequency of $\nu_{8a}$ for a number of substituted pyrimidines was reported by LaFaix and Lebas[35].

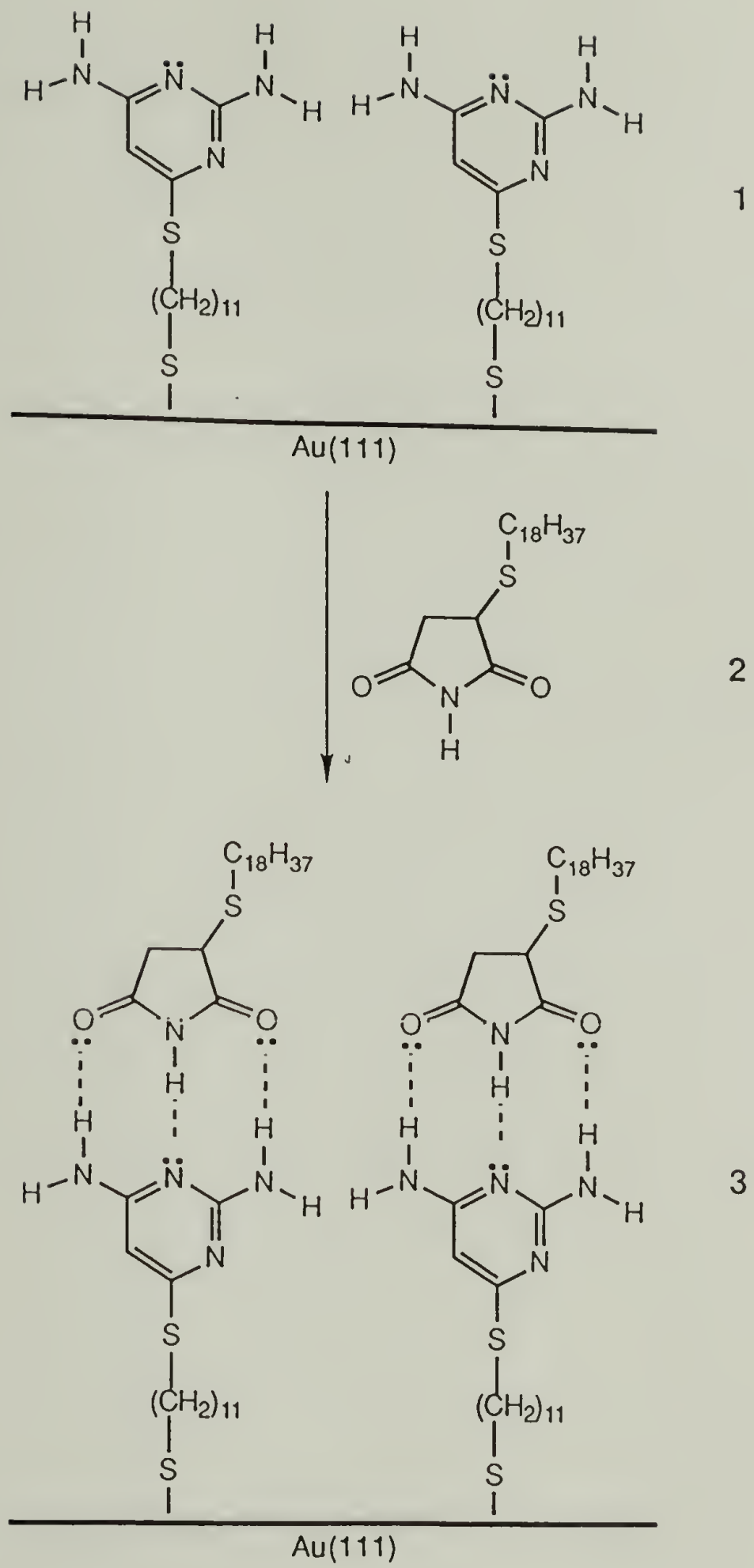


Figure 2.1 Formation of bilayer **3**. Recognition of the monolayer **1** (host) by the succinimide **2** (guest) results in the formation of a bilayer **3**, which is stabilized by the formation of the three hydrogen bonds per host guest pair.

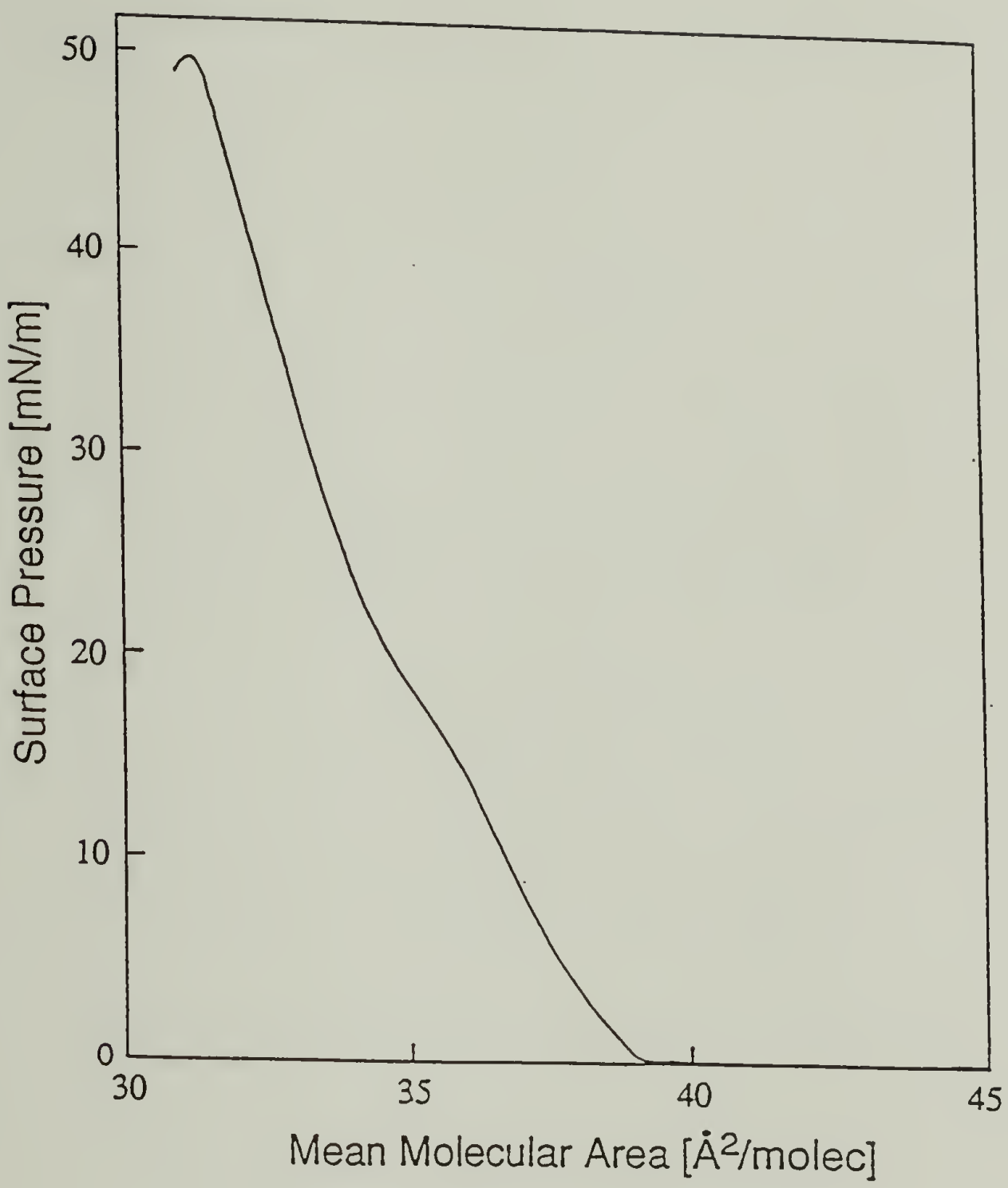


Figure 2.2 The π-A isotherm for **2**.

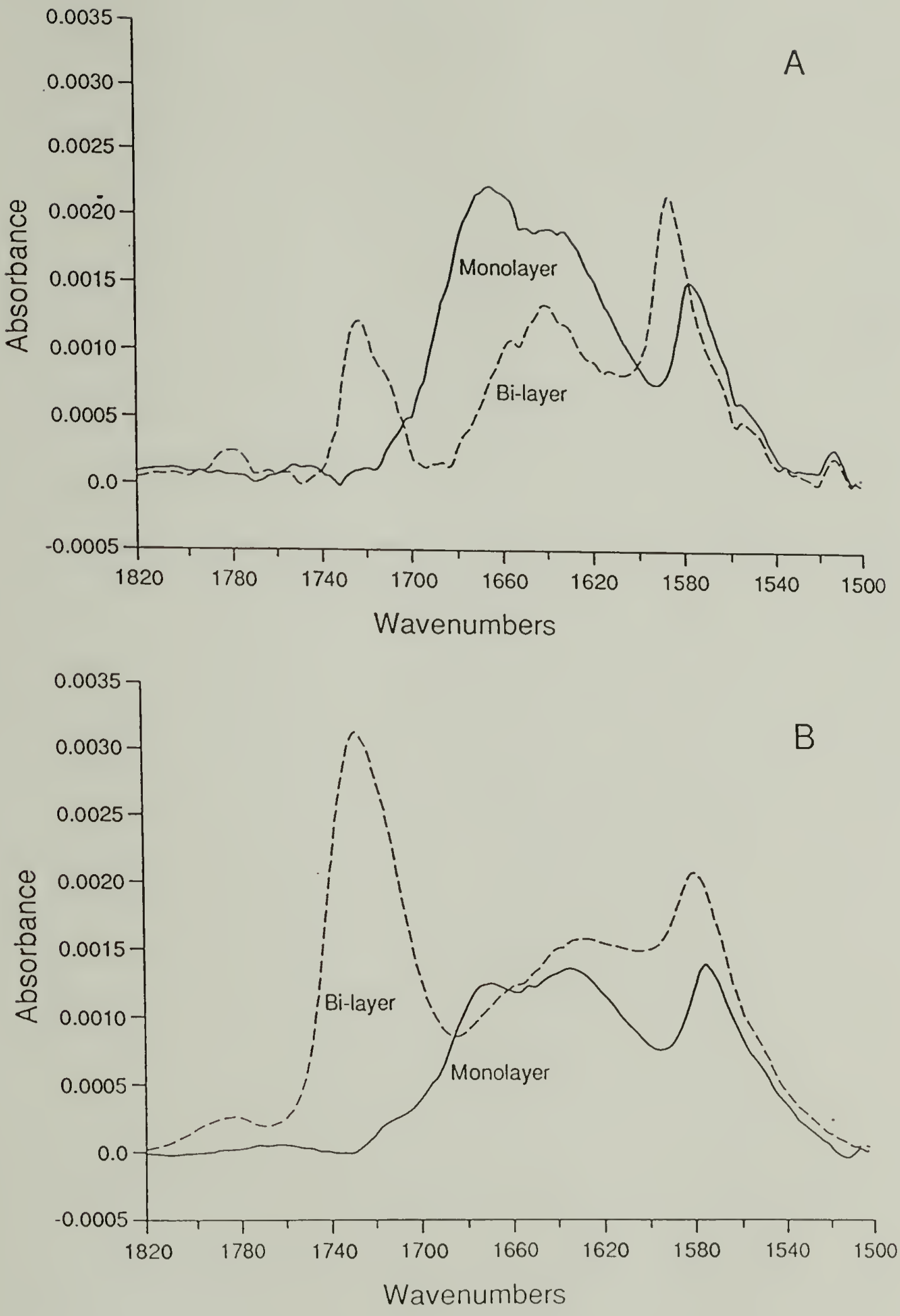


Figure 2.3 Infrared external reflection-absorption spectra with a p-polarized beam of the self-assembled monolayer on gold (**1**) and bilayers (**3**) in the mid frequency region. (**A**) The monolayer and the Langmuir-Blodgett bilayer. (**B**) The monolayer and the solution self-assembled bilayer.

After transfer of **2**, there are some notable changes. First, there is a reduction in the amino scissoring intensity at 1665 $cm^{-1}$ indicating a conformational change within the monolayer as the pyrimidine ring repositions itself to interact with **2**. [Notice that in a p-polarized IR spectrum, only the perpendicular components of the transition dipoles of the adsorbate are visualized[36].] Secondly, the symmetric and asymmetric carbonyl bands of the succinimide **2** appear at 1781 and 1722 $cm^{-1}$ [37]. Finally, the hydrogen bonding interaction raises the frequency of the ring stretching band at 1576 $cm^{-1}$ by 9 $cm^{-1}$. A change in the ring stretching frequency with hydrogen bonding has been observed previously in diaminotriazine systems[29]. Kurihara *et al.* report that Langmuir-Blodgett films of an amphiphilic diaminotriazine transferred from 0.01 M aqueous thymidine exhibit a C=N stretching vibration at 1557 $cm^{-1}$. Transfer from water shifts the vibration to 1571 $cm^{-1}$, consistent with the observations of Stidham and DiLella[38] and Takahashi *et al.*[39] on hydration of nitrogen heterocycles. In addition, DiLella and Stidham have shown in the Raman spectrum of pyridine that $\nu_8$ shifts to higher frequency upon hydrogen bonding to water and Takahashi *et al.* observed a similar shift in the infrared spectrum.

### 2.3.3 Solution Self-Assembled Bilayer

In a second experiment we prepared a bilayer by solution self-assembly. Thus, a sample of monolayer **1** was immersed in a 1.0 mM toluene solution of **2** for 1.8 days, rinsed with solvent, and dried under nitrogen. The same trends that were observed previously are seen in Figure 2.3B. The carbonyl stretching bands at 1781 and 1726 $cm^{-1}$ confirm the presence of **2**. Hydrogen bonding is evident by an increase of 4 $cm^{-1}$ to 1578 $cm^{-1}$ for the $\nu_8$ band. Again we observe the effects of conformational changes in the amino scissoring bands.

### 2.3.4 High Frequency Infrared Region

The high frequency infrared region characterizes the alkyl chains in the mono- and bilayers. There, the frequency of the asymmetric methylene stretching band, $d^-$ ($\nu_{as}CH_2$), at 2921 $cm^{-1}$ indicates that the monolayer is liquid-like[40]. With the Langmuir-Blodgett transfer of **2** to the monolayer, however, there is a shift to a more solid-like frequency at 2919 $cm^{-1}$ (Figure 2.4). The frequency in the KBr spectrum of pure **2** is 2919 $cm^{-1}$. The IR spectrum recorded one week later showed virtually no change, thus indicating the stability of the bilayer. Compression of **2** at the air-water interface should result in extended alkyl chains. Apparently, once compressed, the transferred **2** retains the extended structure. Notice that $CH_2$ groups from both molecules contribute to the observed IR spectrum; however, it is impossible to suggest conformational changes in monolayer **1** due to bilayer formation without specific deuteration. Ellipsometric measurements confirm that the alkyl chain is extended, in that there is a 25 Å increase in thickness upon adsorption of **2**.

In the self-assembled bilayer there is a shift in $d^-$ to 2923 $cm^{-1}$; i.e., the bilayer is clearly liquid-like. This is not surprising, since the overlayer has not been closely packed prior to bilayer formation. An increase of only 16 Å in the film thickness is observed, suggesting that the succinimide overlayer is less dense than that prepared by Langmuir-Blodgett transfer, and that the alkyl chains are disordered. Although it may be inferred from the relative intensities of the asymmetric carbonyl bands in Figures 2.3A and 2.3B that there is more succinimide in the self-assembled bilayer, the relative intensities of the asymmetric methylene stretching vibrations in Figure 2.4 suggest the opposite, in agreement with ellipsometric results. Differences in packing and conformation in the overlayers probably account for the observed variation in the infrared intensities.

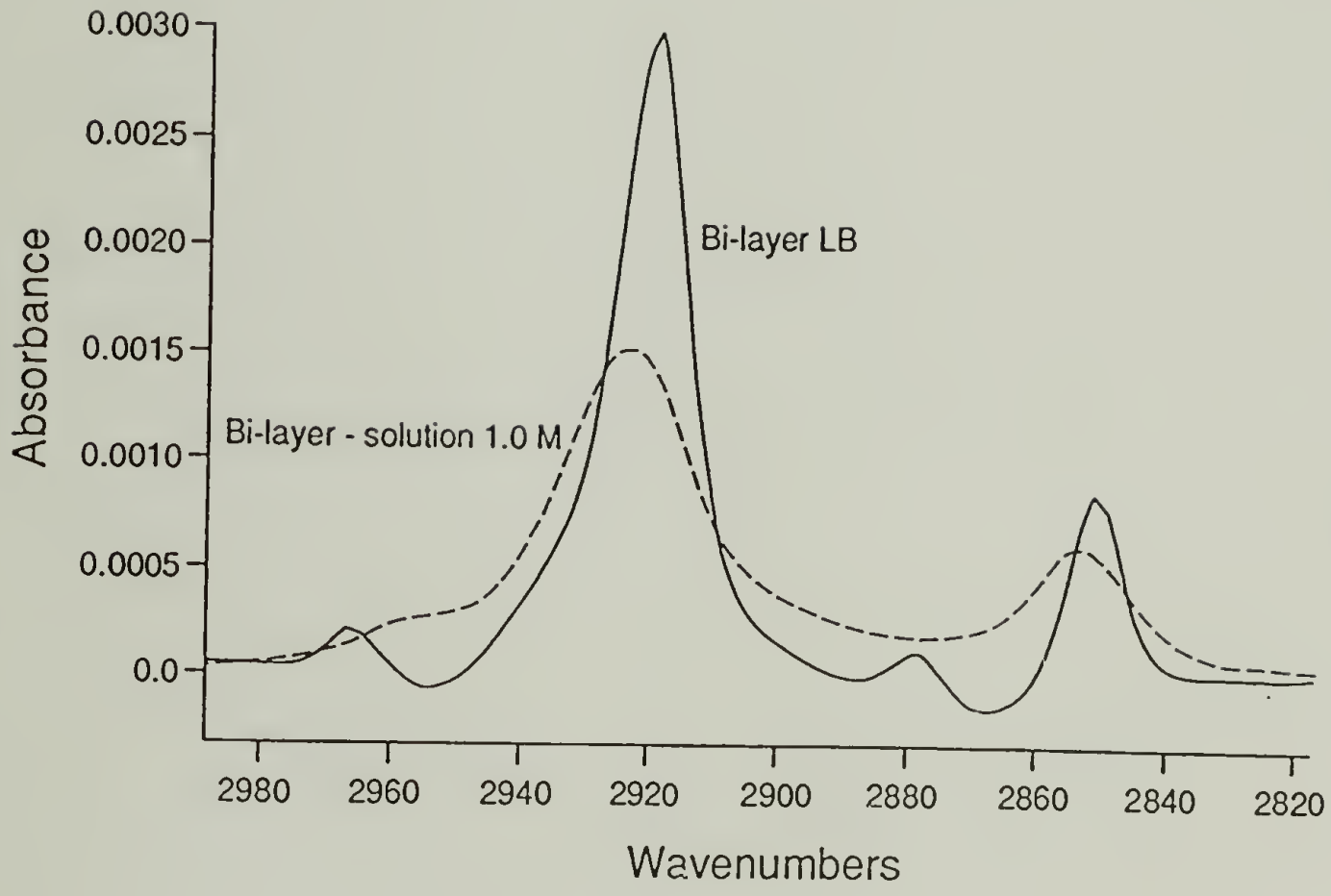


Figure 2.4 Infrared external reflection-absorption spectra with a p-polarized beam of the Langmuir-Blodgett and the solution self-assembled bilayers.

### 2.3.5 X-Ray Photoelectron Spectroscopy

The bilayers were examined by angle resolved X-ray photoelectron spectroscopy (XPS). In Table 2.1 the atomic concentrations for several electron take off angles (ETOA) are given. The concentration of gold is greater for the self-assembled sample, supporting a less densely covered surface. The one anomaly is the oxygen content for the solution self-assembled bilayer at 15° ETOA, which is likely a result of surface contamination. Succinimide overlayer calculations (14 Å) reveal that the more rigorous washing of the bilayer with solvent has removed more of **2** of this sample. The trends in elemental concentration as a function of ETOA are similar for the bilayers. Ellipsometric measurements of both bilayers before and after exposure to the high vacuum of the XPS showed no change in thickness and no apparent loss of material.

### 2.3.6 Concentration Effects

The extent of bilayer formation depends on the concentration of the succinimide in the solution used in the self-assembly step. Thus, as the concentration of **2** is reduced from 1.0 to 0.5 to 0.25 mM, there is a corresponding reduction in coverage as indicated by a reduction in the intensity of the asymmetric carbonyl band at 1727 $cm^{-1}$, and the asymmetric methylene band at 2923 $cm^{-1}$ (Figure 2.5). In all of these bilayer spectra there is an increase in the ring stretching frequency with hydrogen bonding. At concentrations below 1.0 mM, there are conformational changes due to the repositioning of the pyrimidine ring as described above. Intensity changes indicate that the 4-amino group is in a more nearly perpendicular orientation, and the 2-amino group and the ring are oriented parallel to the monolayer plane. One possible explanation for these conformational changes is that there is only one amino group and one carbonyl group involved in the recognition, similar to that found in base pairing mismatch[41].

Table 2.1 Atomic Percent versus Electron Take-off Angle

| | Solution Self-assembled bilayer *atomic percent* | | | | Langmuir-Blodgett bilayer *atomic percent* | | | |
|---|---|---|---|---|---|---|---|---|
| Element | 15 ° | 25° | 45° | 75° | 15° | 25° | 45° | 75° |
| C | 71.0 | 67.6 | 60.6 | 56.5 | 85.3 | 78.4 | 73.1 | 68.4 |
| O | 9.6 | 8.1 | 8.8 | 7.6 | 5.0 | 5.2 | 5.1 | 5.7 |
| N | 8.9 | 9.0 | 9.3 | 9.7 | 3.3 | 6.0 | 6.6 | 6.7 |
| S | 2.2 | 3.6 | 2.6 | 2.1 | 2.2 | 3.9 | 3.4 | 3.8 |
| Au | 8.4 | 11.7 | 18.8 | 24.2 | 4.2 | 6.6 | 11.8 | 15.4 |

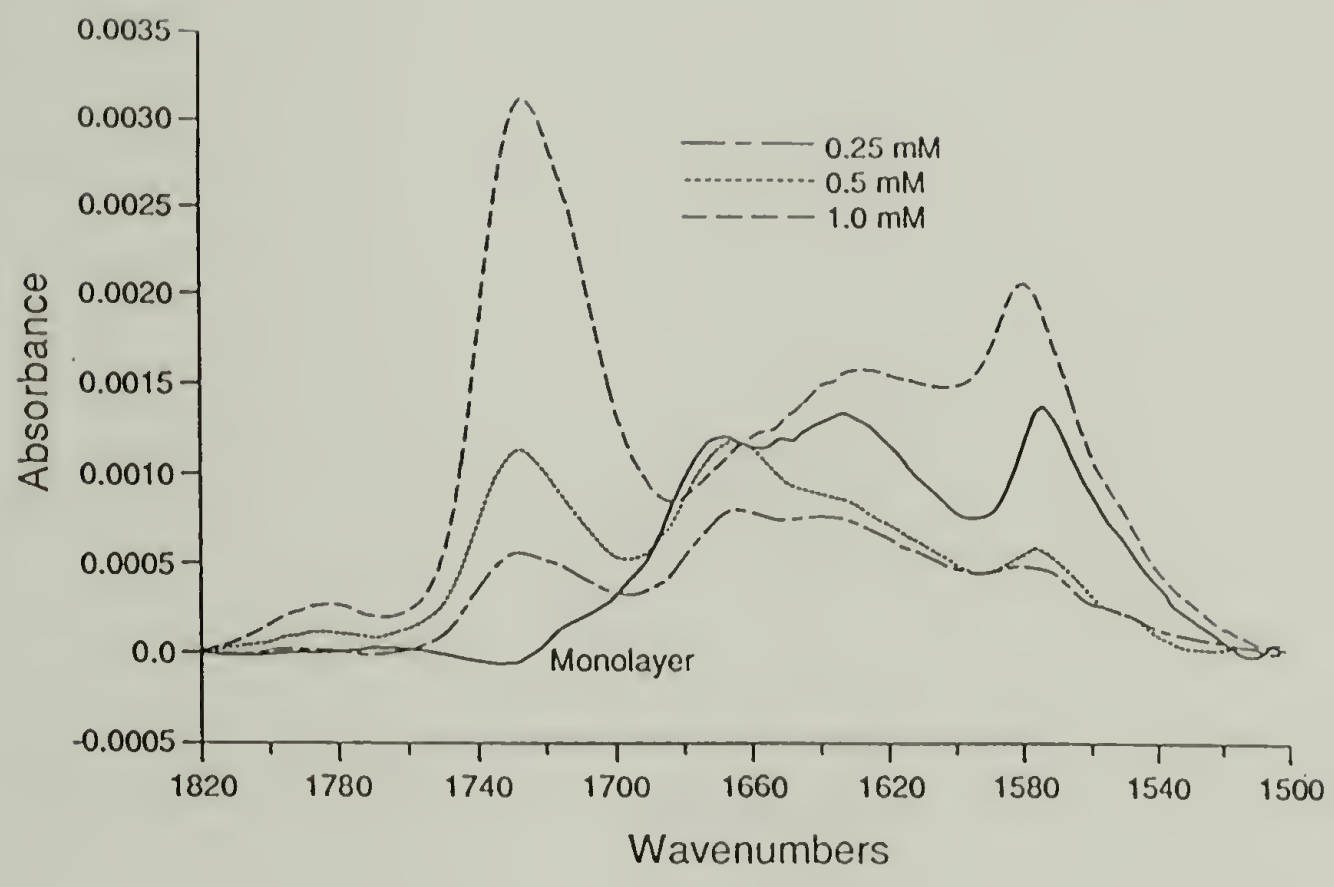


Figure 2.5 Infrared external reflection-absorption spectra with a p-polarized beam of the self-assembled monolayer on gold (**1**) and the solution self-assembled bilayers (**3**) formed from 1.0 mM, 0.5 mM and 0.25 mM solutions.

The breadth of the asymmetric carbonyl band indicates the possibility of several orientations.

## 2.4 Conclusions

The molecular recognition of components with complementary hydrogen bond donors and acceptors has created Langmuir-Blodgett and self-assembled bilayers stabilized by relatively weak hydrogen bonding interactions. This suggests that the prospects for building semi-permanent solid state structures with weak, non-covalent interactions by reversible recognition are good, with the logical extension being the incorporation of specific functionalities into guest-host partners to construct sensors and devices. Finally, beyond the specific host-guest system reported here, there is the prospect that the techniques described herein will be utilized for obtaining binding constants for host-guest systems[42].

(1) Lehn, J.-M. *Angew. Chem. Int. Ed. Engl.* **1988**, 27, 90.

(2) Ringsdorf, H.; Schlarb, B.; Venzmer, *J. Angew. Chem. Int. Ed. Engl.* **1988,** 27, 113.

(3) Lindsey, J. S. New *J. Chem.* **1991**, 15, 153.

(4) Schneider, H.-J. Angew. Chem. Int. Ed. Engl. **1991**, 30, 1417.

(5) Van Binst, G. *Design and Synthesis of Organic Molecules Based on Molecular Recognition*; Proceedings of the Solvay Conference on Chemistry; Springer-Verlag: New York, **1986**; 2-4 and references within.

(6) Chaiken, I.; Chiancone, E.; Fontana, A.; Neri, P. *Macromolecular Biorecognition Principles and Methods*; Humana Press: Clifton, New Jersey, **1987**.

(7) Alberts, B.; Bray, D.; Lewis, J.; Raff, M.; Roberts, K.; Watson, J. D. Molecular *Biology of the Cell*, Garland: New York, **1983**; 91-98.

(8) Whitesides, G. M.; Mathias, J. P.; Seto, C. T. *Science* **1991**, 254, 1312.

(9) Cram, D. *J. Angew. Chem. Int. Engl.* **1988**, 27, 1009.

(10) Whitesides, G. M.; Simanek, E. E.; Mathias, J. P.; Seto, C. T.; Chin, D. N.; Mammen, M.; Gordon, D. M. *Acc. Chem. Res.* **1995**, 28, 37.

(11) Bethel, D. *Advances in Physical Organic Chemistry*; Academic Press: New York, **1993**, 28; 45-138.

(12) Quian, P.; Matsuda, M.; Miyashita, T. *J. Am. Chem. Soc.* **1993,** 115, 5624.

(13) Tsuruta, T.; Doyama, M.; Seno, M.; Imanishi, Y. eds *New Functional Materials: Synthesis and Function Control of Biofunctionality Materials*; Elvsevier: New York, **1993**, **C**; 607-614.

(14) Ikeura, Y.; Kurihara, K.; Kunitake, T. *J . Am. Chem. Soc.* **1991**, 113, 7342.

(15) Budach, W.; Ahuja, R. C.; Mobius, D.; Schrepp, W. *Thin Solid Films* **1992**, 210/211, 434.

(16) Rojas, M. T.; Koniger, R.; Stoddart, J. F.; Kaifer, A. E. *J. Am. Chem. Soc.* **1995**, 117, 336.

(17) Samuelson, L.A.; Kaplan, D. L.; Lim, J. O.; Kamath, M.; Marx, K. A.; Tripathy, S. K. *Thin Solid Films* **1994,** 242, 55.

(18) Chailapakul, O.; Crooks, R. M. *Langmuir* **1993**, 9, 884.

(19) Spinke, M.; Liley, M.; Schmitt, F.-J.; Gruder, H.-J.; Angemaier, L.; Knoll, W. *J. Chem. Phys.* **1993**, 99, 7012.

(20) Fujita, K.; Kimura, S.; Imanishi, Y. *J. Am. Chem. Soc.* **1994**, 116, 2185.

(21) Ahlers, M.; Muller, W.; Reichert, A.; Ringsdorf, H.; Venzmer, *J. Angew. Chem. Int. Ed. Engl.* **1990**, 29, 1269.

(22) Jencks, W. P. *In Design and Synthesis of Organic Molecules Based on Molecular Recognition*; Van Binst, G., Ed.; XVIIIth Solvay Conference on Chemistry; Springer-Verlag: New York, 1983; 59.

(23) Motesharei, K.; Myles, D. C.; *J. Am.. Chem.. Soc.* **1994**, 116, 7413.

(24) Hamilton, A. D.; van Engen, D. *J. Am. Chem. Soc.* **1987**, 109, 5035

(25) Park, T. K.; Schroeder, J.; Rebek, J., Jr. *J. Am. Chem. Soc.* **1991**, 113, 5125.

(26) Feng, Q.; Park, T. K.; Rebek, J., Jr. *Science* **1992**, 256, 1179.

(27) Lehn, J.-M. *Pure & Appl.Chem.* **1994**, 66, 1961.

(28) Ahuja, R.; Caruso, P.-L.; Mobius, D.; Wolfgang, P.; Ringsdorf, H.; Wildburg, G. *Angew. Chem. Int. Ed. Engl.* **1993**, 32, 1033.

(29) Kurihara, K.; Ohto, K.; Honda, Y.; Kunitake, T. *J. Am. Chem. Soc.* **1991**, 113, 5077.

(30) Roberts, S. M., Ed.; *Biomolecular Recognition: Chemical and Biological Problems II; Second International Chemical and Biochemical Problems in Molecular Recognition*; Royal Society of Chemistry: Cambridge, 1992.

(31) Lehn, J.-M. *Angew. Chem. Int. Ed. Engl.* **1990**, 29, 1304.

(32) Ulman, A. *An Introduction to Ultrathin Organic Films: From Langmuir-Blodgett to Self-Assembly*; Academic Press, Inc.: New York, 1991.

(33) Evans, S.; Urankar, E.; Ulman, A.; Ferris, N. *J. Am. Chem. Soc.* **1991**, 113, 4121.

(34) Thompson, W. K. *J. Chem. Soc.* **1962**, 617.

(35) LaFaix, A. J.; Lebas, J. M. Spectrochim. Acta. **1970**, 26A, 1243.

(36) Greenler, R. J. *J. Chem. Phys.* **1966**, 44 , 310.

(37) Uno, T.; Machida, K. *Bull. Chem. Soc.* (Japan) **1962**, 35, 276.

(38) Stidham, H. D.; DiLella, D. P. *J. Raman Spectroscopy* **1979**, 8, 180.

(39) Takahashi, H.; Mamola, K.; Plyler, E. K. *J. Mol. Spectroscopy* **1966**, 21, 217.

(40) Porter, M. D.; Bright, T. B.; Allara, D. L.; Chidsey, C. E. D. *J. Am. Chem. Soc.* **1987**, 109, 3559.

(41) Kennard, O.; Hunter, W. *Angew. Chem. Int. Ed. Engl.* **1991**, 30, 1254.

(42) We thank one of the referees for suggesting this possibility.

# CHAPTER 3

## PEPTIDE-DERIVED SELF-ASSEMBLED MONOLAYERS: ADSORPTION OF N-STEAROYL L-CYSTEINE METHYL ESTER ON GOLD

### 3.1 Abstract

The work reported herein concerns the assembly of N-stearoyl L-cysteine methyl ester ($CH_3(CH_2)_{16}COCysOMe$, **1**) on the surface of gold. This compound serves as a simple model of a related polypeptide, which has been designed to adopt a β-sheet architecture on metallic and oxide surfaces. We describe the preparation of monolayers of **1**, and characterization of these layers via ellipsometry, vibrational spectroscopy and x-ray photoelectron spectroscopy. The results are most consistent with a disordered array of the alkyl chains, in which close packing is frustrated by a mismatch in the cross-sectional areas of the cysteinyl ester headgroup and the stearoyl chains of the thiol. Despite the disorder, the alkyl chains form a hydrophobic surface layer, with an advancing contact angle for water comparable to that observed for octadecanethiol on gold.

### 3.2 Introduction

We have been exploring the synthesis and assembly of genetically engineered artificial proteins, a new class of macromolecular materials characterized by uniformity of size and molecular structure[1]. Through a process of *de novo* protein design and biological synthesis, we have prepared a family of such materials[2-5], and we have begun to investigate their assembly into predetermined crystalline arrays and liquid

begun to investigate their assembly into predetermined crystalline arrays and liquid crystal phases. Much of the eventual utility of genetically engineered polymers will be based on their assembly at surfaces and interfaces, and on our capacity to exploit the resulting assemblies as sensors, catalysts and biomaterials. A critical issue in such developments will be the identification of strategies for controlling not only molecular architecture, but supramolecular architecture as well, such that structures can be engineered at length scales ranging from molecular to macroscopic.

Consider, for example, the polymeric surface assembly represented in schematic form in Figure 3.1. In this hypothetical structure the metal surface directs the orientation of the adsorbed polymer chain through strong, favorable interactions with the periodically spaced functional groups (Y) of the chain. Lateral hydrogen bonds would then be expected to provide a driving force for the polymer to fold into a regular lamellar[1], and to stabilize the resulting monolayer. Tam-Chang et al.[6] have demonstrated enhanced stability for short chain alkanethiol monolayers containing amide bonds; extension of the alkyl chain (e.g., to $C_{12}$) masks the enhanced stability as assessed by the rate of exchange of hexadecane thiol[6]. Novel interfaces can then be engineered further through elaboration of the "outer surface" functionality (X).

The structures of such monolayers will be governed by interactions of the side chain functionality with the substrate, by inter- and intramolecular hydrogen bonding interactions, and by chain connectivity. In order to simplify the problem, we have begun by examining the assembly of a model compound, N-stearoyl-L-cysteine methyl ester ($C_{17}H_{35}COCysOCH_3$, **1**) on gold[7]. Studies of **1** enable us to probe the cysteine-substrate interaction without the complications that arise from hydrogen bonding or long-chain effects. The presence of the $C_{18}$ chain facilitates characterization of these monolayers, through their analogy to similar assemblies prepared from alkanethiols[8].

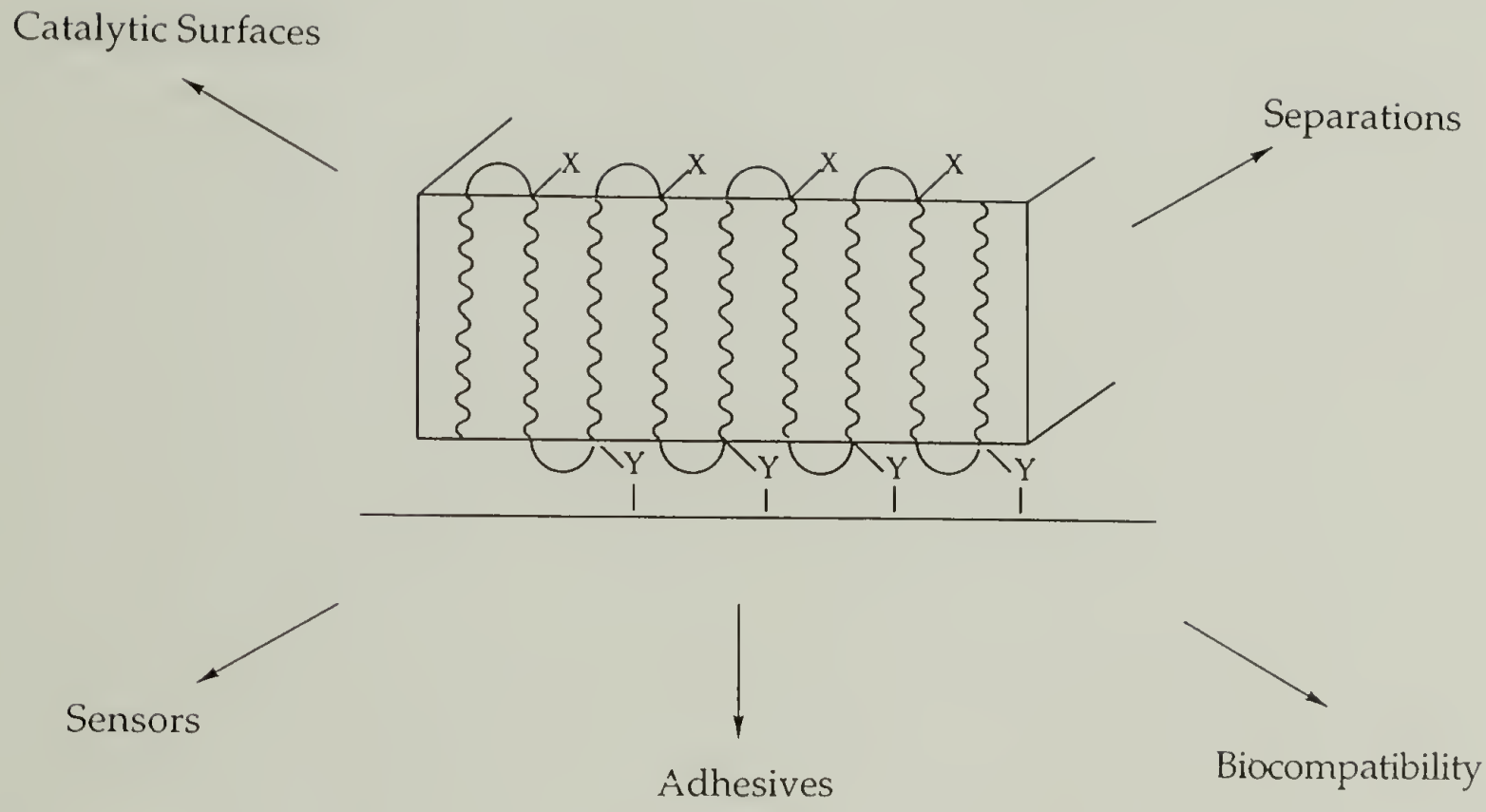


Figure 3.1 Engineered interface constructed via self-assembly of periodic polypeptides on metallic and oxide surfaces.

## 3.3 Experimental Section

### 3.3.1 Materials

Methylene chloride and methanol were dried by distillation from $CaH_2$. Double distilled water and ethanol were filtered (4 μm) before use. All other chemicals were purchased from Aldrich Chemical Company, Bachem and Advanced Chemtech and used without further purification.

### 3.3.2 Methods

TLC was effected with silica gel 60 $F_{254}$ (Merck) on precoated aluminum plates with elution by $CHCl_3/CH_3OH/HOAc$ (v/v, 9/1/0.1), spots being visualized by means of a universal UV lamp Model 51402 operating at 254 nm, iodine, the ninhydrin test, or the $Cl_2$/toluidine test. Flash column chromatography was performed with the use of silica gel 60 (Merck mesh size 230-400).

$^1H$ NMR spectra were recorded on a Bruker AC-200 (200 MHz $^1H$) spectrometer using deuterated chloroform as solvent. Melting point measurements were made on a Fisher-Johns melting point apparatus and are uncorrected. Infrared spectra were recorded on a Perkin Elmer 1600 Spectrometer.

### 3.3.3 Synthesis

**Fmoc-Cys(Acm)-OMe.** To a stirred suspension of Fmoc-S-(Acm)-L-cysteine (4.73 g, 11.4 mmol) in dry methylene chloride (65 mL) was added pyridine (0.92 mL, 11.4 mmol) under nitrogen. The mixture was cooled to -20 to -10° C before cyanuric acid (2.0 mL, 22.8 mmol) was added. A precipitate formed within the first 30 min.

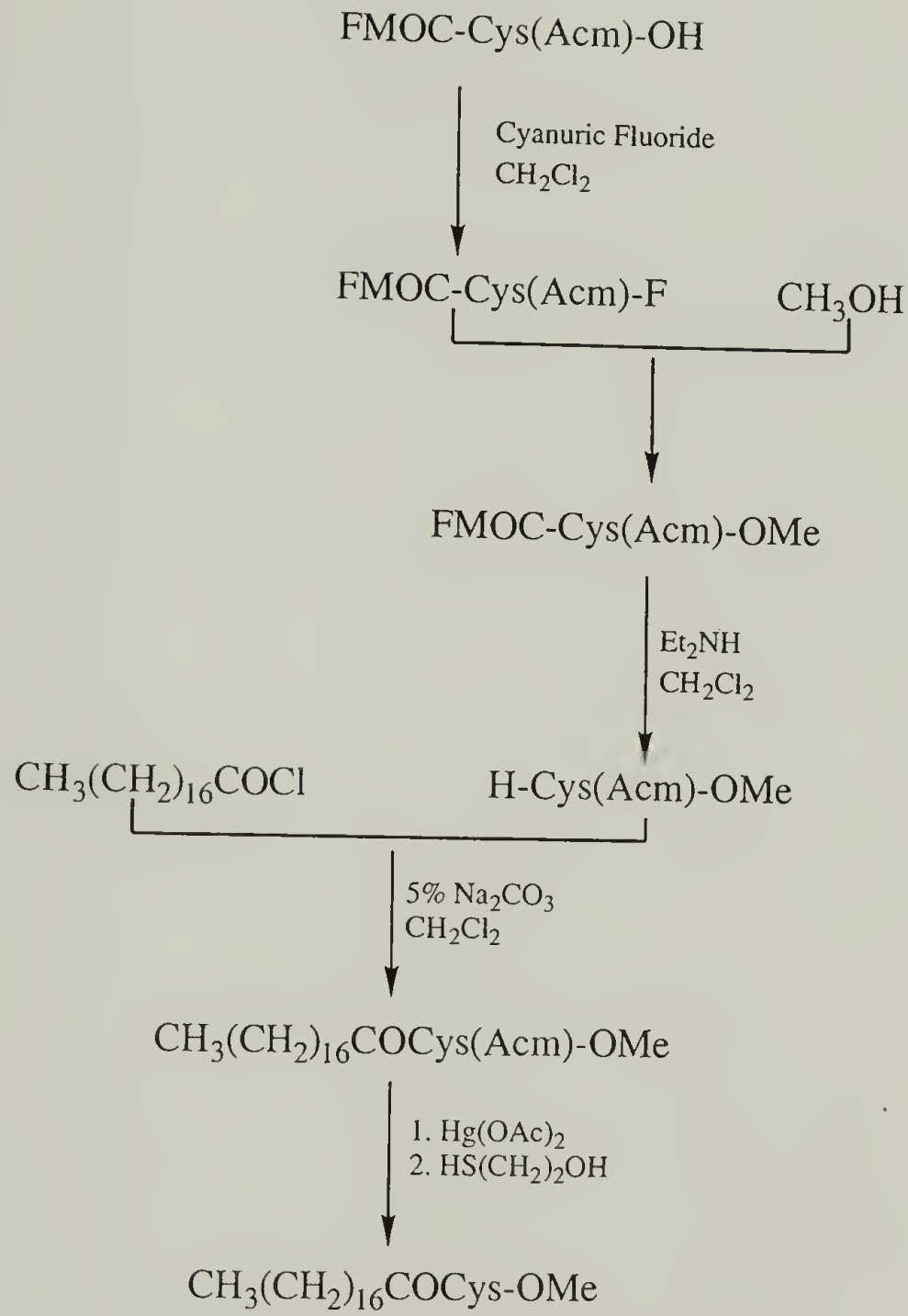


Scheme 3.1 Synthesis of Stearoyl -L-cysteine methyl ester.

After 1.5 hr a sample of the reaction mixture was quenched in dry methanol and showed methyl ester, but no starting acid by TLC analysis. After 4 hr dry methanol (125 mL) was added. The temperature was maintained at -10° C for 1 hr, pyridine (1 mL) was added and the reaction temperature was slowly increased to ambient overnight. The solvents were evaporated under reduced pressure and the solid partitioned between methylene chloride (150 mL) and water (80 mL). The aqueous solution was extracted with methylene chloride (20 mL) and the combined methylene chloride fractions were extracted with 5 % HCl (2 x 20 mL), 5 % $NaHCO_3$, and $H_2O$, and dried over $MgSO_4$. Evaporation of the solvent on a rotary evaporator gave a white solid which was recrystallized from methanol/water to give 4.67 g (95.7 %) of the ester. TLC analysis showed one spot at Rf=0.53, mp 152-153 °C. $^1H$ NMR ($CDCl_3$) δ 2.0 (s, 3H, $COCH_3$), 3.0 (q, 2H, $CHCH_2S$), 3.8 (s, 3H, $COOCH_3$), 4.1–4.5 (s, 2H, $SCH_2N$, 3H, $CHCH_2OCO$), 4.6 (t, 1H, CHCO), 6.0 (d, 1H, NHCH), 6.5 (s, 1H, NHCO), 7.2-7.9 (m, 8H, aryl). Anal. Calcd for $C_{22}H_{24}N_2O_4S$: C, 61.66; H, 5.65; N, 6.54; S, 7.48. Found: C, 61.69; H, 5.62; N, 6.32; S, 7.60.

**$H_{35}C_{17}$COCys(Acm)$OCH_3$** Fmoc-Cys(Acm)-$OCH_3$ (0.754 g, 1.76 mmol) was dissolved in a solution of 18 mL diethyl amine and methylene chloride (1/9). After 4 hr the solvent was removed by evaporation under reduced pressure. Three times the residue was triturated with hexane followed by evaporation of the solvent. The solid was dried further on a vacuum pump. To a solution of H-Cys(Acm)-OMe in 20 mL of dry methylene chloride was added dropwise stearoyl chloride (0.587 g, 1.94 mmol) in 20 mL of dry methylene chloride followed by pyridine (142 mL). The reaction was stirred overnight at room temperature. The methylene chloride was extracted with 20 mL of water. The water was extracted with methylene chloride (20 mL). The combined methylene chloride fractions were extracted with 10 % HCl (3 x 5 mL), 5 % $Na_2CO_3$ (2 x 5 mL), and saturated NaCl (1 x 5 mL), dried over $MgSO_4$ and evaporated

on a rotary evaporator. The solid was dissolved in chloroform and the solution was evaporated onto silica gel and loaded on top of a silica gel column. The solid was purified by flash chromatography with ethyl acetate/hexane 95/5 (v/v) as eluent. The fractions containing the amino acid ester were collected, dried over magnesium sulfate and evaporated to give 0.729 g (87.7 %) of $H_{35}C_{17}COCys(Acm)OCH_3$ as a white solid. The solid was recrystallized from methanol. TLC analysis showed one spot at $R_f$=0.55, mp 121.5-122.0 °C. $^1H$ NMR ($CDCl_3$) δ 0.9 (t, 3H, $CH_3$), 1.3 (s, 30H, $CH_2$), 2.1 (s, 3H, $COCH_3$), 2.3 (t, 2H, $CH_2CO$), 3.0 (m, 2H, $CHCH_2S$), 3.8 (s, 3H, $COOCH_3$), 4.4 (m, 2H, $CH_2N$), 4.8 (m, 1H, CHCO), 6.7 (d, 1H, NHCH), 6.9 (t, 1H, NHCO) Anal. Calcd for $C_{25}H_{48}N_2O_4S$: C, 63.52; H, 10.23; N, 5.97; S, 6.78. Found: C, 63.46; H, 10.33; N, 5.90; S, 6.79.

**$H_{35}C_{17}COCysOCH_3$** To a stirred suspension of $H_{35}C_{17}COCys(Acm)OCH_3$ (0.242 g, 0.512 mmol) in 50 % aqueous acetic acid (10 mL) was added mercuric acetate (0.163 g, 0.512 mmol). The mixture was stirred for 3 hr at 40° C. The reaction was complete as determined by TLC analysis. β-Mercaptoethanol (2.2 mL) was added to the mixture and stirred for 3.5 hr. The aqueous solution was filtered and washed with water. The solid was dissolved in chloroform and dried over $MgSO_4$. Evaporation of the solvent gave 0.188 g of white solid. The solid was dissolved in chloroform and the solution was evaporated under nitrogen onto silica gel and loaded on top of a silica gel column. The solid was purified by flash chromatography under nitrogen with ethyl acetate/hexane 60/40 (v/v) as eluent. The fractions containing the amino acid ester were collected, dried over magnesium sulfate and evaporated to give 0.112 g (55 %) of **1** as a white solid. The solid was recrystallized from methanol under nitrogen. TLC analysis showed one spot at $R_f$= 0.53 with elution by ethyl acetate/hexane (v/v, 50/50), mp 85.5-86.5 °C (lit[9]. mp, 85.5-87.0 °C). $^1H$ NMR

($CDCl_3$) δ 0.9 (t, 3H, $CH_3$), 1.3 (s, 30H, $CH_2$), 2.3 (t, 2H, $CH_2CO$), 3.1 (q, 2H, $CH_2S$), 3.8 (s, 3H, $OCH_3$), 4.9 (m, 1H, CH), 6.4 (d, 1H, NH).

### 3.3.4 Sample Preparation

#### 3.3.4.1 Substrate

Silicon wafers were etched in 10/1 $NH_4F$/HF solution for 1 min and cleaned for 15 min in methanolic choline solution (Summa), rinsed with filtered water and dried under a stream of nitrogen. An oxide surface was grown thermally at 1100° in an oxygen atmosphere. The substrate was primed with 100 Å of titanium in a CHA Industries SE600 electron beam vacuum deposition chamber at a rate of 5-10 Å/s, followed by 2000 Å of gold (99.99%), deposited at the same rate. This treatment produces a textured gold 111 surface[10].

#### 3.3.4.2 Monolayers

Monolayers of **1** were formed by immersing the gold substrate (prepared within 1.5 hr) into a 5 μM ethanolic solution at 44-47 °C overnight. The formation conditions for the octadecanethiol control monolayer were 1 μM and 51-56 °C. Samples were removed from solution, washed with ethanol, dried with nitrogen and dried further under vacuum overnight.

### 3.3.5 Thin Film Characterization

Four monolayers were formed and characterized for this study. Monolayer thickness was measured using a Rudolf Auto-El$^R$ II null ellipsometer equipped with a

helium-neon laser (632.8 nm) assuming a refractive index of 1.5 for the monolayer. A minimum of 6 spots were measured on each sample. Advancing water contact angle measurements were done using a Rame-Hart goniometer. Six drops were measured on one sample. X-ray photoelectron spectra (XPS) were acquired with a Perkin-Elmer 5100 instrument; Mg was used as the X-ray source. Three samples were analyzed (one spot per sample). Data were collected at 15° and 75° take-off angles (TOA). Reflectance infrared spectra were acquired on a Perkin-Elmer 2000 FTIR spectrometer equipped with a narrow-band mercury cadmium telluride (MCT) detector. The p-polarized radiation was incident on the sample at 80° using an external reflection cell (Graesby Specac). The spectra were obtained by coaddition of 2048 scans at 2 $cm^{-1}$ resolution. The spectra of three monolayers were analyzed and are essentially identical. Normal incidence transmission spectra of KBr pellets of the bulk material were acquired on a Perkin Elmer 1600 instrument.

## 3.4 Results and Discussion

### 3.4.1 Monolayer Formation

Hydrophobically terminated amino acid ester monolayers were formed by immersing gold substrates into ethanolic solutions of **1.** Films were assembled at slightly elevated temperatures (44-47°C) and from dilute solutions. Film thickness for the monolayer of **1** assembled on Au (111) was 17±2 Å, as measured by ellipsometry; this is somewhat less than the ~28 Å thickness anticipated for an analogous $C_{21}$ alkanethiol monolayer on gold[8]. We attribute the reduction in film thickness to the size of the cysteine methyl ester "headgroup" of **1**. It appears that formation of a densely packed monolayer is prohibited by the steric requirements of the amino acid ester, which are greater, in terms of cross-section, than those of the acyl chain. Examination of a set of compact headgroup conformers revealed none of projected cross-section less

than 1.5 fold larger than that of the alkane. It has been shown that the introduction of the amide functionality alone does not prevent the formation of ordered monolayers from fluorinated thiols[11], though the larger cross-section of fluoroalkanes (5.6 Å interchain spacing) relative to hydrocarbon chains (4.5 Å interchain distance)[12] makes direct comparison of these systems difficult. Whitesides and coworkers have proposed that N-dodecyl-2-mercaptoacetamide **2** forms monolayers on gold in which the "organization of the hydrocarbon chain is unlike that found in an n-alkanethiolate SAM", and they attribute this to a distortion of the alkyl chain lattice due to lateral hydrogen bonding interactions[6]. Use of our techniques with simple long-chain alkanethiols affords well ordered films[10,13]; a thickness of 21±2 Å was determined for a monolayer prepared by chemisorption of octadecanethiol (**3**) on gold as a control[8].

$H_{25}C_{12}NHCOCH_2SH$ **2**

Advancing water contact angles were measured to determine the wetting properties of these films. The advancing contact angles of the octadecanethiol (**3**) control ($\theta_a(H_2O)$=109±4°) and the monolayer film of **1** ($\theta_a(H_2O)$=109±1°) were identical, indicating that the interface is hydrophobic despite the disorder of the acyl chains (*vide infra*)[8,14].

### 3.4.2 Angle Resolved X-ray Photoelectron Spectroscopy

The concentration of each element in the monolayer as a function of analysis depth is given in Table 1.1 along with the relative atomic concentrations for compounds **1** and **3**. The angle resolved study confirms the expected inhomogeneity along the surface normal for both monolayers, with an increase in sulfur concentration at the larger detector angle. In Figure 3.2 a high resolution scan of the carbon 1s region demonstrates the expected polymethylene character of the octadecanethiol[8,14]. In the N-stearoyl L-cysteine film a shoulder appears at higher binding energy, representing the carbon atoms of the amino acid ester[16]. Deconvolution of the carbon 1s peak (Figure 3.3) shows the expected increase in the relative intensity of the headgroup signals with increasing take-off angle.

Table 3.1 XPS Elemental Composition.

| Sample | | Atomic Concentrations C | O | N | S |
|---|---|---|---|---|---|
| $CH_3(CH_2)_{16}COCys\text{-}OCH_3$ 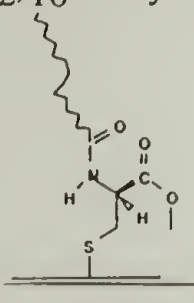 | expected[a] | 81.5 | 11.1 | 3.7 | 3.7 |
| | observed | | | | |
| | 15° TOA | 83.2 | 12.4 | 2.1 | 2.3 |
| | 75° TOA | 82.9 | 10.5 | 3.0 | 3.7 |
| $CH_3(CH_2)_{17}SH$  | expected[b] | 94.7 | | | 5.3 |
| | observed | | | | |
| | 15° TOA | 94.9 | 3.2 | 0.0 | 1.9 |
| | 75° TOA | 95.7 | 0.9 | 0.0 | 3.4 |

a. calculated elemental analysis for $C_{22}NO_3S$
b. calculated elemental analysis for $C_{18}S$

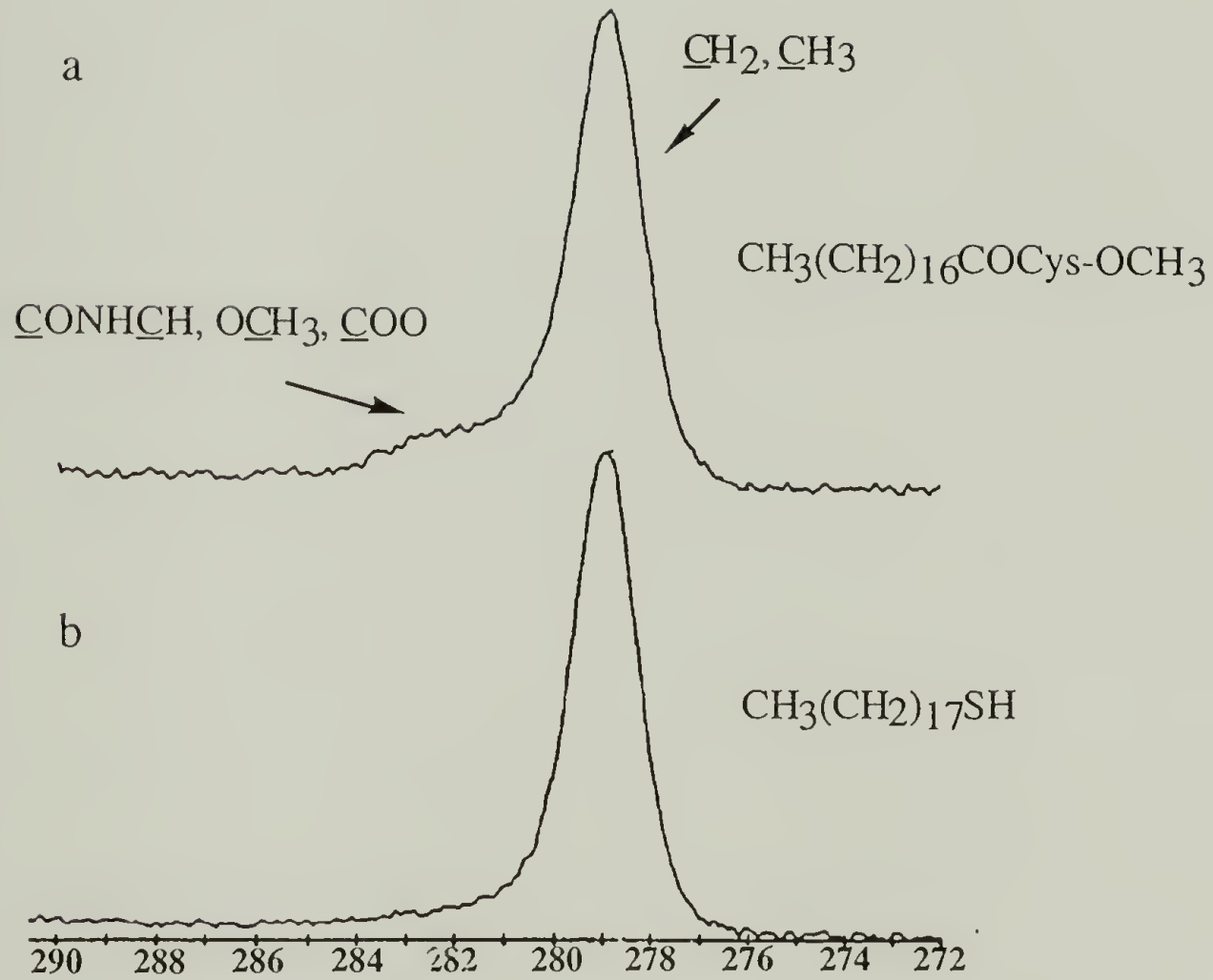


Figure 3.2 XPS $C_{1s}$ spectra of monolayers of **1** (a) and **3** (b) on gold.

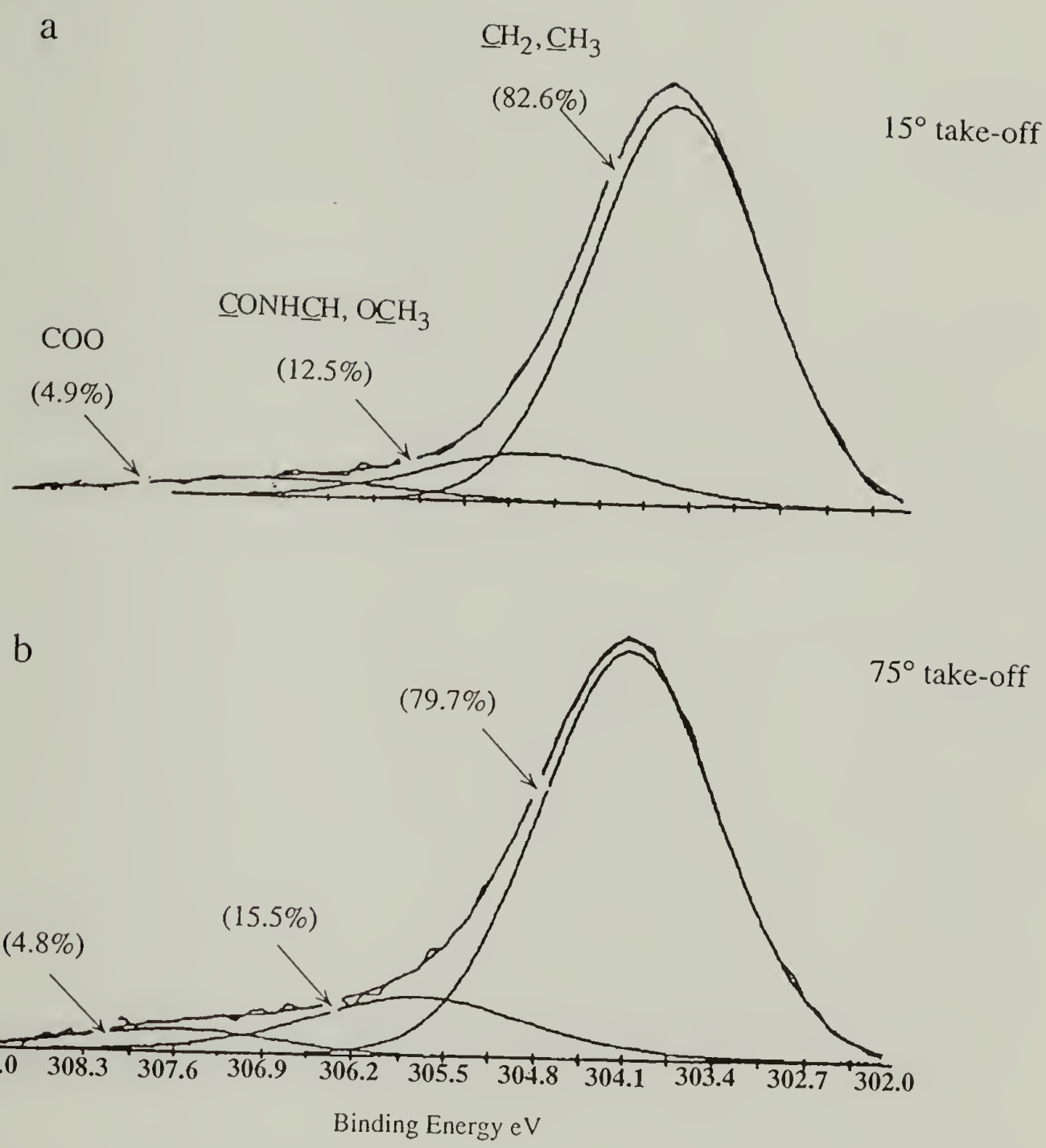


Figure 3.3 XPS $C_{1s}$ spectra of $H_{35}C_{17}COCysOCH_3$ on gold at 15° (a) and 75° (b) take-off angles.

### 3.4.3 External Reflectance Infrared Spectroscopy

The external reflectance infrared spectrum of a monolayer provides structural information about monolayer packing, orientation and conformation[17]. In the high frequency region (Figure 3.4), analysis of the alkyl chain stretching vibrations permits characterization of the packing density of the alkyl chains. The frequency (2925 $cm^{-1}$) and bandwidth (21 $cm^{-1}$) of the methylene antisymmetric vibration ($\nu_{as}$, $CH_2$) clearly indicate a liquid-like, disordered alkyl chain in the N-stearoyl L-cysteine monolayer (Figures 3.4a and 3.5), in marked contrast to the solid-like, ordered structure in the octadecanethiol monolayer (2919 $cm^{-1}$, 10 $cm^{-1}$) (Figure 4b)[18]. Tam-Chang et al.[6] report a frequency of ca. 2922 $cm^{-1}$ for the antisymmetric $CH_2$ stretch in monolayer of **2**, and suggest that "gauche conformations are heavily weighted in the structure" [6].

The orientation of methyl groups in alkanethiol monolayers has been inferred from the intensities of the asymmetric and symmetric methyl vibrations[19]. In **1**, however, the methyl stretching intensity originates from a combination of the terminal methyl of the alkyl chain and the ester methyl[15], and detailed analysis is precluded. Further evidence that the conformational order of the all-trans extended chain has been lost (Figure 3.6) is provided by the reduction in intensity of the methylene wagging and twisting vibrations near 1300 $cm^{-1}$ in the spectrum of the monolayer (cf. bands at 1343 and 1322 $cm^{-1}$ in the spectrum of crystalline **1**; Figure 3.6b)[15,20].

Information about headgroup orientation can be gained from an analysis of the intensities of the ester, amide I, and amide II vibrational bands in the infrared spectrum of the monolayer (Figure 3.6) since only the components of the transition dipoles perpendicular to the metal surface are observed in the reflectance spectrum[21]. The transition dipole for the amide I vibration is nearly along the C-O bond axis, and the weak amide I signal in the spectrum of the monolayers suggests that the carbonyl group

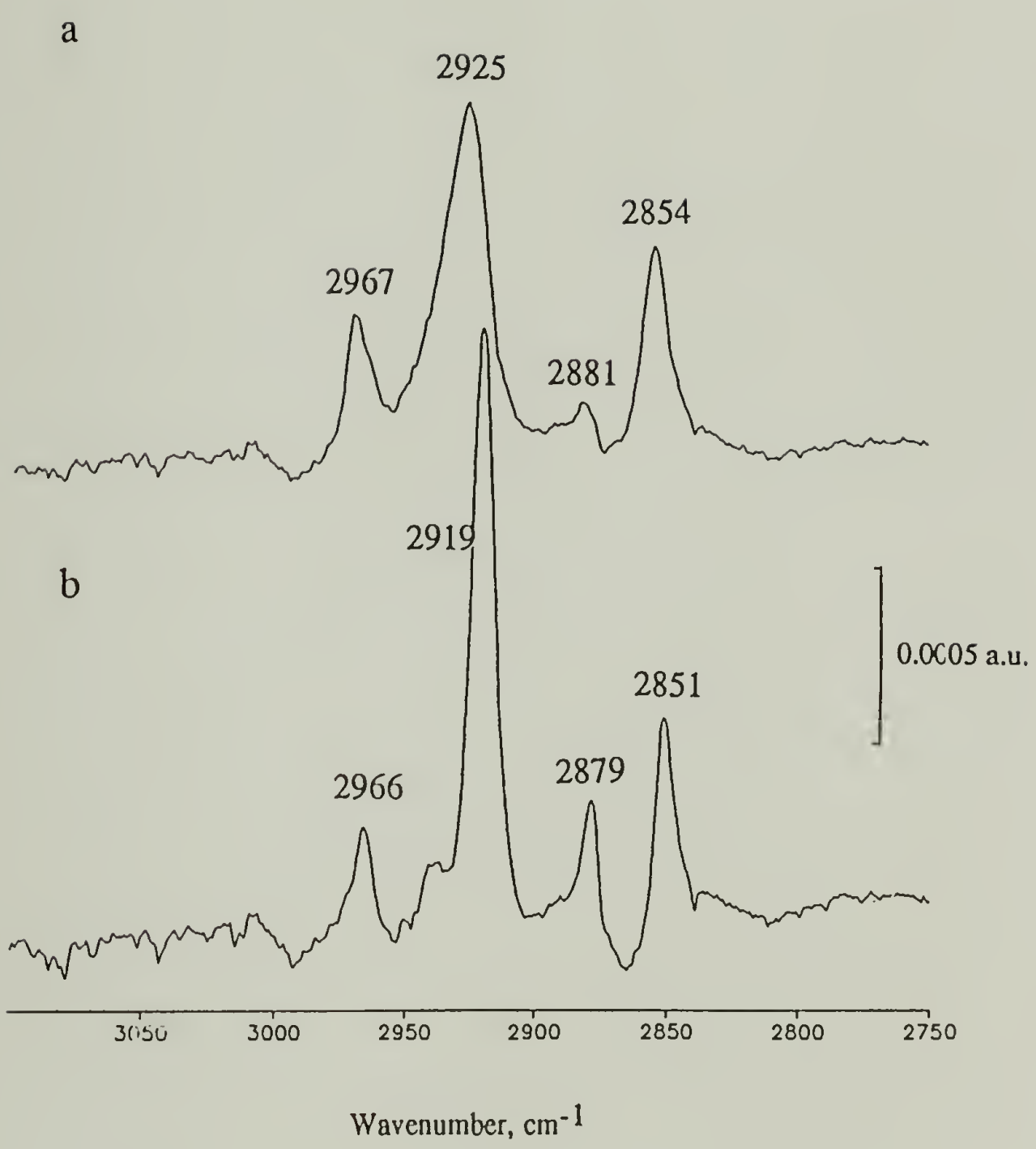


Figure 3.4 FTIR spectra (high frequency region) of monolayers of **1** (a) and **3** (b) on gold.

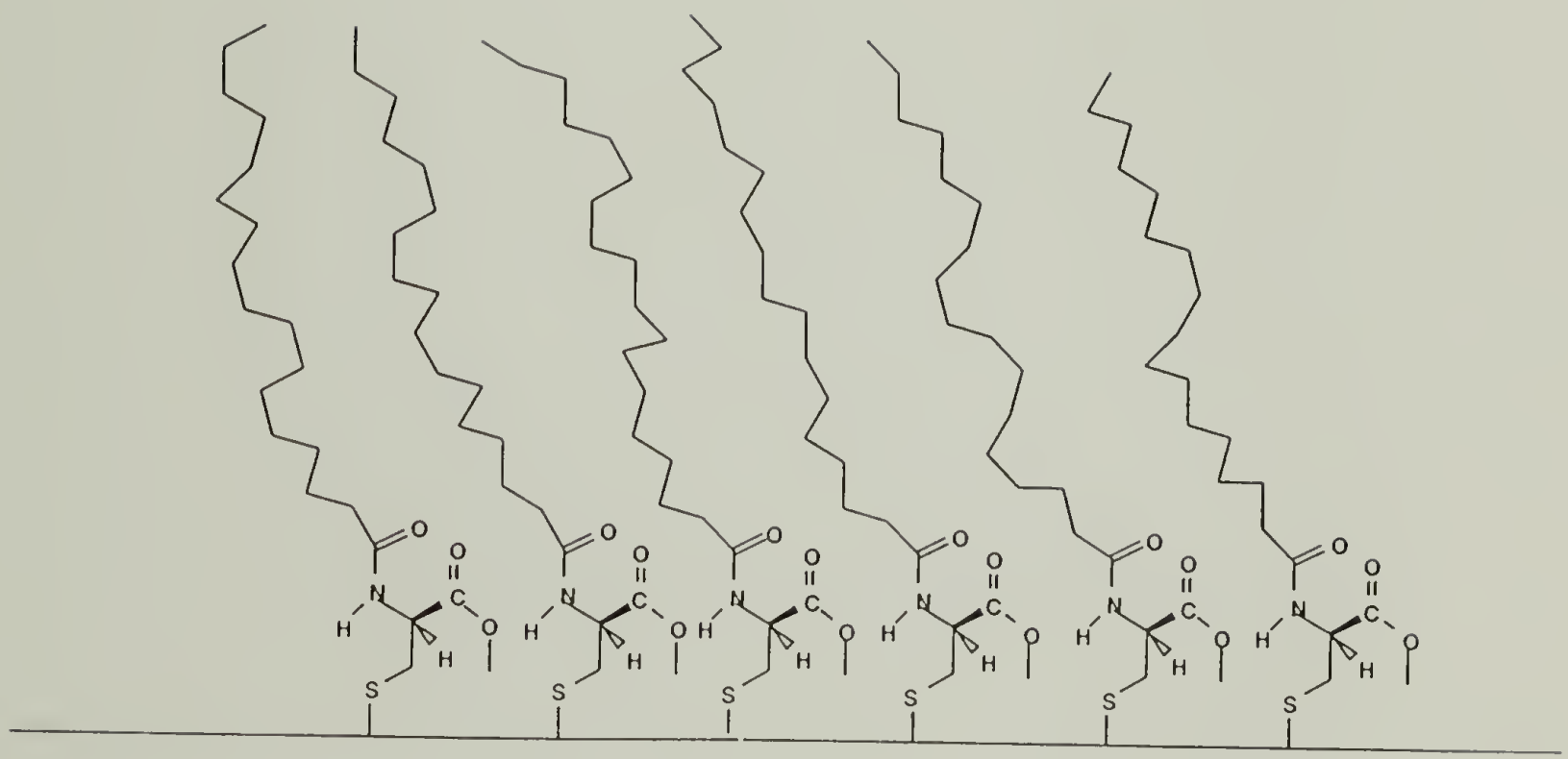

Figure 3.5 Schematic of self-assembled monolayer of H35C17CysOCH3 on gold, emphasizing the disorder of the hydrocarbon tails indicated by the external reflectance infrared spectrum.

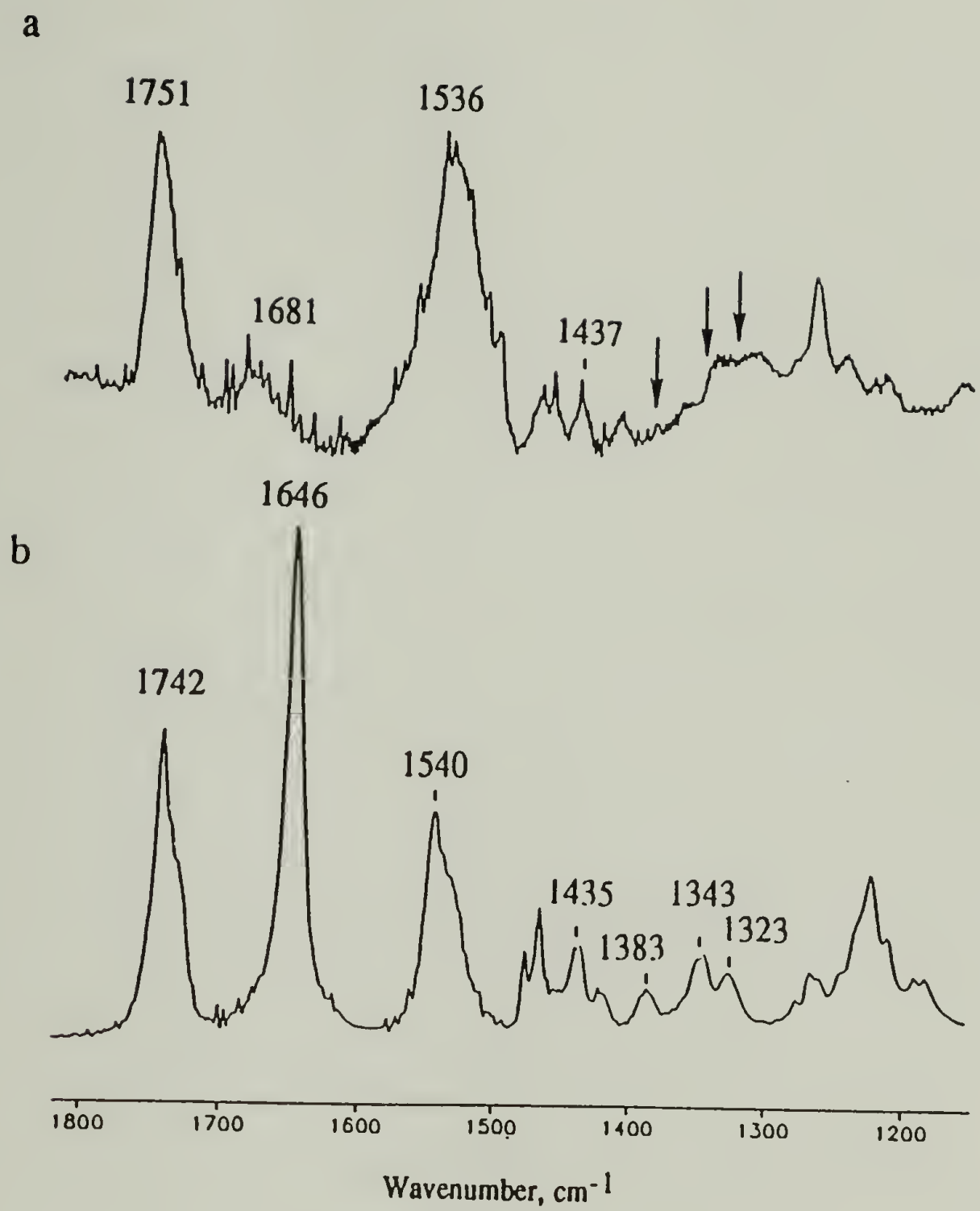


Figure 3.6 FTIR spectra (mid frequency region) of $H_{35}C_{17}COCysOCH_3$ as monolayer on gold (a) and in bulk (b). Missing vibrations in the region of 1390 to 1320 $cm^{-1}$ are marked with arrows in spectrum a (see text).

must be oriented nearly parallel to the surface. The dipole moment direction has been determined experimentally for N-methylacetamide to lie between 15° and 25° from the C-O bond direction[22]. The amide I frequency (1681 $cm^{-1}$) indicates that in the monolayer the carbonyl is not strongly hydrogen bonded. In support of this interpretation, we note that this vibration appears at 1684 $cm^{-1}$ in spectra of dilute solutions of **1** in $CCl_4$, but shifts to 1646 $cm^{-1}$ in a bulk crystalline sample where hydrogen bonding would be expected to occur.

The transition dipole of the amide II vibration lies nearly along the C-N bond[23]. The strong amide II band in the spectrum of the monolayer (Figure 3.6) suggests that the C-N bond must be oriented nearly perpendicular to the metal surface to give such a high intensity. A similar pattern of relative amide band intensities has been noted by Whitesides and and coworkers[6] interpreted in terms of lateral hydrogen-bonding interactions that align the amide C=O bond nearly parallel to the plane of the substrate.

Insight into the conformation of the ester is derived from analysis of the carbonyl stretching vibration and the symmetric methyl bending mode of the methoxy group. The high intensity of the ester carbonyl suggests a substantial component of the transition dipole normal to the metal surface. The 9 $cm^{-1}$ frequency shift (to 1751 $cm^{-1}$) from the crystalline bulk frequency (1742 $cm^{-1}$) further implies that the carbonyl is isolated and prohibited from hydrogen bonding[24]. The O-$CH_3$ bond must also lie out of the substrate plane. The symmetric methyl bending mode vibration, which is parallel to the O-C bond axis for $OCH_3$[15], appears at 1435 $cm^{-1}$ in the bulk sample and at 1437 $cm^{-1}$ in the monolayer. The band intensity (relative to that of the ester carbonyl) is reduced somewhat in the monolayer, but the diminution in intensity is far less than that observed for the amide I vibration.

Table 3.2 Infrared Spectral Mode Assignments.

| | frequency, $cm^{-1}$ | | | |
|---|---|---|---|---|
| | monolayers | | bulk and solution of **1** | |
| mode assignment | **1** | **3** | KBr | $CCl_4$ |
| N-H str | | | 3325 | 3429 |
| $CH_3$ C-H str (asym, ip), $r^-$ | 2967 | 2966 | | |
| $CH_3$ C-H str (asym, op), $r^-$ | | | 2954 | 2961 |
| $CH_3$ C-H str (sym, FR), $r^+$ | | 2938 | | |
| $CH_2$ C-H str (asym), $d^-$ | 2925 | 2919 | 2917 | 2926 |
| $CH_3$ C-H str (sym, FR), $r^+$ | 2881 | 2879 | | |
| $CH_2$ C-H str (sym), $d^+$ | 2853 | 2851 | 2850 | 2854 |
| ester C=O str | 1751 | | 1742 | 1749 |
| Amide I | 1681 | | 1646 | 1684 |
| Amide II | 1536 | | 1540 | |
| $CH_3O$ $CH_3$ bend (sym) | 1437 | | 1435 | |
| $CH_3$ $CH_3$ bend (sym) | | | 1382 | |
| $CH_2$ chain wag/twist | | | 1343 | |
| $CH_2$ chain wag/twist | | | 1322 | |

## 3.5 Conclusion

In this preliminary study we have demonstrated that N-stearoyl-L-cysteine methyl ester is capable of forming monolayers on gold. The acyl chains in the monolayer are disordered, probably as a result of the large cross-section of the amino acid ester headgroup. Future studies will explore hydrogen bonding interactions within the monolayer through an investigation of the adsorption of cysteine oligopeptides as models for polymer **1**.

(1) Krejchi, M. T.; Atkins, E. D. T.; Waddon, A. J.; Fournier, M. J.; Mason, T. L.; Tirrell, D. A. *Science* **1994**, *265*, 1427.

(2) McGrath, K. P.; Fournier, M. J.; Mason, T. L.; Tirrell, D. A. *J. Am. Chem. Soc.* **1992**, *114*, 727.

(3) Kothakota, S.; Fournier, M. J.; Mason, T. L.; Tirrell, D. A. *J. Am. Chem. Soc.* **1995**, *117*, 536.

(4) Tirrell, J. G.; Fournier, M. J.; Mason, T. L.; Tirrell, D. A. *C&EN* **1994**, *Dec. 19*, 40.

(5) Yoshikawa, E.; Fournier, M. J.; Mason, T. L.; Tirrell, D. A. *Macromolecules* **1994**, *27*, 5471.

(6) Tam-Chang, S.-W.; Biebuyck, H. A.; Whitesides, G. M.; Jeon, N.; Nuzzo, R. G. *Langmuir* **1995**, *11*, 437.

(7) Dawson, S. L.; Fournier, M. J.; Mason, T. L.; Tirrell, D. A. *Polym. Prepr.* **1994**, *35*, 413.

(8) Bain, C. D.; Troughton, E. B.; Toa, Y.-T.; Evall, J.; Whitesides, G. M.; Nuzzo, R. G. *J. Am. Chem. Soc* **1989**, *111*, 321.

(9) Zeeland, F. J.; Havinga, E. *Rec. Trav. Chim.* **1958**, *77*, 267.

(10) Dubois, L. H.; Nuzzo, R. G. *Annu. Rev. Phys. Chem.* **1992**, *43*, 437.

(11) Lenk, T. J. ;. V. M. H., C. L. Hoffmann, J. F. Rabolt, D. G. Castner, C. Erdelen, H. Rinsdorf *Langmuir* **1994**, *10*, 4610.

(12) Fenter, P.; Eisenberger, P.; Liang, K. S. *Phys. Rev. Lett.* **1993**, *70*, 2443.

(13) Ulman, A. *An Introduction to Ultrathin Films: from Langmuir-Blodgett to Self-Assembly;* Academic Press: Boston, 1991; p. 280.

(14) Dubois, L. H.; Zegarski, B. R.; Nuzzo, R. G. *J. Am. Chem. Soc.* **1990**, *112*, 570.

(15) Nuzzo, R. G.; Dubois, L. H.; Allara, D. A. *J. Am. Chem. Soc.* **1990**, *112*, 558.

(16) Uvdal, K.; Bodö, P.; Liedberg, B. *J. Colloid and Interface Sci.* **1992**, *149*, 162.

(17) Evans, S. D.; E.Goppert-Berarducci, K.; Urankar, E.; Gerenser, L. J.; Ulman, A.; Snyder, R. G. *Langmuir* **1991**, *7*, 2700.

(18) Porter, M. D.; Bright, T. B.; Allara, D.; Chidsey, C. E. D. *J. Am. Chem. Soc.* **1987**, *109*, 3559.

(19) Labinis, P. E.; Whitesides, G. M.; Allara, D. L.; Tao, Y.-T.; Parikh, A. N.; Nuzzo, R. G. *J. Am. Chem. Soc.* **1991**, *113*, 7152-7167 and references therein.

(20) Snyder, R. G.; Schachtschneider, J. H. *Spectrochim. Acta* **1963**, *19*, 8.

(21) Greenler, R. J. *J. Chem. Phys.* **1966**, *44*, 310.

(22) Bradbury, E. M.; Elliot, A. *Polymer* **1963**, *4*, 47.

(23) Krimm, S.; Bandekar, J. *Adv. Protein Chem.* **1986**, *38*, 181.

(24) Colthup, N. B. et al. *Introduction to Infrared and Raman Spectroscopy;* Academic Press: Boston, 1990; pp. 210-213.

# CHAPTER 4

# PARALLEL β -SHEET OLIGOPEPTIDE SELF-ASSEMBLED MONOLAYERS: ADSORPTION OF N-ACYL-(L-ALAGLY)3-L-CYSTEINE METHYL ESTER ON GOLD

## 4.1 Abstract

The work reported herein concerns the assembly of N-Acetyl-(L-AlaGly)3-L-cysteine methyl ester ($CH_3O(AlaGly)_3CysOCH_3$, **2**) on the surface of gold. This compound serves as a model of a related polypeptide, which has been designed to adopt a β-sheet architecture on metallic and oxide surfaces. We describe the synthesis of the oligopeptide, preparation of monolayers of **2** assembled under different solution conditions, and characterization of these layers via ellipsometry, x-ray reflectivity, vibrational spectroscopy and x-ray photoelectron spectroscopy. The oligopeptide chemisorbs to gold via the cysteine thiol and forms monolayers. The infrared data demonstrates that the oligopeptide tertiary structure in monolayer **2** is different than what is typically seen in peptide structures. The implication is that the gold (111) surface forces an uncharacteristic peptide packing.

## 4.2 Introduction

Recently, there has been a significant convergence between the fields of biology and material science. Fundamental biological processes such as molecular recognition are routinely influencing the design and engineering of materials such as sensors and devices, while concurrently, synthetic materials, specifically medical implants, are

routinely optimized for biological compatibility. Understanding how to direct assembly at surfaces and interfaces is critical for continued growth in both of these areas.

One approach to the fabrication of well ordered monolayer structures is the chemisorption of alkyl thiols and dialkyl disulfides on gold. These materials have served well as model compounds for the adsorption of proteins to surfaces[1-6] and, to a lesser extent, as models to enhance the understanding of molecular recognition[7-9]. For some applications, thin films with enhanced stability will be required. Introduction of intermolecular hydrogen bonding, bonds which are stronger than van der Waals interactions that typically hold together monolayers, is accomplished by the addition of an amide functionality into the adsorbate[10-16]. A novel approach reported by Whitesell and Chang[17] was the in situ formation of a hydrogen bonded α-helical polypeptide network supported on gold.

We have previously demonstrated through a process of de novo protein design and biological synthesis[18-20], the assembly of polypeptides into predetermined crystalline arrays[21,22], liquid crystalline phases[23], and thermally reversible hydrogel networks[24]. Of particular interest is the sequence [-(AlaGly)3CysGly(AlaGly)3GluGly-]n (**1**) which has been designed to adopt folded β-sheet structures on metallic and oxide surfaces. In artificial proteins of this kind, the pendant functionality is expected to direct the assembly of the chain on metal surfaces. This hypothetical structure, stabilized by hydrogen bond formation, is shown in Figure 4.1. The functionality (X) provides a convenient synthetic route to engineered interfaces for catalytic surfaces, separation systems, sensors, and biocompatability.

Identification of conditions for forming regular, well-ordered polypeptide structures at surfaces is crucial for the successful assembly of **1**. In order to simplify the problem, our initial efforts have focused on the self-assembly of two model

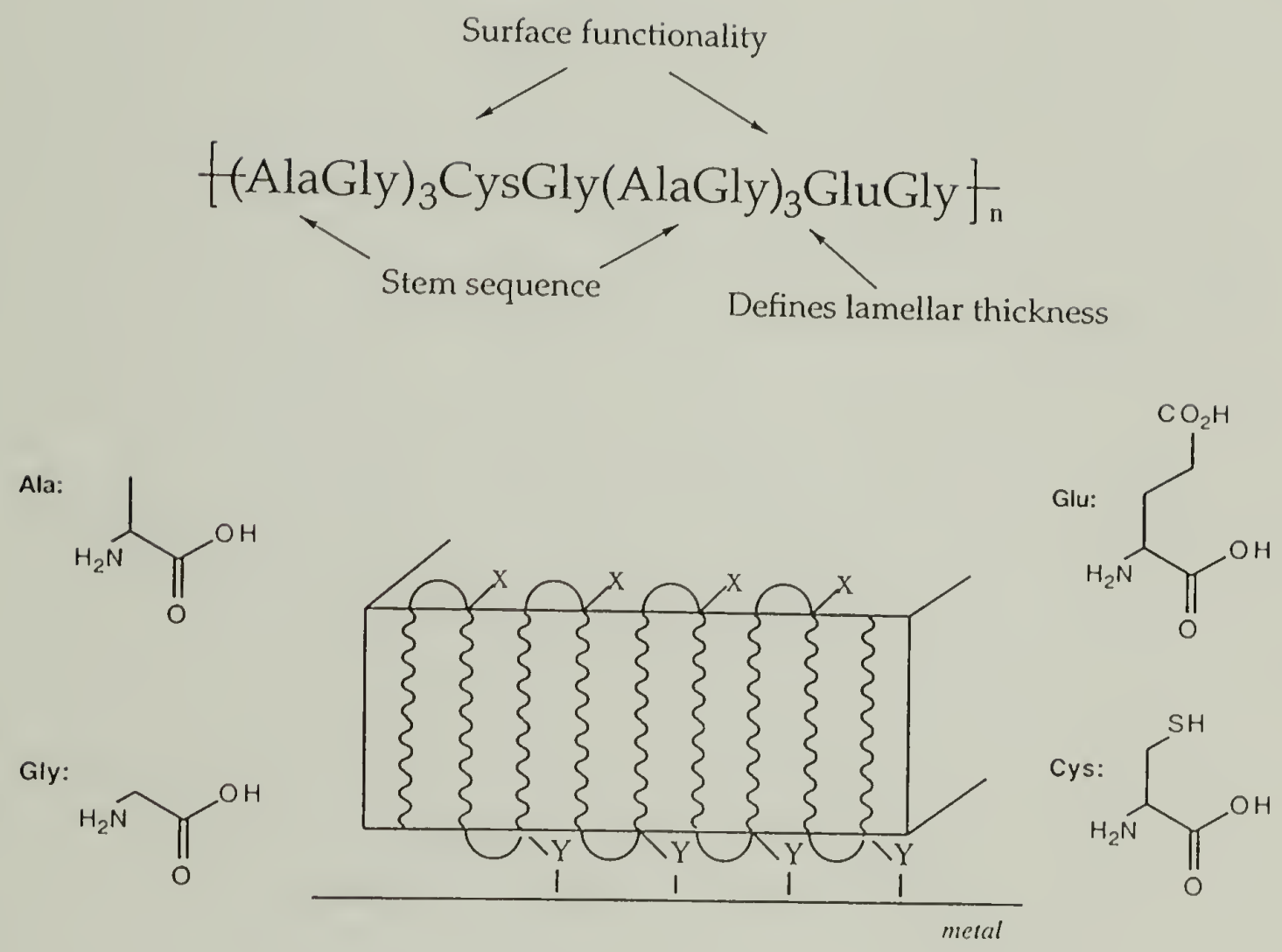


Figure 4.1 Design strategy for folded polypeptides and idealized adsorption on metal surfaces.

$$\left[(\text{AlaGly})_3\text{Cys}\text{Gly}(\text{AlaGly})_3\text{GluGly}\right]_n$$

$$CH_3CO\text{-}(\text{AlaGly})_3\text{Cys}\text{-}OCH_3$$

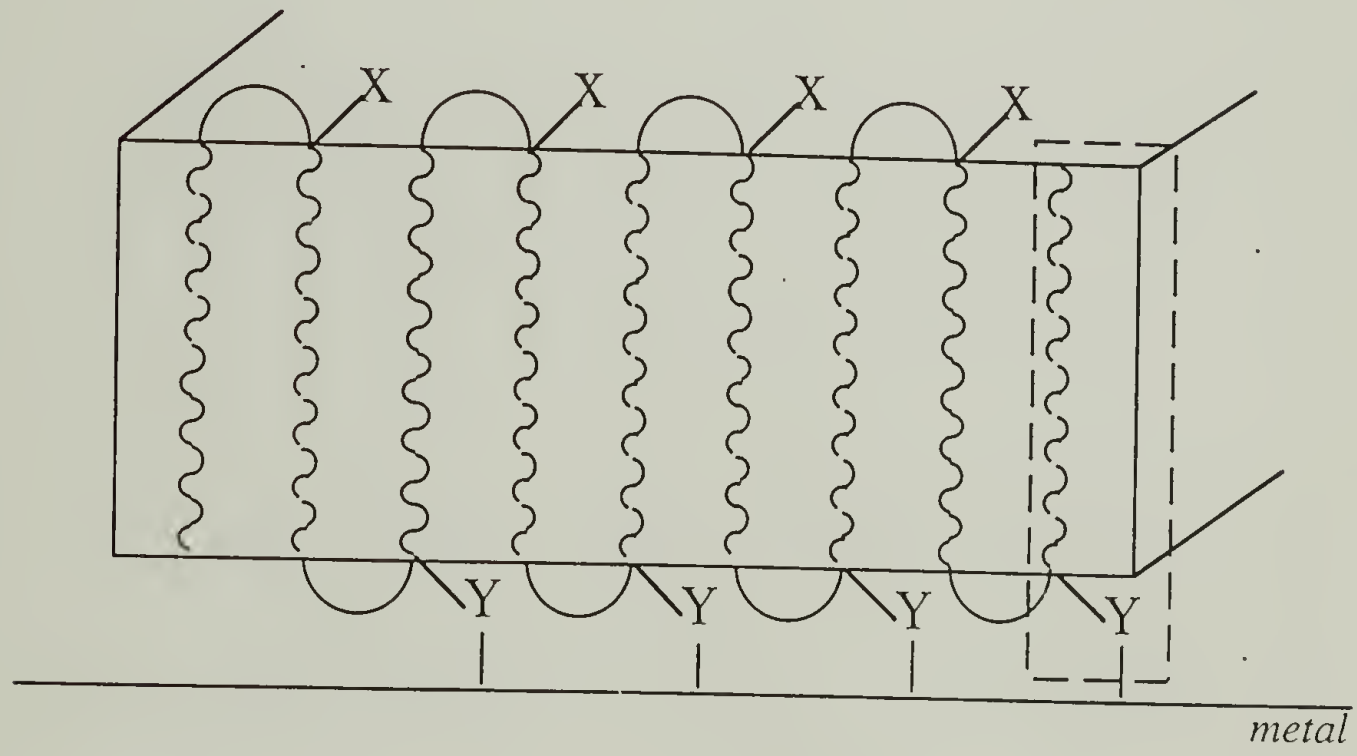


Figure 4.2 Oligopeptide depicting the polypeptide section which is modeled.

compounds[11, 12] which capture the substrate and lateral interactions, but defer complications associated with chain connectivity. The oligopeptide **2**, $CH_3O(AlaGly)_3CysOCH_3$, a strand of the β-sheet, represented in Figure 4.2, serves as a model for the polypeptide **1**, is capable of hydrogen bonding and is anticipated to form a parallel β-sheet structure when chemisorbed on gold.

## 4.3 Experimental Section

### 4.3.1 Materials

Methylene chloride and methanol were dried by distillation from $CaH_2$. Thionyl chloride was purified by distillation from linseed oil. Dimethy amine was removed from N,N-dimethyl formamide by distillation under reduced pressure, or by aspiration for 20 min or by bubbling nitrogen through the solvent for 20 min. Water was deionized and distilled. Water and ethanol were filtered (4 μm) before use and freed of oxygen by aspiration or by bubbling nitrogen or argon through the solvent for 20 min. All other chemicals were purchased from Aldrich Chemical Company, Richleieu Biotechnologies Inc., Lancaster, Bachem or Advanced Chemtech and used without further purification.

### 4.3.2 Methods

Thin layer chromatography (TLC) was effected with silica gel 60 $F_{254}$ (Merck) on precoated aluminum plates with elution by $CHCl_3/CH_3OH/HOAc$ (v/v, 9/1/0.1), spots being visualized by means of a universal UV lamp Model 51402 operating at 254 nm, iodine, the ninhydrin test, the $Cl_2$/toluidine test or by Ellman's reagent. Column

chromatography was performed with the use of silica gel 60 (Merck mesh size 230-400) and gel chromatography with Sephadex G-10 (Sigma).

$^1$H NMR spectra were recorded on Bruker AC-200 (200 MHz $^1$H), Varian XL-200 (200 MHz $^1$H), and Bruker DPX-300 (300 MHz $^1$H) spectrometers using deuterated chloroform, DMSO, and trifluoroacetic acid as solvents. Chemical shift values are based on known chemical shifts of solvent peaks as references. Melting point measurements were made on a Fisher-Johns melting point apparatus and are uncorrected. Infrared spectra were recorded on a Perkin Elmer 1600 Spectrometer.

4.3.3 Synthesis

**N-((9-Fluorenylmethyl)oxy)carbonyl-L-alanyl-chloride (3).**

N-((9-Fluorenylmethyl)oxy)carbonyl (Fmoc)-L-Alanine (11.39 g, 0.0346 mol) was suspended in dry methylene chloride (40 mL) in a three neck 500 ml round-bottom flask under nitrogen. Thionyl chloride (29 mL, 0.360 mol) was added dropwise over 20 min with concomitant formation of yellow color. The solution was heated at reflux for 1.5 h. A sample of the reaction mixture was quenched in excess dry methanol and showed methyl ester, but no starting acid by TLC analysis. Excess thionyl chloride and methylene chloride were evaporated under reduced pressure. The solid was redissolved in dry methylene chloride followed by evaporation of the solvent. This process was repeated again before the solid was dried overnight in vacuo. The solid was recrystallized with dry methylene chloride/hexane to give 10.70 g (0.0324 mol, 94 %) of **3**. TLC analysis of the methyl ester (FMOCAlaOCH$_3$) showed product at $R_f$=0.90, no starting acid and a very slight impurity at $R_f$=0.72, mp 113-114 °C ( lit.[25] 112-114 °C). $^1$H NMR ($CDCl_3$) δ 0.8 (d, 3H, $CH_3$), 4.1 (t, H, CH), 4.2 - 4.6 (d, 2H, $CH_2O$, m, 1H, NCHCO), 5.1 (d, 1H, NH), 7.0 - 7.8 (m, 8H, aryl). Anal. Calcd for

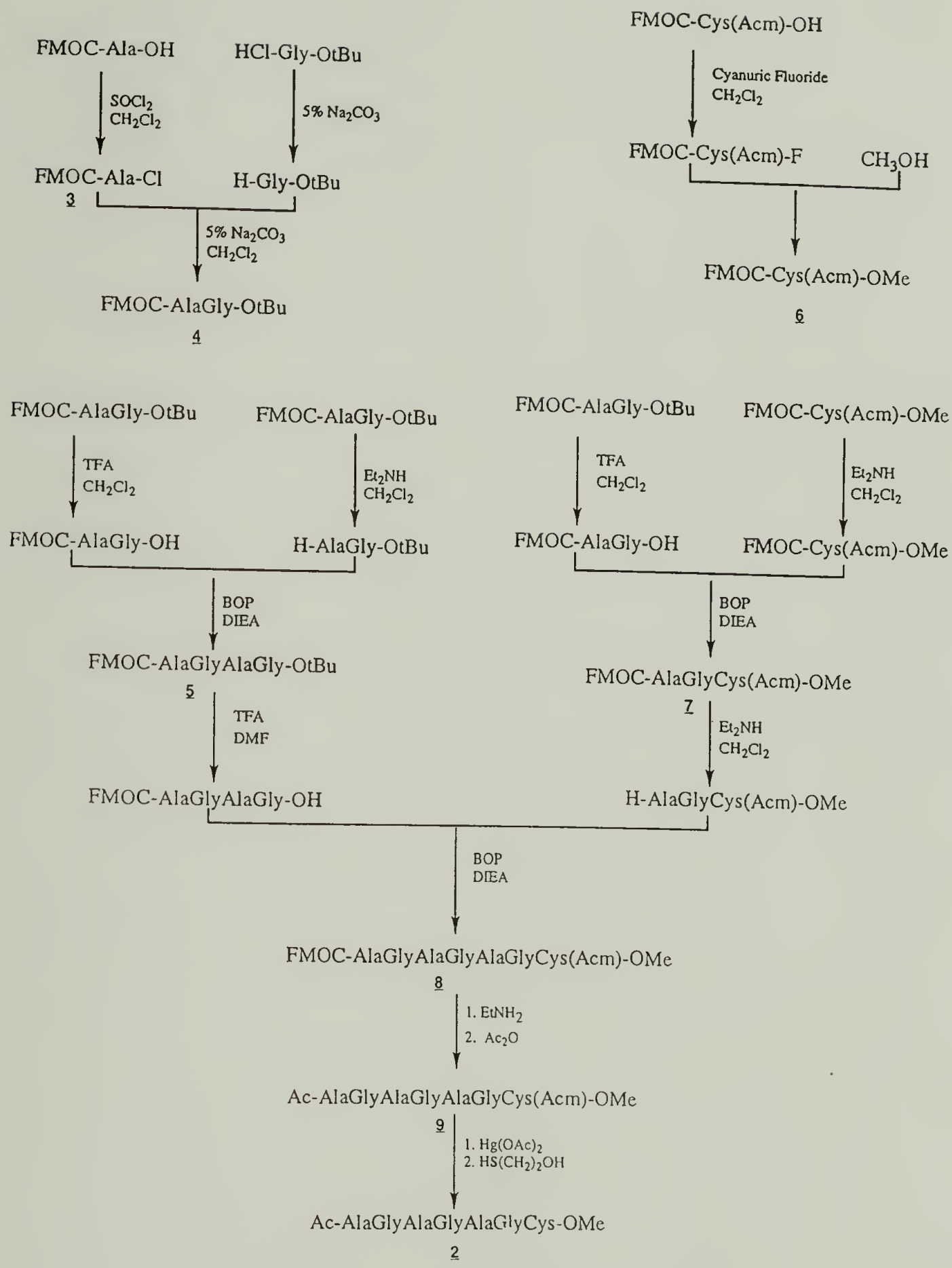


Scheme 4.1 Synthesis of N-Acetyl-L-alanylglycyl-L-alanylglycyl-L-alanylglycyl-L-cysteine methyl ester.

$C_{18}H_{16}NO_3Cl$: C, 65.55; H, 4.89; N, 4.25; Cl, 10.75. Found: C, 65.82; H, 4.92; N, 4.36; Cl, 10.97.

**N-((9-Fluorenylmethyl)oxy)carbonyl-L-alanylglycine tert-butyl ester (4).** In a 1 liter round bottom flask glycine tert-butyl ester hydrochloride (5.03 g, 30 mmol) was neutralized with 300 mL of 5 % aqueous sodium carbonate. After stirring for 5 min, 200 mL of methylene chloride was added and stirred for an additional 5 min. FMOC-L-alanyl chloride (12.0 g, 0.0364 mol) dissolved in 200 mL of dry methylene chloride was added dropwise to the two phase mixture over 20 min. The reaction was stirred for 1 h at room temperature. The layers were separated. The aqueous layer was washed with methylene chloride. N-Methyl piperazine (1.5 mL) was added to the combined methylene chloride solution and stirred for 1 min. The methylene chloride solution was washed successively with 5 % hydrochloric acid (2 x 50 mL), 5 % sodium bicarbonate (2 x 50 mL), and saturated sodium chloride (2x 50 mL) and dried over anhydrous magnesium sulfate. The solvent was evaporated under reduced pressure. The solid was purified on a silica gel column with ethyl acetate/hexane (80/20, v/v) as eluant. The solution was dried with anhydrous magnesium sulfate and the solvent was removed under reduced pressure to give 12.14 g (0.0286 mol, 95 %) of **4**. TLC analysis showed one spot at $R_f = 0.86$, mp 128.5-129.5 °C. $^1H$ NMR ($CDCl_3$) δ 1.2 (d, 3H, $CHC\underline{H}_3$), 1.4 (s, 9H, $C(CH_3)_3$), 3.8 (d, 2H, $CH_2COO$), 4.1 - 4.8 (t, 1H, $C\underline{H}CH_2O$; d, 2H, $CHC\underline{H}_2O$: m, 1H, NCHCO), 5.3 (t, 1H, $N\underline{H}CH_2$), 6.3 (d, 1H, $N\underline{H}CH$), 7.2 - 7.7 (m, 8H, aryl). Anal. Calcd for $C_{24}H_{28}N_2O_5$: C, 67.91; H, 6.65; N, 6.60. Found: C, 67.87; H, 6.72; N, 6.47.

**N-((9-Fluorenylmethyl)oxy)carbonyl-L-alanylglycyl-L-alanylglycine tert-butyl ester (5).** Compound **5** was prepared in three steps. To remove the tert-butyl group, compound **4** (12.73 g, 0.030 mol) was dissolved in 60 mL of methylene

chloride/trifluoroacetic acid (1/1, v/v) and stirred at room temperature for 4 h. Evaporation of the solvent and trifluoroacetic acid yielded a solid which was further purified by trituration with diethyl ether and coevaporation of trifluoroacetic acid with the solvent. After two iterations, no trifluoroacetic acid could be detected and the solid was dried in vacuo. The removal of the FMOC group was accomplished by stirring compound **4** (12.73 g, 0.030 mol) with 200 ml of methylene chloride containing 30 mL of diethylamine at room temperature for 4 h. The solvent and excess diethylamine were removed under reduced pressure. The solid was triturated with hexane followed by removal of the solvent as described above until no diethyl amine could be detected and then dried in vacuo. The deprotected segments, Fmoc-(AlaGly)$_2$-OH and H-(AlaGly)$_2$-OtBu, were coupled by combining the segments, each dissolved in 150 mL of N,N-dimethylformamide, in a flask followed by sequential addition of benzotriazolyloxytris(dimethylamino) phosphonium hexafluorophosphate (13.23 g, 0.030 mol) and 30 mL of diisopropylamine. After 1 h the pH of the solution was measured (with moist indicator paper) and adjusted to pH 8 with diisopropylethyl amine (DIEA). The solution was allowed to stir overnight. A white solid formed. The solvent was removed under reduced pressure and was washed with ethyl acetate, diethyl ether, 5 % citric acid, 5 % NaHCO$_3$, H$_2$O, and diethyl ether. The solid was recrystallized with N,N-dimethyl formamide/diethyl ether to give 12.7 g (0.023 mol, 77 %) of **5**. TLC analysis showed one spot at R$_f$= 0.32, mp 196-197 °C. $^1$H NMR (DMSO) δ 1.2 (d, 6H, CHC<u>H</u>$_3$), 1.4 (s, 9H, C(CH$_3$)$_3$), 3.8 (d, 4H, CH$_2$COO), 4.1 (t, 1H, C<u>H</u>CH$_2$O), 4.2 - 4.4 ( d, 2H, CHC<u>H</u>$_2$O: m, 2H, NCHCO), 7.3 - 8.0 (m, 8H, aryl), 8.2 – 8.3 (t, 1H, N<u>H</u>CH$_2$; d, 1H, N<u>H</u>CH). Anal. Calcd for C$_{29}$H$_{36}$N$_4$O$_7$: C, 63.03; H, 6.56; N, 10.14 . Found: C, 63.00; H, 6.71; N, 10.09.

**N-((9-Fluorenylmethyl)oxy)carbonyl-S-acetoamidomethyl-LCysteine methyl ester (6).** Fmoc-Cys(acm)-OMe was available from previous studies[12].

**N-((9-Fluorenylmethyl)oxy)carbonyl-L-alanylglycyl-S-acetoamidomethyl-L-cysteine methyl ester (7).** In a round bottom flask FMOC-AlaGly-OtBu (1.64 g, 3.86 mmol) was deblocked with 60 ml of trifluoroacetic acid/methylene chloride (1/1, v/v). The solution was stirred at room temperature for 4.5 h. The solution was evaporated under reduced pressure. Three times the resultant solid was triturated with diethyl ether and each time the solvent was evaporated under reduced pressure. The solid was further dried in vacuo until no residual TFA could be detected. FMOC-Cys(Acm)-OMe (1.65 g, 3.86 mmol) was deblocked with 4.4 ml of diethyl amine in 10 ml of methylene chloride/acetonitrile (4/1, v/v). Deblocking was complete after 4 h. Completeness of the reaction was checked by TLC. The solution was concentrated under reduced pressure and the resultant solid was triturated with hexane and dried as described above. Each of the deblocked peptides was dissolved in 40 ml of dimethyl formamide/acetonitrile (10/30, v/v) and combined. To this solution was added benzotriazolyloxytris(dimethylamino) phosphonium hexafluorophosphate (1.706 g, 3.86 mmol) followed by 4.4 ml of diisopropylethylamine. After 1 hr the pH was adjusted to 8 with diisopropylamine and the reaction was stirred overnight. The solvent was removed under reduced pressure and the resultant residue was dissolved in ethyl acetate and extracted with 5% citric acid (2 x 20 ml), water (10 ml), 5% $NaHCO_3$ (2 x 20 ml), and water (10 ml ) and dried with magnesium sulfate. The solid was further purified by chromatography on a silica gel column with ethyl acetate/hexane (80/20, v/v) as eluant. From the fractions containing pure 7, 1.48 g (2.67 mol, 69 %) of the tripeptide was obtained, mp 182.5-183 °C. $^1$H NMR (DMSO) d 1.2 (d, 3H, CHC$\underline{H}_3$), 1.8 (s, 3H, $CH_3$), 2.8 (q, 2H, CHC$\underline{H}_2$S), 3.6 (s, 3H, $COOCH_3$), 3.8 (d, 2H, $CH_2COO$), 4.0 (t, 1H, C$\underline{H}CH_2CO$), 4.1-4.5 (d, 2H, CHO; m, 1H, $NCH(CH_3)CO$, s, 2H, $SCH_2N$), 4.5 ($NCH(CH_2)CO$), 7.3-7.9 (m, 8H, aryl), 8.1-8.5 (m, 1H, N$\underline{H}$CH($CH_2$), 1H, N$\underline{H}$CH($CH_3$), 1H, N$\underline{H}$CH($CH_2$S, 1H, $NHCOCH_3$). Anal. Calcd for $C_{27}H_{32}N_4O_7S$: C, 58.30; H, 5.79; N, 10.07; S, 5.76. Found: C, 58.40; H, 5.70; N, 9.86; S, 5.56.

**N-((9-Fluorenylmethyl)oxy)carbonyl-L-alanylglycyl-L-alanylglycyl-L-alanylglycyl-S-acetoamidomethyl-L-cysteine methyl ester (8).** Compound **5** (1.38 g, 2.5 mmol) was treated with 20 mL of triflouroacetic acid and stirred at room temperature for 2 h. The solid was concentrated under reduced pressure and triturated with diethyl ether three times and dried in vacuo. Treatment of compound **7** (1.39 g, 2.5 mmol) with 25 mL of diethyl amine/N,N-dimethyl formamide (1/9, v/v) required 1.5 h at room temperature for complete deprotection of the FMOC group as monitored by TLC analysis. The solvent and excess diethylamine were removed under reduced pressure. The solid was triturated with hexane and residual diethylamine was removed by coevaporation of the solvent. The solid was purified in this manner three times and dried in vacuo. The deprotected segments, $Fmoc(AlaGly)_2OH$ and $HAlaGlyCys(acm)OCH_3$, were each dissolved in 12.5 mL of dimethyl formamide and combined followed by the sequential addition of benzotriazolyloxytris(dimethylamino) phosphonium hexafluorophosphate (1.11g, 2.5 mmol) and 2.5 mL of diisopropylethylamine. The pH was adjusted and the solution was stirred at room temperature overnight. A precipitate formed slowly. After coupling was complete, the solvent was evaporated under reduced pressure. The solid was washed successively with diethyl ether (2 x 80 mL), 10 % HCl (2 x 20 mL), 5 % $NaHCO_3$, and $H_2O$. Recrystallization of the dry solid with N,N-dimethyl formamide/diethyl ether gave a white solid. The filtrate was evaporated and the resultant solid was recrystallized a second time with N,N-dimethyl formamide/diethyl ether. Compound **8** was combined and 1.78 g (2.19 mmol, 88 %) was obtained. TLC analysis showed one spot at $R_f$=0.43 with elution by chloroform/methanol/acetic acid (80/20/1, v/v/v), mp 200 °C dec. $^1H$ NMR (DMSO) δ 1.2 (d, 9H, $CHC\underline{H}_3$), 1.8 (s, 3H, $NCOCH_3$), 2.8 (q, 2H, $CHC\underline{H}_2S$), 3.6 (s, 3H, $COOCH_3$), 3.8 (d, 6H, $NCH_2CO$), 4.0 (t, 1H, $C\underline{H}CH_2CO$), 4.1–4.5 (m, 2H, $CH_2O$; 1H, $NCH(CH_3)CO$, s, 2H, $SCH_2N$), 4.5 ($NCH(CH_2)S$), 7.3-7.8 (m, 8H, aryl), 7.9–8.5 (m, 3H, $N\underline{H}CH(CH_2)$, 3H, $N\underline{H}CH(CH_3)$, 1H, $N\underline{H}CH(CH_2S$, 1H, $NHCOCH_3$).

Anal. Calcd for $C_{37}H_{48}N_8O_{11}S$: C, 54.67; H, 5.95; N, 13.78; S, 3.95. Found: C, 54.94; H, 5.87; N, 13.51; S, 3.72.

**N-Acetyl-L-alanylglycyl-L-alanylglycyl-L-alanylglycyl-S-acetoamidomethyl-L-cysteine methyl ester (9).** Compound **8** (1.02 g, 1.25 mmol) was treated with 16.2 mL of diethyl amine/N,N-dimethyl formamide (19/1, v/v) and stirred for 3 h at room temperature. The solvent was evaporated and the residue was triturated twice with hexane and subsequently dissolved in N,N-dimethylformamide to which 1 mL of freshly distilled acetic anhydride was added. The solution was stirred at room temperature overnight. Evaporation of the solvent on a rotary evaporator yielded a white solid which was recrystallization from water/methanol to give 0.699 g (1.1 mmol, 87 %) of **9**. TLC analysis showed one spot at $R_f = 0.59$ with elution by chloroform/methanol/acetic acid (60/40/1, v/v/v), mp 252-254 °C dec. $^1H$ NMR (DMSO) δ 1.2 (d, 9H, $CHC\underline{H}_3$), 1.8 (s, 3H, $NCOCH_3$, 3H, $CH_3CON$), 2.8 (q, 2H, $CHC\underline{H}_2S$), 3.6 (s, 3H, $COOCH_3$), 3.8 (d, 6H, $NCH_2CO$), 4.2 (m, 3H, $C\underline{H}(CH_3)CO$, 2H, $SCH_2N$), 4.4 (m, 1H, $NC\underline{H}(CH_2)S$) 7.9 – 8.5 (m, 3H, $N\underline{H}CH(CH_2)$, 3H, $N\underline{H}CH(CH_3)$, 1H, $N\underline{H}CH(CH_2S$, 1H, $N\underline{H}COCH_3$). Anal. Calcd for $C_{24}H_{40}N_8O_{10}S$: C, 45.56; H, 6.37; N, 17.71; S, 5.07. Found: C, 45.09; H, 6.25; N, 17.34; S, 4.88.

**N-Acetyl-L-alanylglycyl-L-alanylglycyl-L-alanylglycyl-L-cysteine methyl ester (2).** To remove the acetoamidomethyl group, mercuric acetate was used. Compound **9** ( 70 mg, 0.11 μmol) was dissolved in 4 mL of water to which 2 mL of glacial acetic acid was added. With the addition of mecuric acetate (76.9 mg, 0.22 μmol), complete deblocking was achieved in 1 h at room temperature. Capture of the mercuric ion was accomplished by first diluting the solution with 46 mL of water and then adding 2-mercaptoethanol (83 μL). The solution was stirred at room temperature for 3 hr. The solution was purified in 8 aliquots applied to a Sephadex G-10 column

( 30 cm x 1.5 cm) and eluted under nitrogen with degassed 10 % aqueous acetic acid. The fractions containing compound **2** (detected by Ellman test) were collected and evaporated under reduced pressure to give 30.1 mg (0.053 μmol, 48 %) of **2**. TLC analysis showed one spot at $R_f = 0.63$ with elution by chloroform/methanol/acetic acid (60/40/1, v/v/v). A small sample was recrystallized from water/methanol/acetic acid under nitrogen to give a white solid, mp 215 °C dec. $^1H$ NMR (DMSO) δ 1.2 (d, 9H, $CHC\underline{H}_3$), 1.8 (s, 3H, $CH_3CON$), 2.8 (q, 2H, $CHC\underline{H}_2S$), 3.6 (s, 3H, $COOCH_3$), 3.8 (d, 6H, $NCH_2CO$), 4.2 (m, 3H, $C\underline{H}(CH_3)CO$), 4.4 (m, 1H, $NC\underline{H}(CH_2)S$) 7.9 – 8.5 (m, 3H, $N\underline{H}CH(CH_2)$, 3H, $N\underline{H}CH(CH_3)$, 1H, $N\underline{H}CH(CH_2S)$. ESMS ($M + H^+$) calcd for $C_{21}H_{35}N_7O_9S$: m/z 562.6, found m/z 562.

4.3.4 Sample Preparation

4.3.4.1 Substrate

Silicon wafers were etched in 10/1 $NH_4F/HF$ solution for 1 min and cleaned for 15 min in methanolic choline solution (Summa), rinsed with filtered water and dried under a stream of nitrogen. An oxide surface was grown thermally at 1100° in an oxygen atmosphere. The substrate was primed with 100 Å of titanium in a CHA Industries SE600 electron beam vacuum deposition chamber at a rate of 5-10 Å/s, followed by 2000 Å of gold (99.99%), deposited at the same rate. This treatment produces a textured gold 111. Gold substrates for the room temperature self-assembly study were prepared without a thermally grown oxide.

4.3.4.2 Monolayers

Monolayers of **2** were formed by immersing the gold substrate (prepared within 1.5 hr) into a 5 μM aqueous solution at 44-47 °C overnight. The formation conditions

for the octadecanethiol (ODT) control monolayer were 1 μM and 51-56 °C. Samples were removed from solution, washed with water or ethanol, respectively, dried with nitrogen and dried further under vacuum overnight. Monolayers of **2** were also prepared by immersion of the gold substrate in 5 μM room temperature aqueous and denaturing solutions (8 M urea) for 2 days, washed with water, dried with nitrogen and dried further under vacuum overnight.

### 4.3.5 Thin Film Characterization

Four monolayers were formed and characterized for this study. Monolayer thickness was measured using a Rudolf Auto-EI$^{R}$ II null ellipsometer equipped with a helium-neon laser (632.8 nm) assuming a refractive index of 1.5 for alkylthiol and 1.54 for oligopeptide overlayers. A minimum of 6 spots were measured on each sample. The X-ray reflectivity measurements were performed at the Exxon X10B beamline at the National Synrotron Light Source using an X-ray wavelength of $\lambda = 1.113$ Å. Advancing and receding water contact angle measurements were done using a Rame-Hart goniometer. Six drops were measured on one sample. X-ray photoelectron spectra (XPS) were acquired with a Perkin-Elmer 5100 instrument; Mg was used as the X-ray source. Three samples were analyzed (one spot per sample). Data were collected at 15°, 45° and 75° take-off angles (TOA). Reflectance infrared spectra were acquired on a Perkin-Elmer 2000 FTIR spectrometer equipped with a narrow-band mercury cadmium telluride (MCT) detector. The p-polarized radiation was incident on the sample at 80° using an external reflection cell (Graesby Specac). The spectra were obtained by coaddition of a minimum of 2048 scans at 2 cm$^{-1}$ resolution. The spectra of three monolayers were analyzed and are essentially identical. Normal incidence

transmission spectra of KBr pellets of the bulk material were acquired on a Perkin Elmer 1600 instrument.

## 4.4 Results and Discussion

### 4.4.1 Monolayer Formation at Elevated Temperature

Oligopeptide monolayers were formed by immersing gold substrates into aqueous solutions of **2**. Films were assembled at slightly elevated temperatures (45-47°C) and from dilute solutions to encourage this strongly associative adsorbate to form a well packed monolayer. Earlier studies have shown that concentration affects adsorption time[1,26]. Although monolayers form almost immediately, it may take much longer to form well-ordered structures. In choosing dilute solution conditions, we wish to form well-ordered monolayers devoid of kinetically trapped adsorbate.

Film thickness for the monolayer of **2** assembled on Au (111) was 15±1 Å, as measured by ellipsometry; slightly more than half the 27 Å thickness anticipated for an extended parallel β-sheet septapeptide, assuming a 3.25 Å residue repeat distance[27]. It is not uncommon to find monolayer thickness measurements to differ from prediction[28], especially for alkyl thiol monolayers[29], but not of this magnitude. While small changes in refractive index give varied thicknesses for alkylthiol monolayers[1, 30], again the difference is minimal. We have observed a thickness of 21±2 Å for a monolayer prepared by chemisorption of octadecanethiol (ODT) on gold as a control[1] and believe that the problem lies in accurately determining thin peptide films thickness and is not due to contamination of the gold substrate. It is curious that others[31] have experienced similar difficulty in accurately determining film thickness of adsorbed proteins on metal surfaces by ellipsometry.

A loose packing density in the monolayer could lead to an error in film thickness determined by ellipsometry[28,29]. Adsorption of alkanethiols onto gold yield a $\sqrt{3}x\sqrt{3})R30$ structure with a spacing of sulfur atoms at 21.7 Å[2][32,33] which is smaller than the area per molecule observed in either the antiparallel[34,35] or parallel[35,36] β-sheet structures observed for L-alanyl-L-alanyl-L-alanine (tri L-alanine), 24.68 Å$^2$ and 24.66 Å$^2$ respectively. The packing density of monolayer **2** will be different from that of a typical alkanethiol monolayer based not only on the size of the L-alanylglycine chain, but also, as we observed in an earlier study[12] with $CH_3(CH_2)_{16}COCysOCH_3$ (**10**), on the steric requirements of the cysteine methyl ester "headgroup" which precluded the formation of a densely packed monolayer.

It is interesting to note that determination of film thickness for monolayers of **2** on gold as measured by low angle x-ray reflectivity reveal a much thicker monolayer. We observed an oligopeptide film that is 24 Å thick. (The preparation time for self-assembly was reduced to one hour in solution for this sample and may be a factor in the monolayer structure formed.) To achieve this film thickness the oligopeptide, if in an extended β-sheet structure, must be tilted approximately 27° from the surface normal. Ellipsometry is an indirect method, whereas x-ray reflectivity is a direct measure of film thickness no matter what the packing density is, provided that there is sufficient electron density contrast between the air, organic layer and substrate interfaces and the substrate is smooth.

Advancing water contact angles were measured to determine the wetting properties of these films. The advancing contact angle on the octadecanethiol (ODT) control was ($\theta_a(H_2O)=109\pm4°$)[1,37] indicating that the interface is hydrophobic, as expected. The contact angle obtained on a monolayer film of **2** was determined to be $\theta_a(H_2O)=43\pm1°$; water spreads more freely, as expected, for the more hydrophilic peptide monolayer interface (Table 4.1).

Table 4.1 Monolayer Formation Conditions, Film Thickness, and Contact Angle for Monolayers.

| Monolayer | Solvent | Concentration | Temperature | Contact Angle *Advancing* |
|---|---|---|---|---|
| **2** | Water | 5 μm | 45 - 47 °C | 43 ± 1° |
| ODT | Water | 1 μm | 51- 56 °C | 109 ± 4° |

4.4.2 Monolayer Formation at Room Temperature

Additional studies to probe how alternate formation conditions might affect packing density were undertaken. Monolayers were assembled from room temperature aqueous and peptide denaturing (8 M urea) solutions. These monolayers were characterized primarily by external reflectance infrared spectroscopy and XPS. Entrapment of urea at the air-solid interface is expected to lower the contact angle. There is only a 3° decrease in contact angle measurement for the monolayer prepared from the denaturing solution, reported in Table 4.2, suggesting minimal or no urea present in the monolayer. (The contact angle on these samples is 11° lower than previously observed.) The difference in advancing and receding contact angle measurements for water on ODT[13] is typically 12°. The hysteresis in wetting, especially for the monolayer assembled from urea, may suggest a different packing in monolayer **2** as compared to alkyl thiols.

Table 4.2 Monolayer **2** Formation Conditions and Contact Angle Measurements.

| Solvent | Concentration | Temperature | Contact Angle | |
|---|---|---|---|---|
| | | | *Advancing* | *Receding* |
| Water | 5 μm | room temperature | 34 ± 4° | 14 ± 4° |
| Water | 5 μm | room temperature | 33 ± 4° | 19 ± 4° |
| 8 M Urea | 5 μm | room temperature | 30 ± 3° | 13 ± 3° |

### 4.4.3 Angle Resolved X-ray Photoelectron Spectroscopy

Figure 4.3 shows a survey spectrum collected at a 75° detector angle of a oligopeptide monolayer. Only the expected elements $S_{2p}$, $C_{1s}$, $N_{1s}$ and $O_{1s}$ were detected. Uvdal[38] has observed two $S_{2p}$ peaks with the adsorption of L-cysteine on gold in a bilayer film characteristic of only one sulfur adsorbed to the gold, the second an unbound thiol. In all monolayers we find only the spin slit doublet, $S_{2p1/2}$ and $S_{2p3/2}$, representing a gold-thiolate species.

The atomic compositions of monolayers assembled at elevated temperature are reported at two angles in Table 4.3 and confirm the expected inhomogeneity along the surface normal. With the ODT control the sulfur increases with increasing angle; i.e., the sulfur concentration is attenuated for the ODT monolayer as reported by others[1]. There is evidence of some oxygen contamination at the air-monolayer interface. In monolayer **2** the atomic concentrations qualitatively exhibit the expected concentrations for the adsorbate. Compare the observed concentrations to those expected. The carbon concentration decreases with increasing take-off angle (TOA). At a 75° TOA , a sampling depth of 40 Å, we would anticipate detecting a signal for the entire monolayer while at 15° TOA we might observe a signal for approximately the first 10 Å or three residues (Ac-L-Ala-Gly-L-Ala-) i.e., half layer; thus, the decreased carbon concentration is what would be expected. In Figure 4.4 the carbon peak multiplicity for three monolayers; monolayer **2**, the control monolayer **10** constructed to study the cysteine methyl ester head group interaction[7], and the control ODT are assigned.

XPS derived elemental concentrations of monolayers fabricated from room temperature solutions are reported in Table 4. 4. The atomic concentrations are

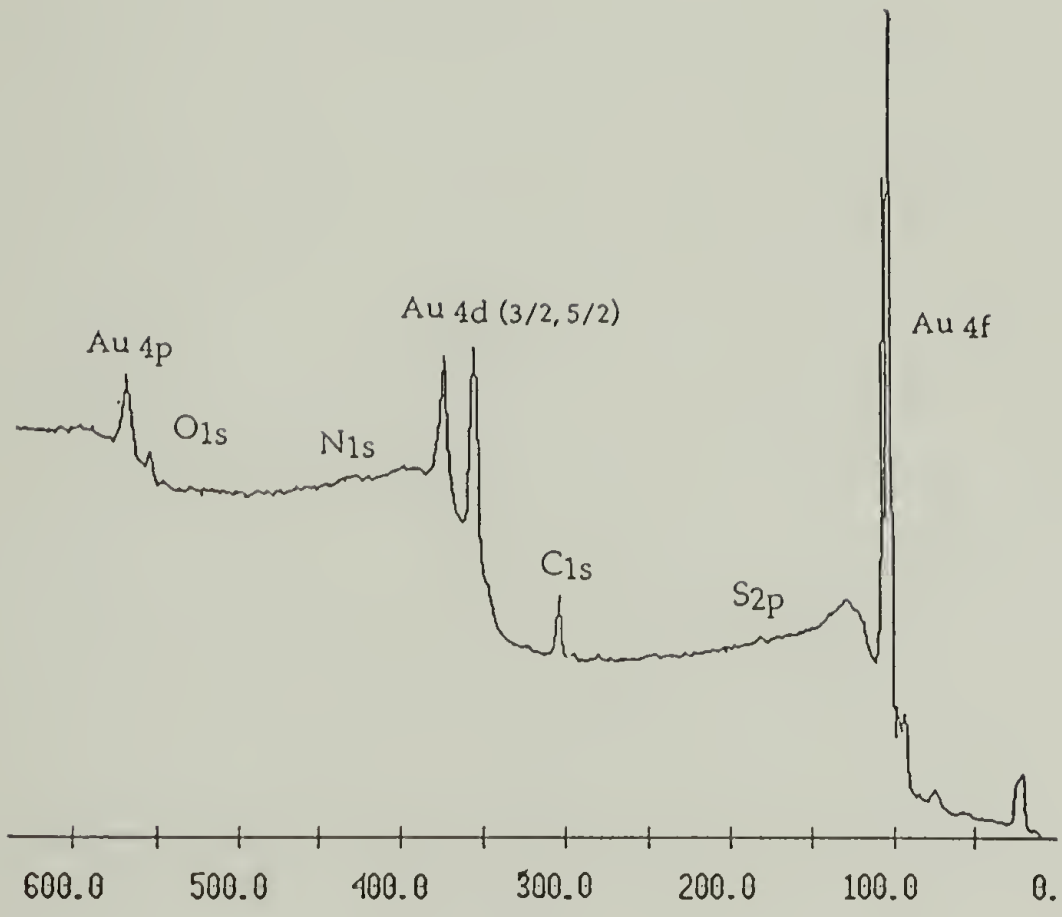


Figure 4.3 XPS survey spectrum of monolayer **2**.

Table 4.3 XPS Elemental Composition for Monolayers Assembled at Elevated Temperature.

| Sample | | Atomic Concentrations C | O | N | S |
|---|---|---|---|---|---|
| $CH_3CO$-$(AlaGly)_3CysOCH_3$ 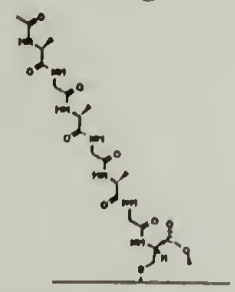 | expected[a] | 55.3 | 23.7 | 18.4 | 2.6 |
| | observed | | | | |
| | 15° TOA | 65.1 | 19.2 | 14.5 | 1.2 |
| | 75° TOA | 63.4 | 19.5 | 14.5 | 2.6 |
| $CH_3(CH_2)_{17}SH$ 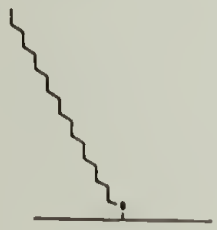 | expected[b] | 94.7 | | | 5.3 |
| | observed | | | | |
| | 15° TOA | 94.9 | 3.2 | 0.0 | 1.9 |
| | 75° TOA | 95.7 | 0.9 | 0.0 | 3.4 |

a. calculated elemental analysis for $C_{34}N_7O_{10}S$
b. calculated elemental analysis for $C_{18}S$

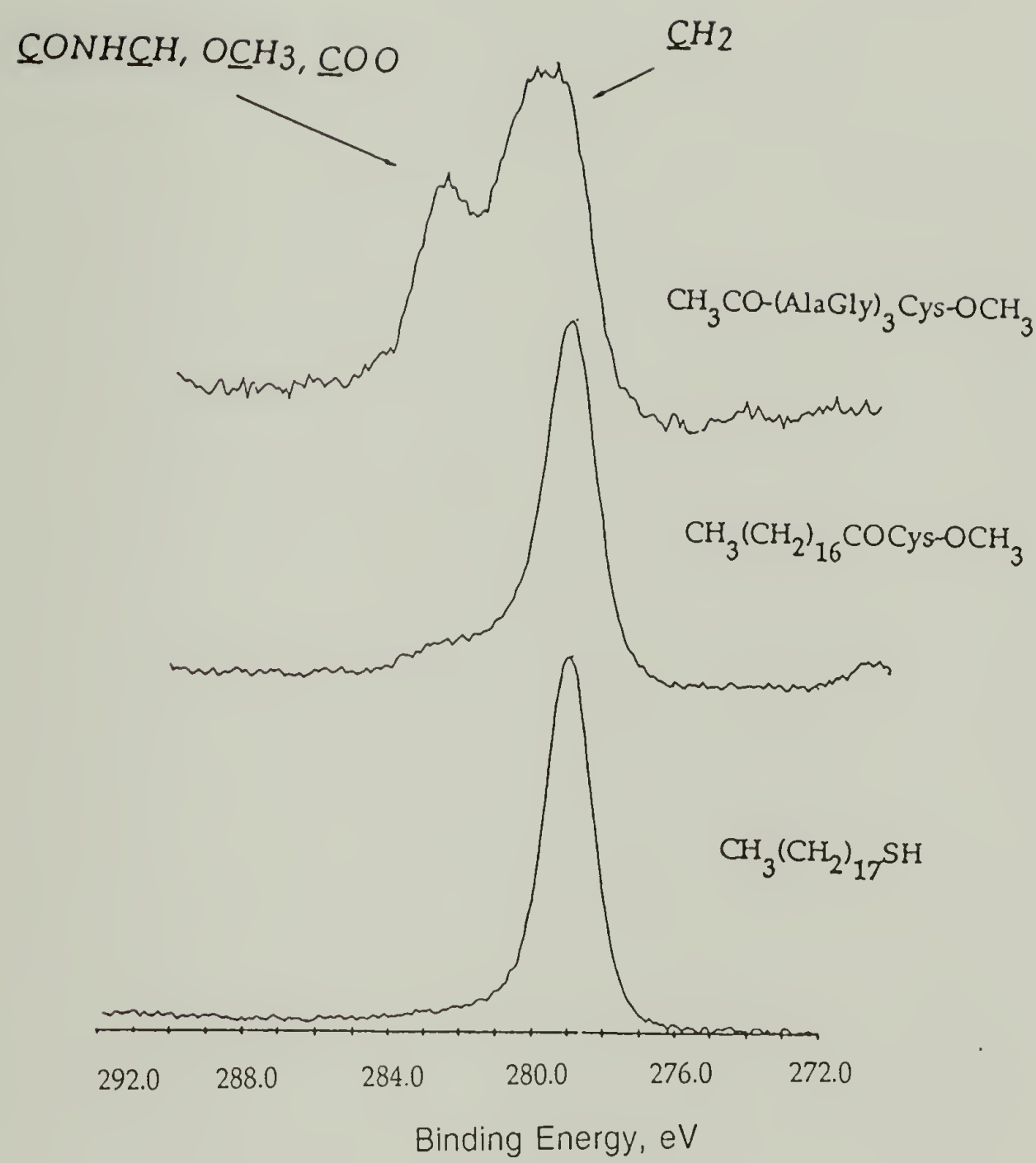


Figure 4.4 XPS $C_{1s}$ spectra of monolayers on gold.

Table 4.4 XPS Elemental Compositions for Monolayers Assembled at Room Temperature.

| Sample | | Atomic Concentrations C | O | N | S |
|---|---|---|---|---|---|
| $CH_3CO$-$(AlaGly)_3CysOCH_3$ | expected[a] | 55.3 | 23.7 | 18.4 | 2.6 |
| Assembled from room temperature aqueous solution | observed | | | | |
| | 15° TOA | 60.4 | 21.0 | 17.5 | 1.2 |
| | 45° TOA | 62.6 | 19.7 | 16.3 | 1.4 |
| | 75° TOA | 63.6 | 19.5 | 15.4 | 1.5 |
| $CH_3CO$-$(AlaGly)_3CysOCH_3$ | expected[a] | 55.3 | 23.7 | 18.4 | 2.6 |
| Assembled from room temperature 8 M urea solution | observed | | | | |
| | 15° TOA | 62.4 | 21.1 | 15.6 | 0.9 |
| | 45° TOA | 62.8 | 20.4 | 15.4 | 1.4 |
| | 75° TOA | 62.7 | 19.1 | 15.9 | 2.3 |

a. calculated elemental analysis for $C_{14}N_7O_{10}S$

comparable to those reported above in Table 4.3 for the samples prepared at elevated temperature. Interestingly, the monolayer prepared in the presence of urea shows no increase in nitrogen which would accompany entrapment of urea. The C/N concentration ratio for monolayers of **2** assembled under different conditions is

presented in Table 4.5. At 75° TOA (40 Å) the atomic composition is determined for the entire monolayer and again there does not appear to be any presence of urea.

Table 4.5 C/N Atomic Concentrations for Monolayer **2**.

| | Aqueous, RT | 8 M Urea, RT |
|---|---|---|
| 75 ° TOA | 4.1 | 3.9 |

4.4.4 External Reflectance Infrared Spectroscopy

4.4.4.1 Mid Frequency

Infrared spectroscopy has been a potent means of investigating protein structure since the 1950's. Linear combinations of independent or normal modes of vibration occur at specific frequencies and are characteristic of distinct functional group adsorption. The in-plane peptide CONH vibrations in the mid-frequency region, i.e., the amide I and II bands, are particularly helpful. The amide I vibration is comprised primarily of CO stretching mode[39,40] with out-of-phase CN stretching and CCN deformation and in-plane NH bend[41] demonstrated by normal mode analysis of N-methylacetamide, a simple trans-peptide analog. The amide II mode is an out-of-phase combination of largely NH in-plane bending and CN stretch.

Only the components of the transition dipole moment which are perpendicular to the metal surface are observed with reflectance spectra[42,43]. Thus, comparing the relative intensities of the vibrational bands further assists in deciphering monolayer

orientation. We have assumed a parallel β-sheet structure for the monolayer **2** with the oligopeptide tilted 32° to comply with the x-ray reflectivity data as shown in Figure 4.5. Examination of the infrared spectrum of monolayer **2** (Figure 4.6) reveals that the amide I vibration at 1675 $cm^{-1}$ is comparable in intensity to the amide II vibration at 1546 $cm^{-1}$. (The noise in the spectrum is due to the presence of water vapor in the infrared chamber). This is clearly not the case in the bulk spectra where the amide I predominates. Referring to Figure 4.5, it is not surprising that the amide I intensity is reduced relative to the amide II intensity with the CO bond oriented almost parallel to the gold surface. The alternately slanting hydrogen bonds ensure that there will be some amide I intensity even if the sheet is normal to the gold surface. With this orientation we would anticipate a substantial transition dipole component normal to the surface representing the amide II vibration.

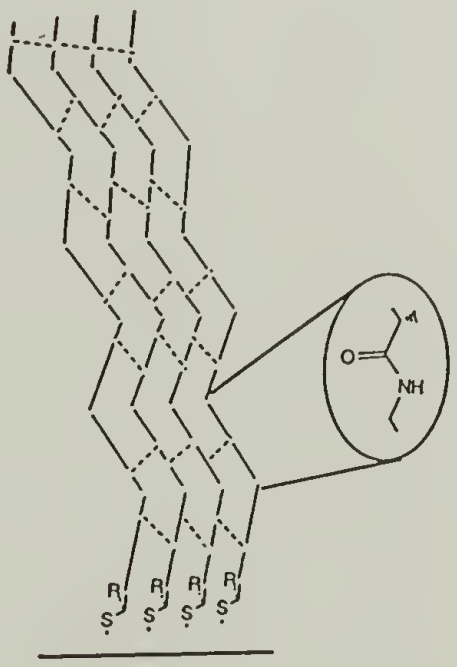


Figure 4.5 Schematic of self-assembled monolayer of **2** on gold with intrasheet hydrogen bonding.

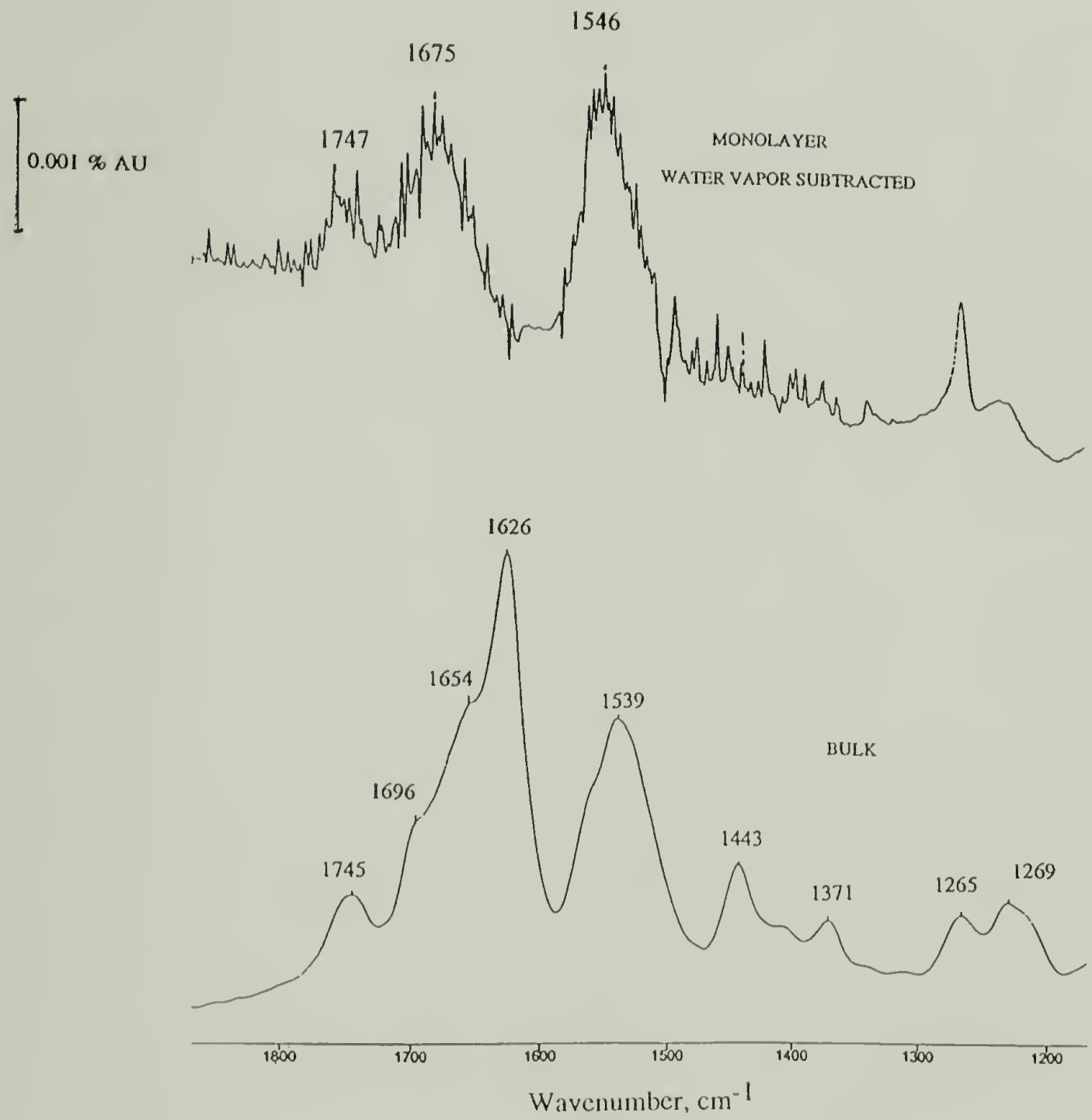


Figure 4.6 FTIR spectra (mid frequency region) of monolayer **2** on gold (top) and **2** bulk (bottom).

4.4.4.2 High Frequency

In the high frequency region of the infrared spectrum, Figure 4.7, only the asymmetric methyl vibration at 2971 $cm^{-1}$ is evident in monolayer **2** suggesting that the $C\alpha$ methyl, methylene and methine hydrogens are positioned parallel to the surface, again consistent with the proposed structure[44]. In some of the models of monolayer **2** constructed in a parallel β-sheet conformation only the terminal N-acyl methyl group is nearly perpendicular to the metal surface. We assume that the packing densities in both monolayers **2** and **10** are similar and are determined largely by the size of the head group. It is interesting to note that with the addition of the three alanyl methyls in monolayer **2** compared to **10** that there is no increase in the intensity of the methyl vibrations at 2971 $cm^{-1}$. In the proposed structure the NH stretching should have minimal intensity based on the proposed structure. Although we have not seen amide A and B vibrational bands which appear at 3289 $cm^{-1}$ and 3076 $cm^{-1}$ in the bulk, we have noted formation of ice on the detector window and discount any information from this region of the spectrum.

4.4.4.3 Consequences of Lattice Structure

What drives the monolayer amide I vibrational band to such a high frequency at 1675 $cm^{-1}$? One possibility is that the gold 111 lattice may force the oligopeptide to organize in a fashion which isolates the chains or prohibits the formation of strong hydrogen bonds, i.e. increased hydrogen-bond distances. It has been demonstrated that even small changes to hydrogen-bond distances change force fields[34] and can appreciably affect the amide I frequency as demonstrated by organizational differences in two similar antiparallel (AP) β-sheet structures, tri L-alanine (1641-1647 $cm^{-1}$) and poly(L-alanine) (1632 $cm^{-1}$)[34]. Even in the parallel β-sheet tripeptides L-valyl-glycyl-

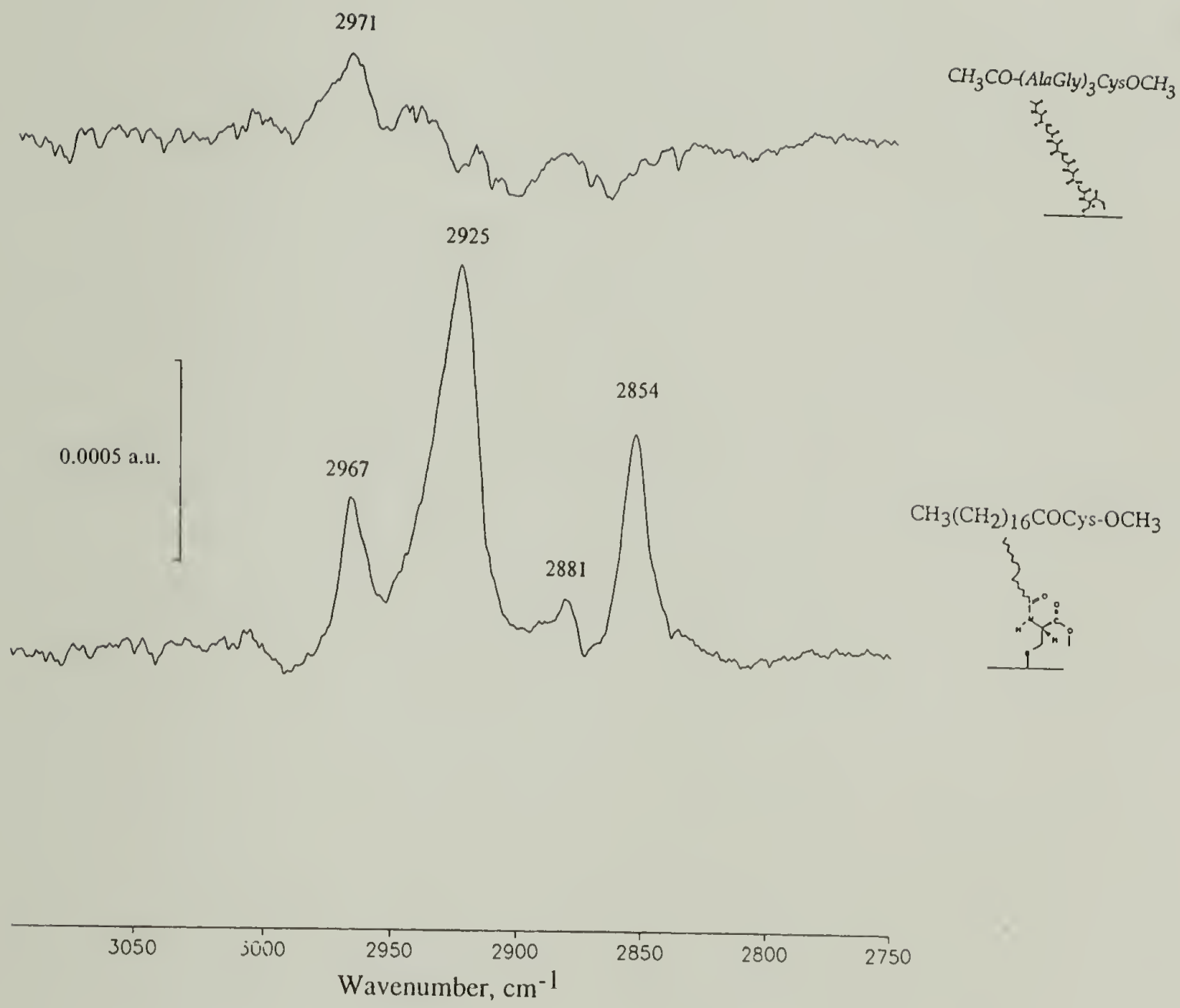


Figure 4.7 FTIR spectra (high frequency region) of monolayers of **2** and **10** on gold.

glycine[45] and L-alanyl-L-alanyl-L-alanine(tri L-alanine)[34] where charged end groups dominate the structure and extend the interior N-O hydrogen bonds to larger distances, the frequency does not reach 1675 $cm^{-1}$, Table 4.6.

Table 4.6 Peptide Hydrogen Bond Distances and Amide I Frequency.

| Peptide | N-O Hydrogen Bond Distance | Amide I |
|---|---|---|
| P β-sheet L-VGG[46] | 3.05 Å | 1645 $cm^{-1}$ |
| P β-sheet tri L-A[36] | 3.28 Å | 1649 $cm^{-1}$ |
| AP β-sheet tri L-A[36] | 2.97 Å | 1641-1647 $cm^{-1}$ |

P = parallel; AP = antiparallel

Several authors have demonstrated that oligo and polypeptides with comparable amino acid composition can form antiparallel or parallel β-sheet structures with appropriate dimensions. Krejchi et al.[21] observed the formation of AP β-structure with poly[(AlaGly)$_3$GluGly)]$_n$, having a 4.74 Å distance between hydrogen-bond chains and in the parallel β-sheet oligopeptide, L-valyl-glycyl-glycine, the distance was found to be 4.8 Å[46]. It would appear that the gold lattice spacing accessed by alkylthiols (4.99 Å) would amply accommodate these hydrogen-bonded β-sheet structures. Secondly, the narrow band width of the amide I vibration argues against formation of a monolayer where the molecules are positioned at inappropriate distances to allow the formation of well ordered hydrogen-bonded chains. Considering intrasheet distances observed in

similar peptides, it is conceivable that the oligopeptide could adsorb on gold and successfully form monolayers with β-sheet like structure.

4.4.4.4 Monolayer Structure

That frequency can be related to conformation[47] has greatly facilitated the understanding of peptide tertiary structure. In monolayer **2**, however, the amide I and II frequencies are inconsistent with assignments for α, β, or random peptide structures[48], a parallel β-structure, envisioned for this monolayer, or the more recently examined oligopeptides listed in Table 4. 7.

Table 4.7 Amide I and Amide II Vibrations in Parallel β Structures.

| Sample | Amide I | Amide II |
|---|---|---|
| monolayer **2** | 1675 $cm^{-1}$ | 1546 $cm^{-1}$ |
| parallel β-polypeptide[48] | 1630 $cm^{-1}$ | 1530 $cm^{-1}$ |
| parallel β tri L-A[35] | 1649 $cm^{-1}$ | 1525 $cm^{-1}$ |
| parallel β L-VGG[45] | 1645 $cm^{-1}$ | 1543 $cm^{-1}$ |
| calculated parallel β poly(L-alanine)[49] | 1642 $cm^{-1}$ | 1553 $cm^{-1}$ |

A calculation by Bandekar and Krimm[49] may explain the frequency-structure inconsistency. They determined by calculating normal modes for a parallel-chain

pleated structure of β poly(L-alanine) that both sheet arrangement and intersheet separation affect the amide I frequency. In this study[49] the sheet separation was varied from 5 to 17 Å for the parallel β poly(L-alanine). The calculated dominant vibrational frequency is given in Table 4.8 for three intersheet distances. For "parallel sheets and an intersheet separation of 5.3 Å (comparable to that in an antiparallel β-poly(L-alanine))" the amide I vibrations would occur at 1669 $cm^{-1}$ (strong Raman band) and 1677 $cm^{-1}$ (strong infrared band) [45] similar to the frequency observed for monolayer **2**. An examination of intersheet distances for oligo and polypeptides with similar amino acid composition are given in Table 4. 9. Clearly, a 5.3-5.4 Å intersheet distance could be anticipated for oligopeptide **2**.

Table 4.8 Dependence of Amide I Vibrations on Intersheet Separation for Parallel β Structures[46].

| Intersheet Distance | Amide I Frequency |
|---|---|
| 5 Å | 1679 $cm^{-1}$ |
| 6 Å | 1672 $cm^{-1}$ |
| 7 Å | 1671 $cm^{-1}$ |

Table 4.9 Intersheet Distance Observed in Polypeptides.

| Peptide | Intersheet Distance |
|---|---|
| AP β poly(L-AG)[50] | 5.4 Å |
| AP β poly(L-alanine)[51] | 5.3 Å |
| AP β poly((AG)3EG)[21] | 5.3 Å |
| AP β poly(G)[52] | 3.4 Å |
| AP silk fibroin[53] | 7.9 Å |
| P β L-VGG[46] | 10.623 Å* |
| P β tri L-A[35] | 10.004 Å* |

* 2 sheets in unit cell; AP = antiparallel; P = parallel

Bandekar and Krimm[49] state that the amide II mode would be insensitive to sheet packing, but remain sensitive to hydrogen bond geometry. For the parallel-chain pleated structure of β poly(L-alanine) the amide II vibration was predicted at 1553 $cm^{-1}$. The observed frequency for monolayer **2** appears at 1546 $cm^{-1}$.

In this study[49] Bandekar and Krimm suggest a possible explanation for the observed amide I and II peak positions befitting the $(L\text{-}Ala\text{-}Gly)_3$ oligopeptide chain. The organization of the oligopeptide chain is a strong driving force for the monolayer structure, yet the structure isn't limited to the interactions of the oligopeptide chain. One must consider the interaction between the gold surface and the cysteine thiol, as well as, the size the cysteinyl head group, both can effect monolayer packing.

Inferring from the thickness measurements (ellipsometry and x-ray reflectivity), the oligopeptide chains must tilt some to achieve a close packed architecture. The extent of tilt remains unresolved. Do the chains tilt in a β-sheet like structure or do

chains randomly collapse to form a more densely packed structure? The narrow bandwidth, compared to the bulk spectrum, would suggest that the monolayer structure isn't random[48]. (The presence of water vapor, clearly confounds the measurement of bandwidth in Figure 4.6. In section 4.4.4.6 the line shape and bandwidth are readily discernible.) It is not possible to precisely define the structure in monolayer **2**. We can say that the organization in monolayer **10** , where the cysteinyl head group-gold interaction was probed, is different than in monolayer **2** based on peak position (1681 and 1536 $cm^{-1}$)[12], intensity and line shape of the amide I and II bands.

Monolayers with an amide functionality incorporated into the adsorbate have appeared in the literature[11,13,15]. The amide I band either appears weakly at 1640-1650 $cm^{-1}$ or not at all, unlike monolayer **2**. More recently, in a study to affect tilt angle and packing of branched thiols, Chechik et al.[54] studied the formation of monolayers wherein the thiolate contained "complementary hydrogen bond donors/acceptors in the alkyl chain". The amide I and amide II vibrations occur at 1670 and 1546 $cm^{-1}$ respectively with the amide II band predominant similar to what was observed in monolayer **2**.

4.4.4.5 Methyl ester

The conformation of the head group functionality was addressed with a simpler model earlier[12]. Based on the methyl ester carbonyl stretching vibration (1748 $cm^{-1}$) the carbonyl remains isolated in this monolayer and is not in a hydrogen bonding environment.

4.4.4.6 Temperature Study

The amide I and amide II vibrations appear at the essentially the same frequencies observed in the elevated temperature studies of monolayer **2**, 1675 and 1546 $cm^{-1}$. The only difference in the monolayers prepared from room temperature solutions, is a slight increase in intensity of the amide I band relative to the monolayer formed at elevated temperature. This change would suggest a concomitant small conformational change in monolayers prepared from lower temperature solutions. More importantly no urea is incorporated into the monolayer prepared under denaturing conditions (no peak observed at 1599 $cm^{-1}$). The amide I and II bandwidths are narrow compared to the bulk spectrum and the line shape is quite symmetrical denoting an ordered monolayer. The ester, amide I and amide II infrared assignments for monolayers of **2** prepared under various conditions are reported in Figure 4.8 and Table 4.10.

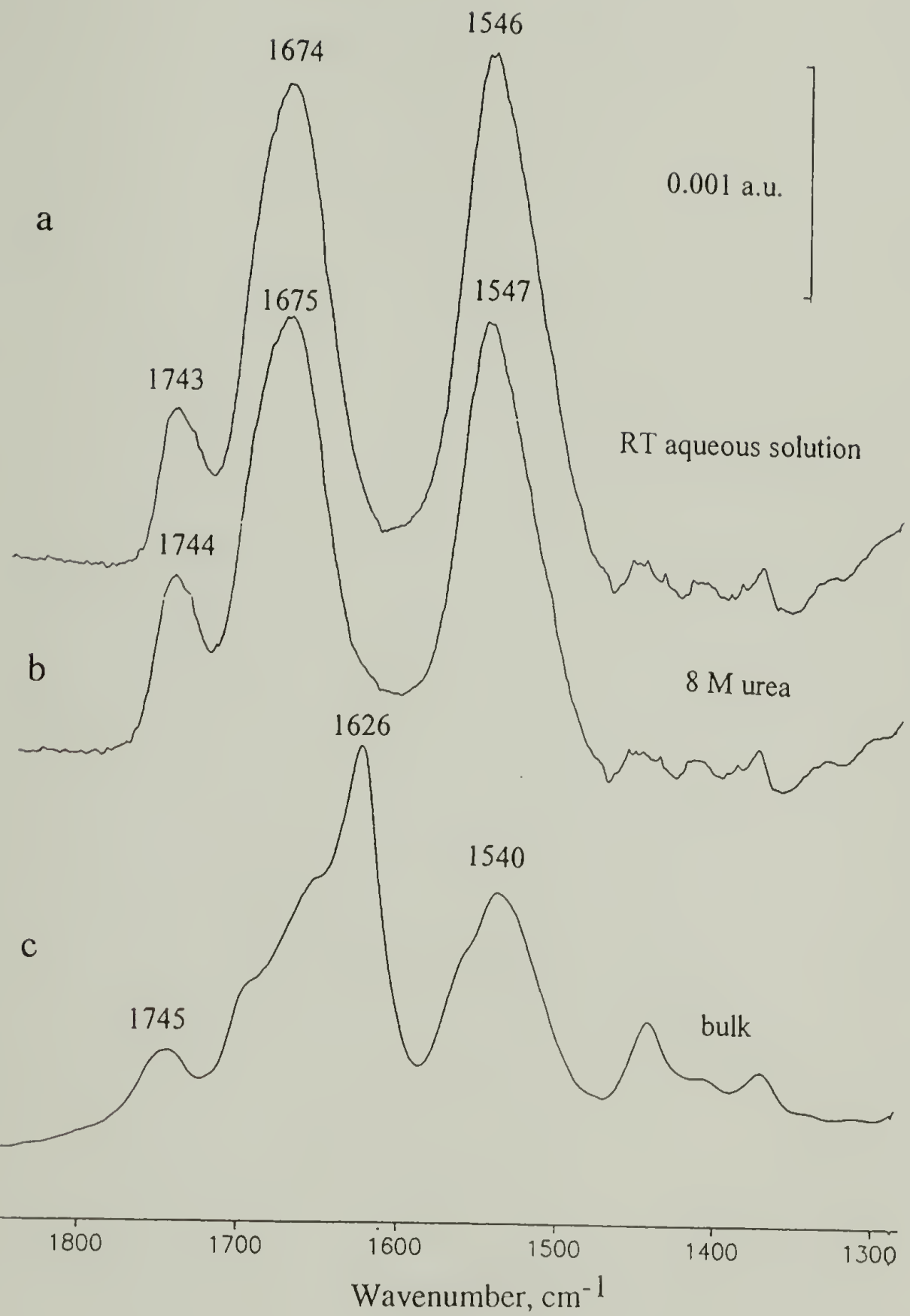


Figure 4.8 FTIR spectra (mid frequency region) of monolayer **2** on gold assembled from RT aqueous solution (a), 8 M urea (b) and in bulk (c).

Table 4.10 Infrared Assignments for Monolayer **2** at Various Preparation Conditions.

| Sample | Ester | Amide I | Amide II |
|---|---|---|---|
| Bulk | 1745 $cm^{-1}$ | 1626 $cm^{-1}$ | 1540 $cm^{-1}$ |
| Monolayer 46° C, aqueous | 1747 $cm^{-1}$ | 1675 $cm^{-1}$ | 1546 $cm^{-1}$ |
| Monolayer RT, aqueous | 1743 $cm^{-1}$ | 1674 $cm^{-1}$ | 1546 $cm^{-1}$ |
| Monolayer RT, aqueous | 1745 $cm^{-1}$ | 1674 $cm^{-1}$ | 1544 $cm^{-1}$ |
| Monolayer RT, 8 M urea | 1744 $cm^{-1}$ | 1675 $cm^{-1}$ | 1547 $cm^{-1}$ |

## 4.5 Conclusion

We have continued to explore a novel approach to the formation of monolayers with the potential for development of uniquely stable films exploiting the potency of hydrogen bonding. An oligopeptide model compound, $CH_3O(AlaGly)_3CysOCH_3$, was synthesized by traditional peptide synthesis and assembled under different solution conditions. Monolayers were characterized via ellipsometry, x-ray reflectivity, contact angle, x-ray photoelectron spectroscopy and vibrational spectroscopy and appear to have similar monolayer structures. X-ray photoelectron spectroscopy confirms that the oligopeptide chemisorbs to gold via the cysteine thiol and successfully forms monolayers. Film thicknesses (from ellipsometry and x-ray reflectivity) indicate that to achieve a close packed architecture the oligopeptide chains are forced to tilt. The extent of tilt remains unresolved. Factors that can influence the packing density in monolayer **2** are conformation and packing of the oligopeptide chain, the gold-cysteine thiol interaction, as well as, the size of the head group functionality. The infrared data demonstrates that the oligopeptide tertiary structure in monolayer **2** is different than what is typically seen in peptide structures. The implication is that the gold (111) surface forces an uncharacteristic peptide packing. This work demonstrates that oligopeptides can form monolayers and indicates the potential for assembling polypeptide monolayers and ultimately that these peptide assemblies could be exploited as sensors, catalysts or biomaterials.

(1) Bain, C. D.; Troughton, E. B.; Toa, Y.-T.; Evall, J.; Whitesides, G. M.; Nuzzo, R. G. *J. Am. Chem. Soc* **1989**, *111*, 321.

(2) Tengvall, P.; Lestelius, M.; Leidberg, B.; Lundstrom, I. *Langmuir* **1992**, 8, 1236.

(3) Mrksich, M.; Whitesides, G. M. In *ACS Symp. Ser, 680 (Poly(ethylene glycol));* J. M. Harris and S. Zalipsky, Ed.; American Chemical Society: Washington, D.C., **1997**; pp 361.

(4) Tidwell, C. D.; Ertel, S. I.; Ratner, B. D.; Tarasevich, B. J.; Atre, S.; Allara, D. L. *Langmuir* **1997**, 13, 3404.

(5) Lestelius, M.; Liedberg, B.; Tengvall, P. *Langmuir* **1997**, 13, 5900.

(6) Patel, N.; Davies, M. C.; Hartshorne, M.; Heaton, R. J.; Roberts, C. J.; Tendler, S. J. B.; Williams, P. M. *Langmuir* **1997**, 13, 6485.

(7) Dawson, S. L.; Elman, J.; Margevich, D. E.; McKenna, W.; Tirrell, D. A.; Ulman, A. In *ACS symp. Ser. 627 Hydrogels and Biodegradable Polymers for Bioapplications*; R. M. Ottenbritte, S. J. Huang and K. Park, Ed.; American Chemical Society: Washington, D. C., **1996**; pp 187.

(8) Matsuura, K.; Ebara, Y.; Okahata, Y. *Thin Solid Films* **1996**, 273, 61.

(9) Friggeri, A.; Veggel, F. C. J. M. v.; Reinhoudt, D. N.; Kooyman, R. P. H. *Langmuir* **1998**, 14, 5457.

(10) Lenk, T. J. ;. V. M. H., C. L. Hoffmann, J. F. Rabolt, D. G. Castner, C. Erdelen, H. Rinsdorf *Langmuir* **1994**, 10, 4610.

(11) Dawson, S. L.; Fournier, M. J.; Mason, T. L.; Tirrell, D. A. *Polym. Prepr.* **1994**, 35, 413.

(12) Dawson, S. L.; Tirrell, D. A. *J. Mol. Recogn.* **1997**, 10, 18.

(13) Tam-Chang, S.-W.; Biebuyck, H. A.; Whitesides, G. M.; Jeon, N.; Nuzzo, R. G. *Langmuir* **1995**, 11, 4371.

(14) Clegg, R. S.; Hutchinson, J. E. *Langmuir* **1996**, 12, 5239.

(15) Sabapathy, R. C.; Bhattacharyya, S.; Leavy, M. C.; Jr., W. E. C.; Hussey, C. L. *Langmuir* **1998**, 14, 124.

(16) Chechik, V.; Schonherr, H.; Vancso, G. J.; Stirling, C. J. M. *Langmuir* **1998**, 14, 3003.

(17) Whitesell, J. K.; Chang, H. K. *Science* **1993**, 261, 73.

(18) McGrath, K. P.; Fournier, M. J.; Mason, T. L.; Tirrell, D. A. *J. Am. Chem. Soc.* **1992**, 114, 727.

(19) Tirrell, J. G.; Fournier, M. J.; Mason, T. L.; Tirrell, D. A. *C&EN* **1994**, Dec. 19, 40.

(20) Kothakota, S.; Fournier, M. J.; Mason, T. L.; Tirrell, D. A. *J. Am. Chem. Soc.* **1995**, 117, 536.

(21) Krejchi, M. T.; Atkins, E. D. T.; Waddon, A. J.; Fournier, M. J.; Mason, T. L.; Tirrell, D. A. *Science* **1994**, 265, 1427.

(22) Yoshikawa, E.; Fournier, M. J.; Mason, T. L.; Tirrell, D. A. *Macromolecules* **1994**, 27, 5471.

(23) Zhang, G.; Fournier, M. J.; Mason, T. L.; Tirrell, D. A. *Macromolecules* **1992**, 25, 3601.

(24) Petka, W. A.; Harden, J. L.; McGrth, K. P.; Wirtz, D.; Tirrell, D. A. *Science* **1998**, 281, 389.

(25) Carpino, L.; Cohen, B. J.; Jr., K. K. S.; Sadat-Aalaee, S. Y.; Tien, J.-H.; Langridge, D. C. *J. Org. Chem.* **1986**, 51, 3732.

(26) Dubois, L. H.; Nuzzo, R. G. *Annu. Rev. Phys. Chem.* **1992**, 43, 437.

(27) Walton, A.; Blackwell, J. *Biopolymers*; Academic Press: New York, **1973**; p 31.

(28) Wasserman, S. R.; Whitesides, G. M.; Tidswell, I. M.; Ocko, B. M.; Pershan, P. S.; Axe, J. D. *J. Am. Chem. Soc.* **1989**, 111, 5852.

(29) Bain, C. D.; Whitesides, G. M. *J. Phys. Chem.* **1989**, 93, 1670.

(30) Porter, M. D.; Bright, T. B.; Allara, D.; Chidsey, C. E. D. *J. Am. Chem. Soc.* **1987**, 109, 3559.

(31) Martensson, J.; Arwin, H. *Langmuir* **1995**, 11, 963.

(32) Strong, L.; Whitesides, G. M. *Langmuir* **1988**, 4, 546.

(33) Camillone, I. N.; Chidsey, C. E. D.; Liu, G.-Y.; Putvinski, T. M.; Scoles, G. *J. Chem. Phys.* **1991**, 94, 8493.

(34) Fawcett, J. K.; Camerman, N.; Camerman, A. *Acta Crystal B* **1975**, 31, 658.

(35) Qian, W.; Bandekar, J.; Krimm, S. *Biopolymers* **1991**, 31, 193.

(36) Hempel, A.; Camerman, N.; Camerman, A. *Biopolymers* **1991**, 31, 187.

(37) Nuzzo, R. G.; Dubois, L. H.; Allara, D. A. *J. Am. Chem. Soc.* **1990**, 112, 558.

(38) Uvdal, K.; Bodö, P.; Liedberg, B. *J. Colloid and Interface Sci.* **1992**, 149, 162.

(39) Miyazawa, T.; Shimanouchi, T.; Mizushima, S. *J. Chem. Phys.* **1956**, 24, 408.

(40) Miyazawa, T. In *Poly-α-Amino Acids Protein Models for Conformational Studies;* G. D. Fasman, Ed.; Marcel Dekker, Inc: New York, **1967**; Vol. 1; pp 69-103.

(41) Krimm, S.; Bandekar, *J. Advan. Protein Chem.* **1986**, 38, 181.

(42) Greenler, R. J. *J. Chem. Phys.* **1966**, 44, 310.

(43) Allara, D. L.; Nuzzo, R. G. *Langmuir* **1985**, 1, 52.

(44) Labinis, P. E.; Whitesides, G. M.; Allara, D. L.; Tao, Y.-T.; Parikh, A. N.; Nuzzo, R. G. *J. Am. Chem. Soc.* **1991**, 113, 7152.

(45) Bandekar, J.; Krimm, S. *Biopolymers* **1988**, 27, 885.

(46) Lalitha, V.; Murali, R.; Subramanian, E. *Int. J. Peptide Protein Res.* **1986**, 27, 472.

(47) Ambrose, E. J.; Elliot, A. *Proc. Roy. Soc. Ser. A* **1951**, 205, 47.

(48) Miyazawa, T.; Blout, E. R. *J. Am. Chem. Soc* **1961**, 83, 712.

(49) Bandekar, J.; Krimm, S. *Biopolymers* **1988**, 27, 909.

(50) Fraser, R. D. B.; MacRae, T. P.; Stewart, F. H. C.; Suzuki, E. *J. Mol. Biol.* **1965**, 11, 706.

(51) Brown, L.; Trotter, I. F. *Trans. Farady Soc.* **1956**, 52, 537.

(52) Nemethy, L.; Printz, M. P. *Macromolecules.* **1972**, 5, 755.

(53) Warwicker, J. O.;. *J. Mol. Biol.* **1960**, 2, 350..

(54) Chechik, V.; Schonherr, H.; Vancso, G. J.; Stirling, C. J. M. *Langmuir* **1998**, 14, 3003.

# APPENDIX A

| ELEMENT | ANALYSIS CALCULATED FOR $C_{22}H_{24}N_2O_4S$ | FOUND |
|---|---|---|
| C | 61.66 | 61.69 |
| H | 5.65 | 5.62 |
| N | 6.54 | 6.32 |
| S | 7.48 | 7.60 |

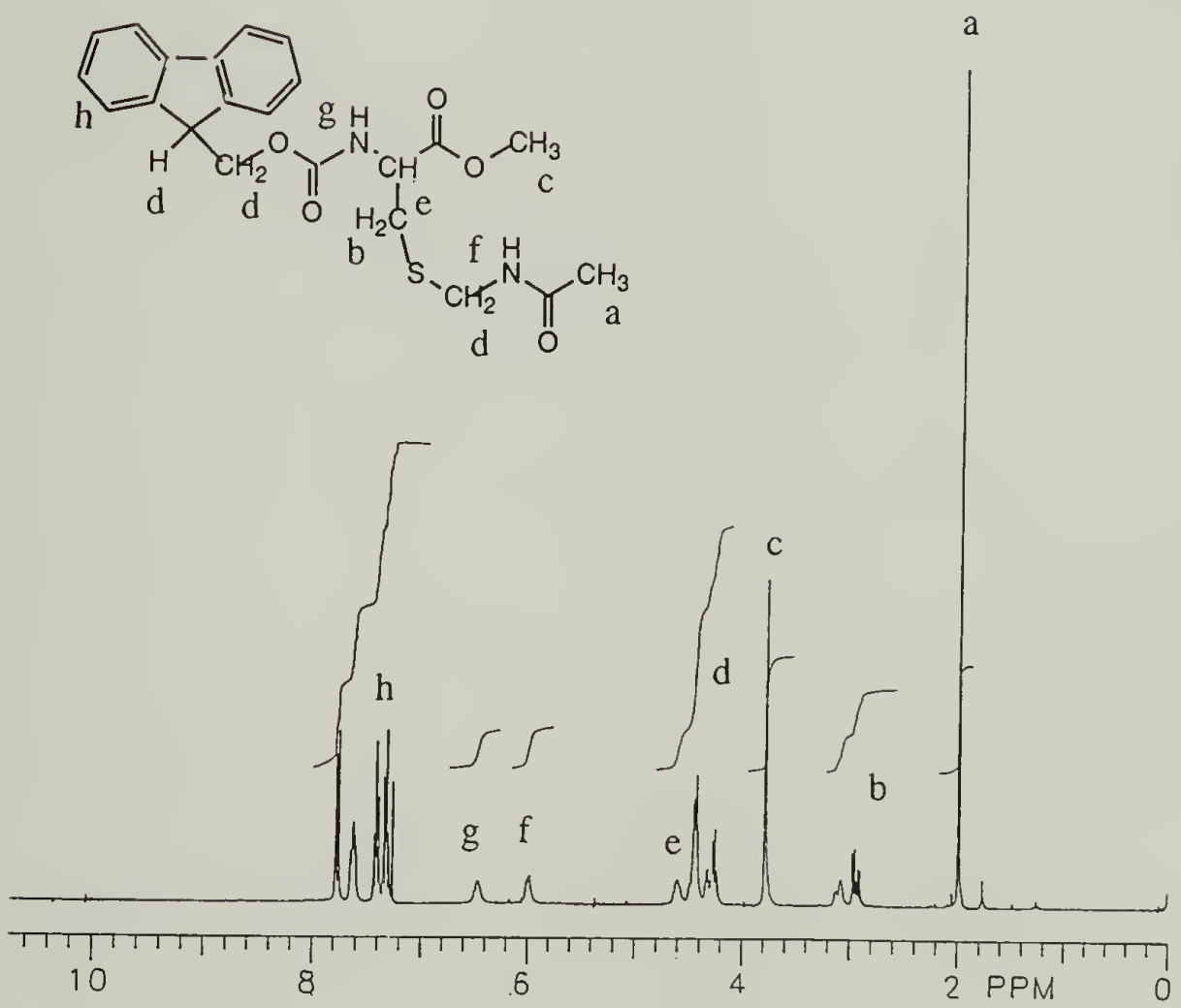


Figure A.1 300-MHz $^1H$ NMR spectra in $CDCl_3$ of FMOC-Cys(acm)-OMe.

| Element | Analysis Calculated for $C_{25}H_{48}N_2O_4S$ | Found |
|---|---|---|
| C | 63.52 | 63.46 |
| H | 10.23 | 10.33 |
| N | 5.97 | 5.90 |
| S | 6.78 | 6.79 |

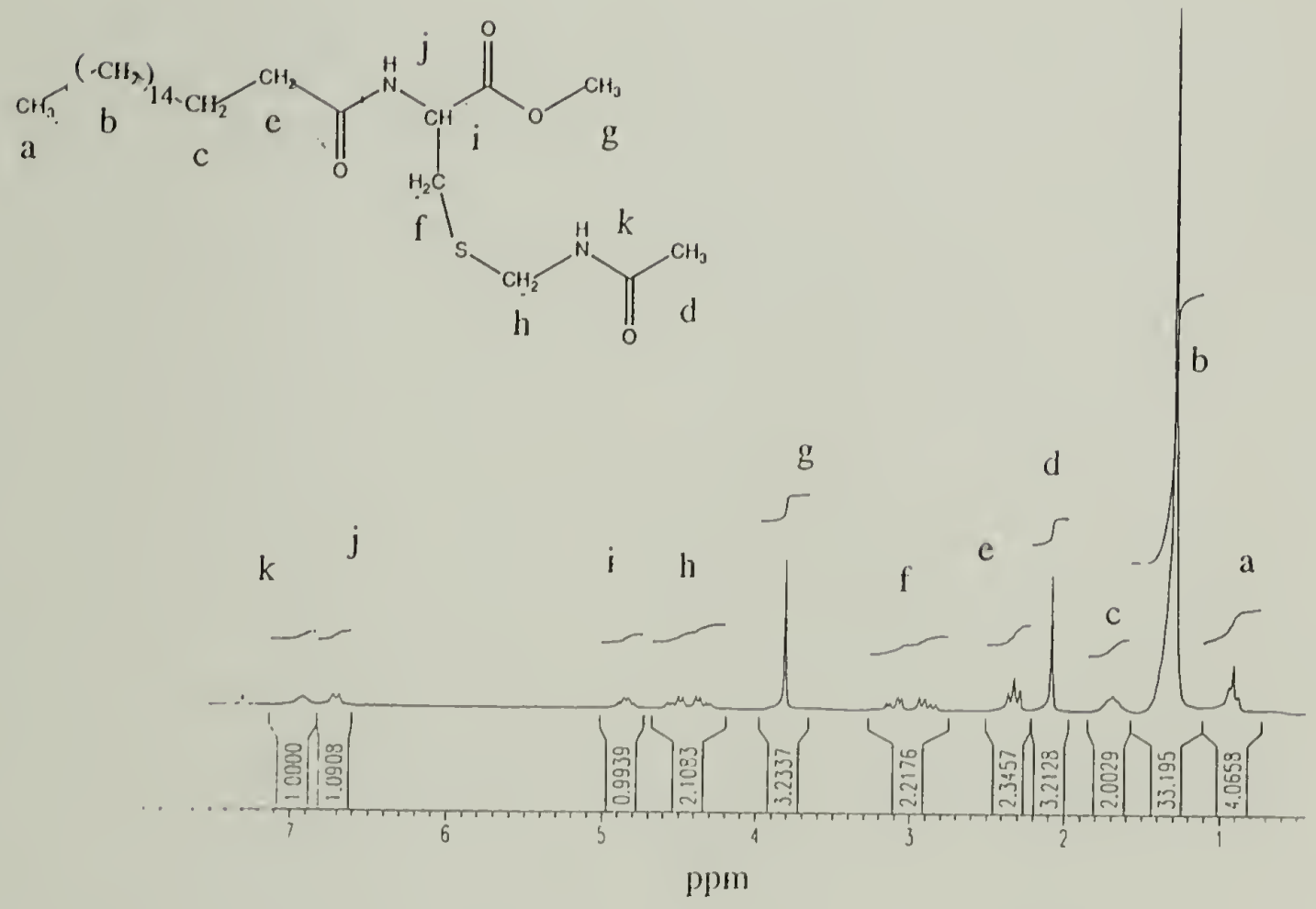


Figure A.2 300-MHz $^1$H NMR spectra in $CDCl_3$ of $H_{35}C_{17}CO$-Cys(acm)-OMe.

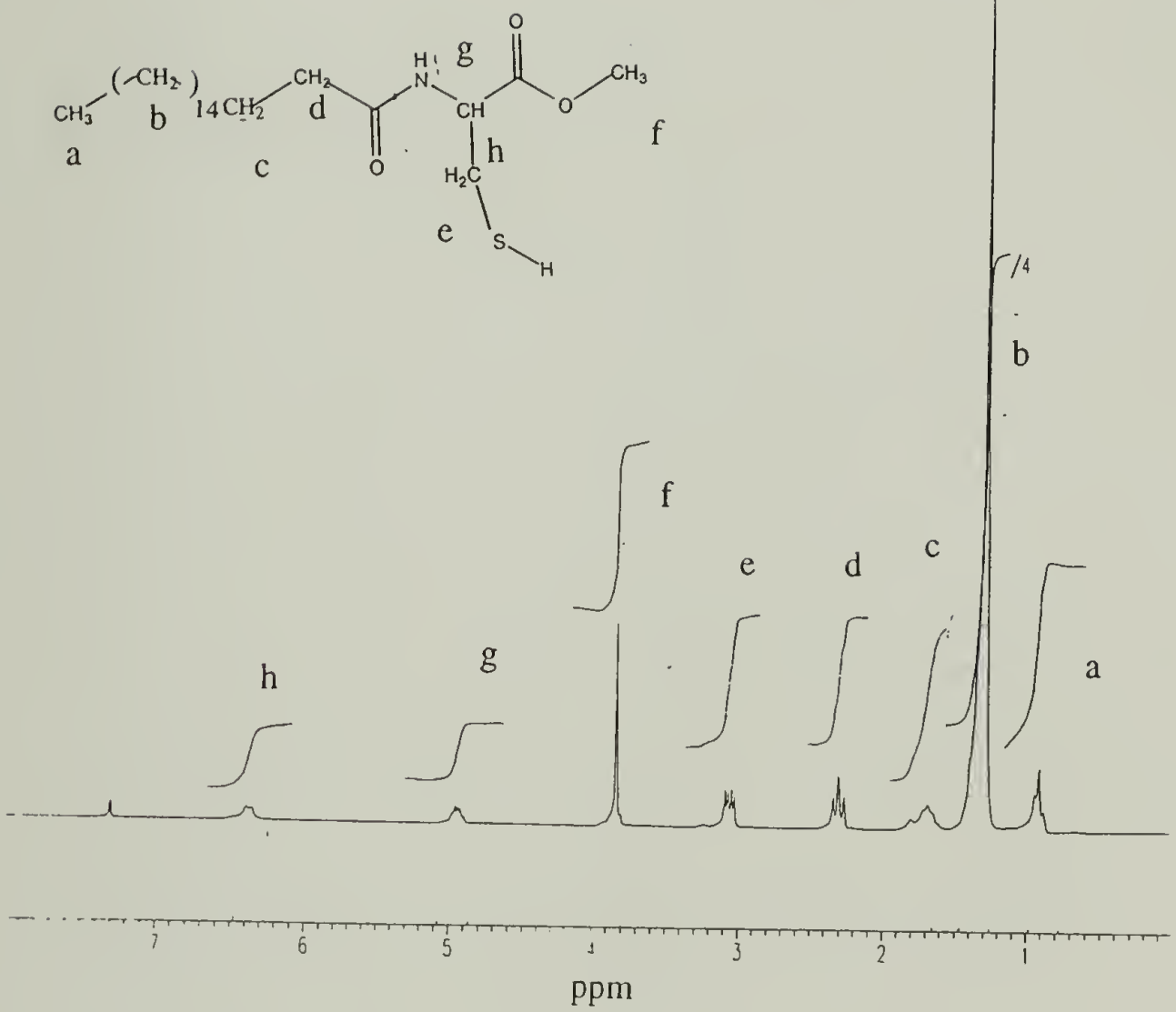


Figure A.3 300-MHz $^{1}H$ NMR spectra in $CDCl_3$ of $H_{35}C_{17}CO$-Cys-OMe.

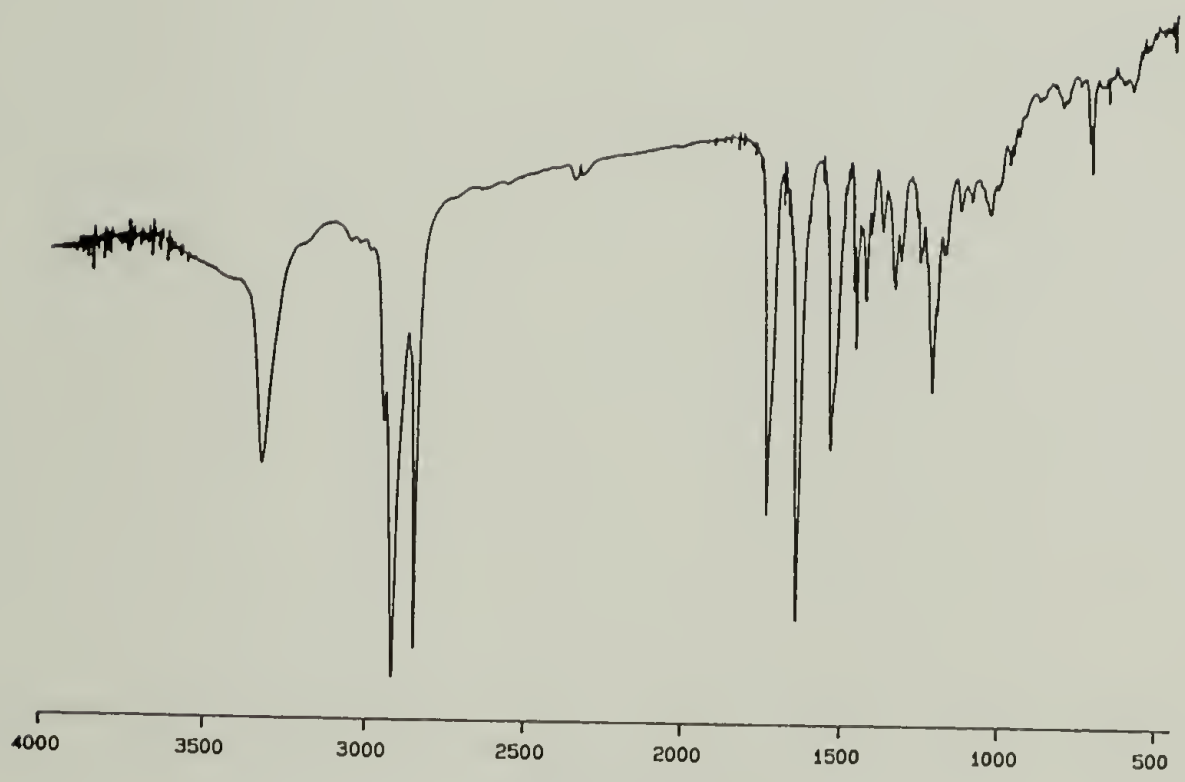


Figure A.4 Solid state IR spectra (KBr) of $H_{35}C_{17}CO$-Cys-OMe.

# APPENDIX B

| ELEMENT | ANALYSIS CALCULATED FOR $C_{18}H_{16}NO_3Cl$ | FOUND |
|---|---|---|
| C | 65.55 | 65.82 |
| H | 4.89 | 4.92 |
| N | 4.25 | 4.36 |
| S | 10.75 | 10.97 |

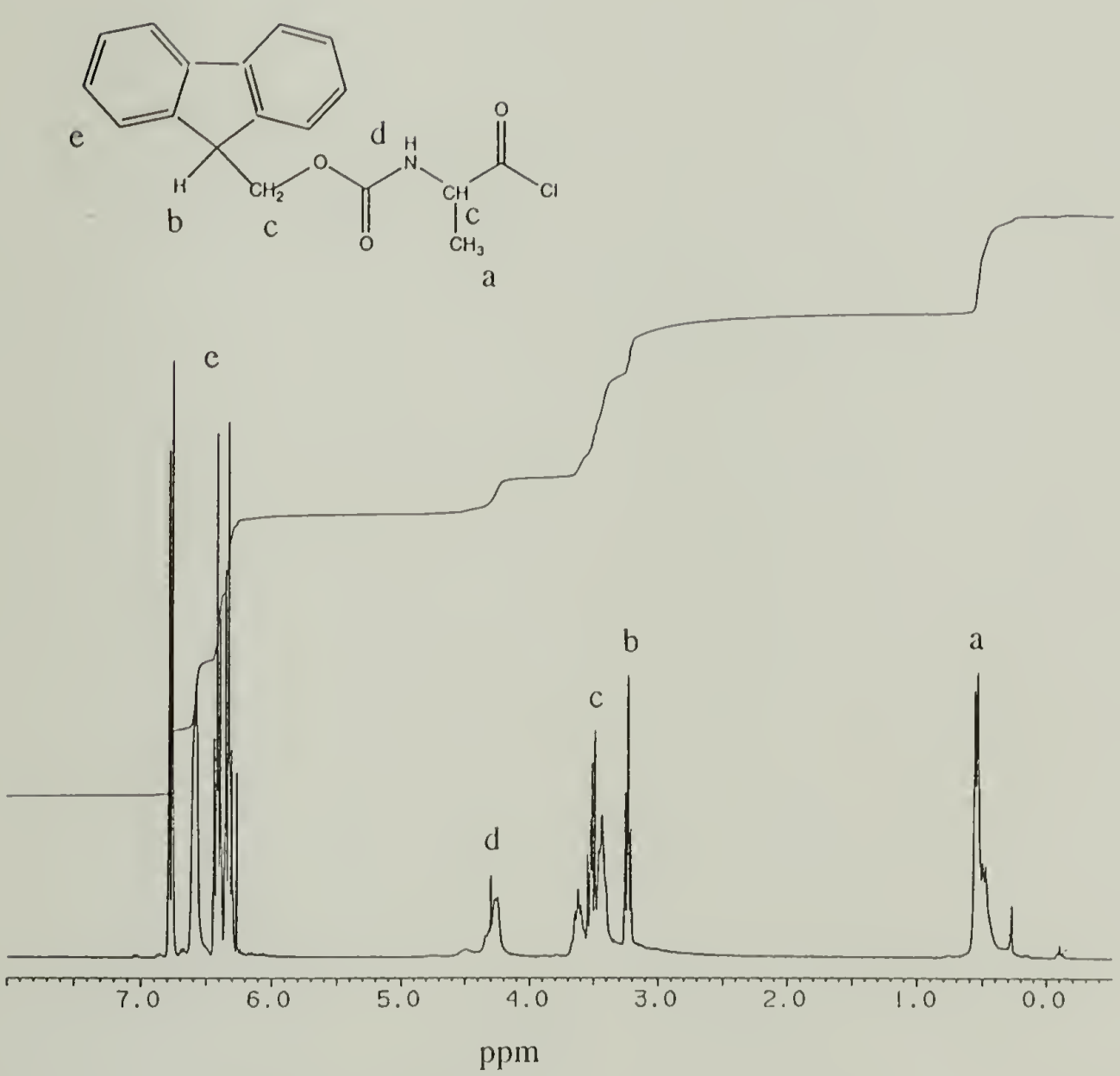


Figure B.1 300-MHz $^1H$ NMR spectra in $CDCl_3$ of FMOC-Ala-Cl.

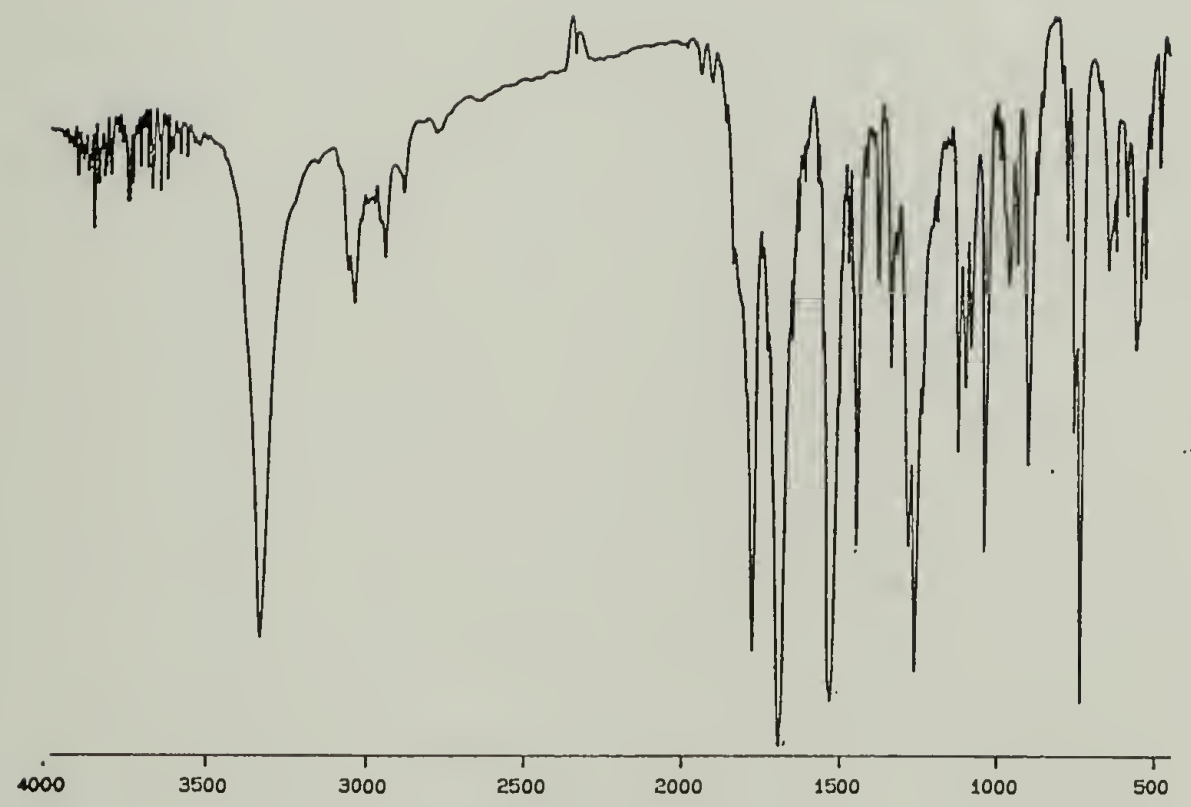


Figure B.2 Solid state IR spectra (KBr) of FMOC-Ala-Cl.

| Element | Analysis Calculated for $C_{24}H_{28}N_2O_5$ | Found |
|---|---|---|
| C | 67.91 | 67.87 |
| H | 6.65 | 6.72 |
| N | 6.60 | 6.47 |

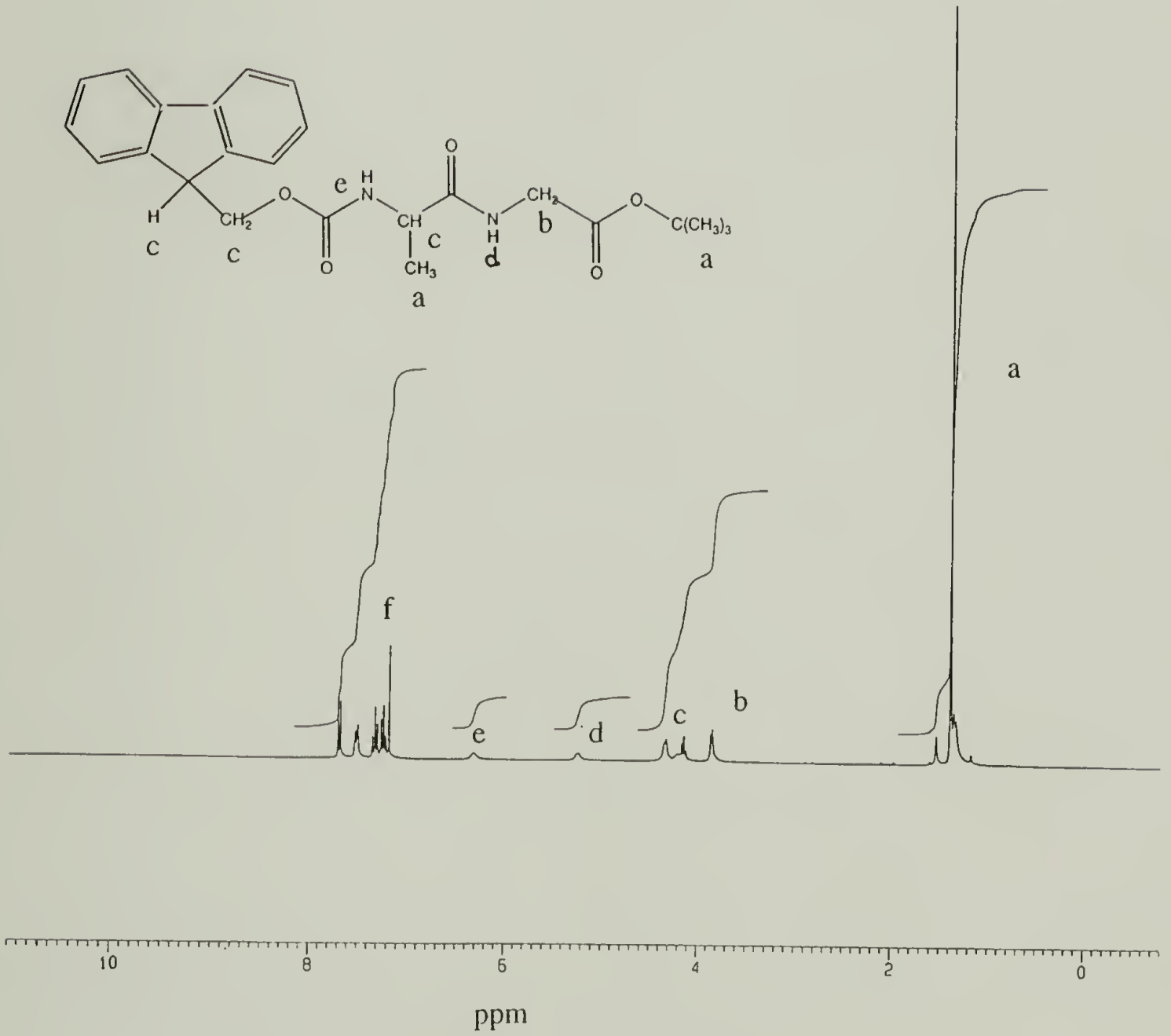


Figure B.3 300-MHz $^1$H NMR spectra in $CDCl_3$ of FMOC-AlaGly-OtBu.

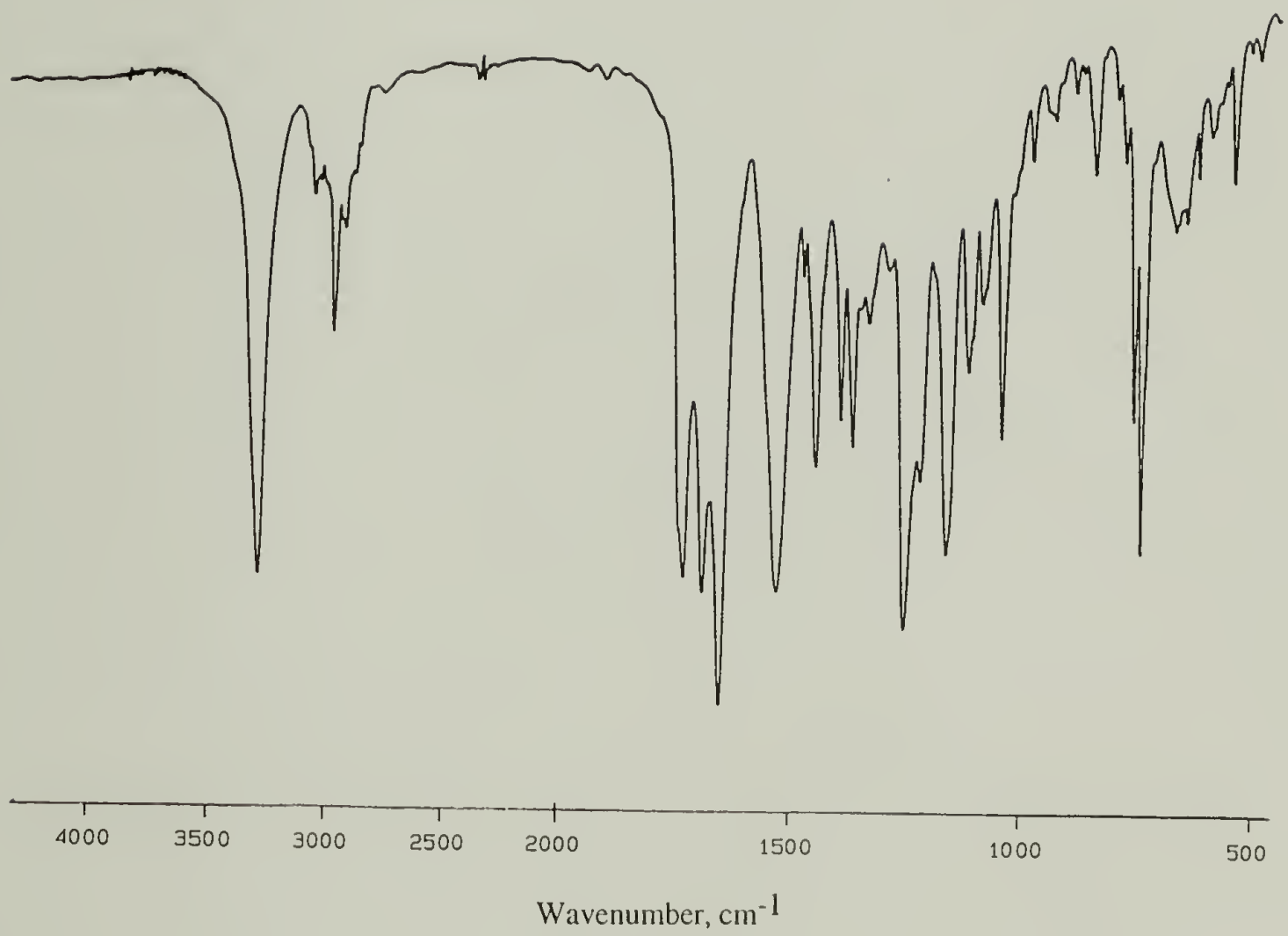


Figure B.4 Solid state IR spectra (KBr) of FMOC-AlaGly-OtBu.

| Element | Analysis Calculated for $C_{29}H_{36}N_4O_7$ | Found |
|---|---|---|
| C | 63.03 | 63.00 |
| H | 6.56 | 6.71 |
| N | 10.14 | 10.09 |

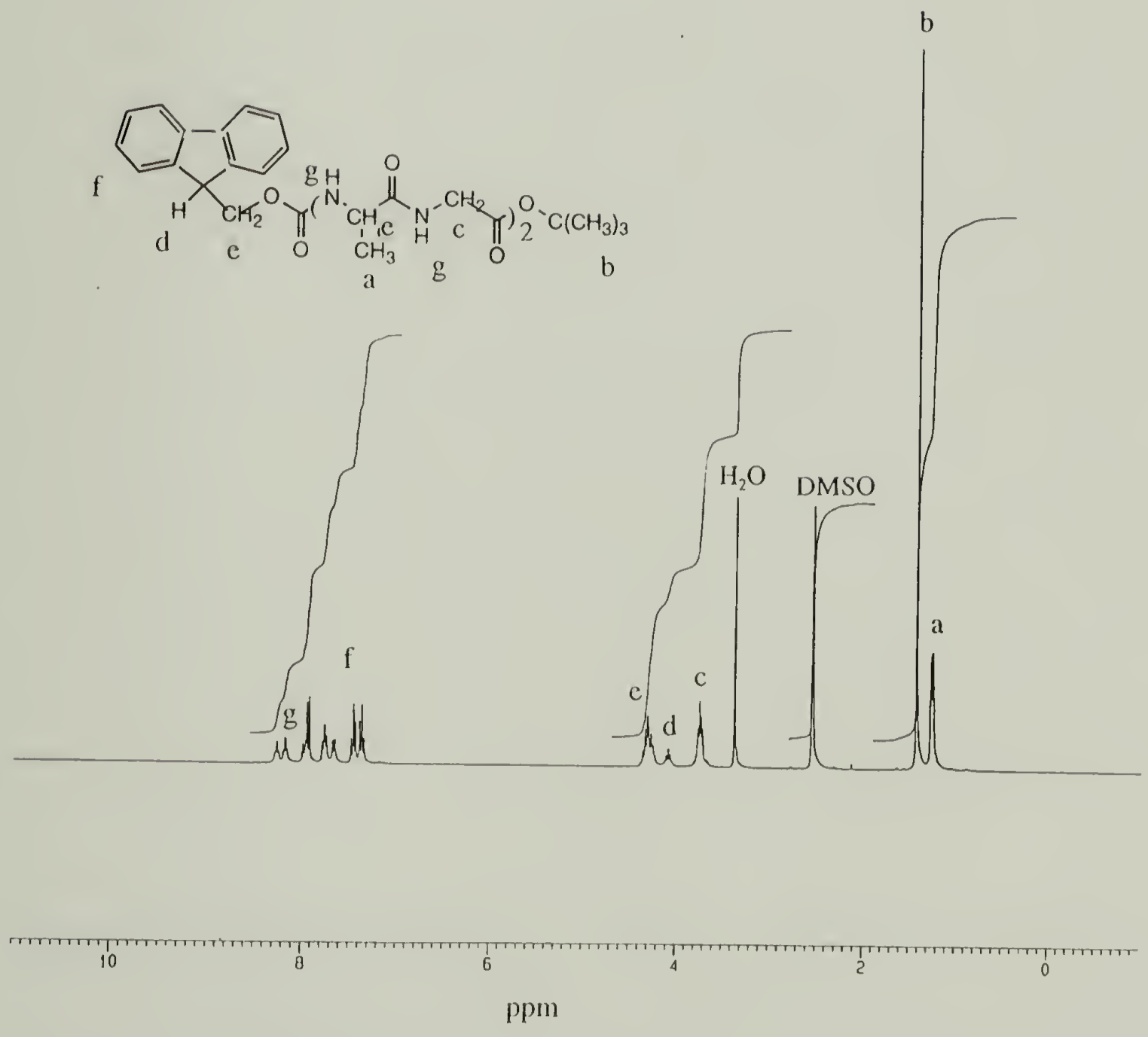


Figure B.5 300-MHz $^1$H NMR spectra in DMSO of FMOC-(AlaGly)$_2$-OtBu.

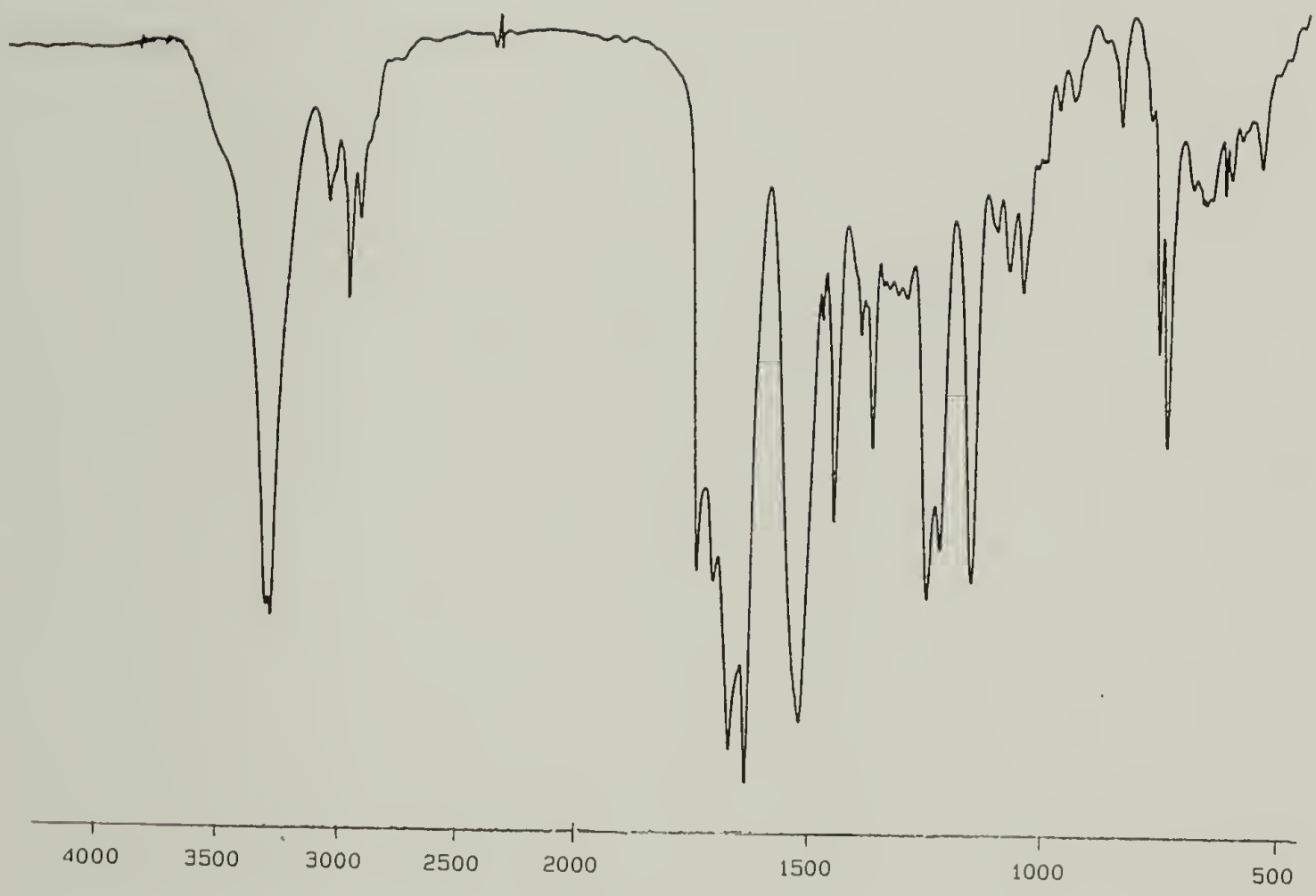


Figure B.6 Solid state IR spectra (KBr) of FMOC-(AlaGly)2-OtBu.

| ELEMENT | ANALYSIS CALCULATED FOR $C_{27}H_{32}N_4O_7S$ | FOUND |
|---|---|---|
| C | 58.30 | 58.40 |
| H | 5.79 | 5.70 |
| N | 10.07 | 9.86 |
| S | 5.76 | 5.56 |

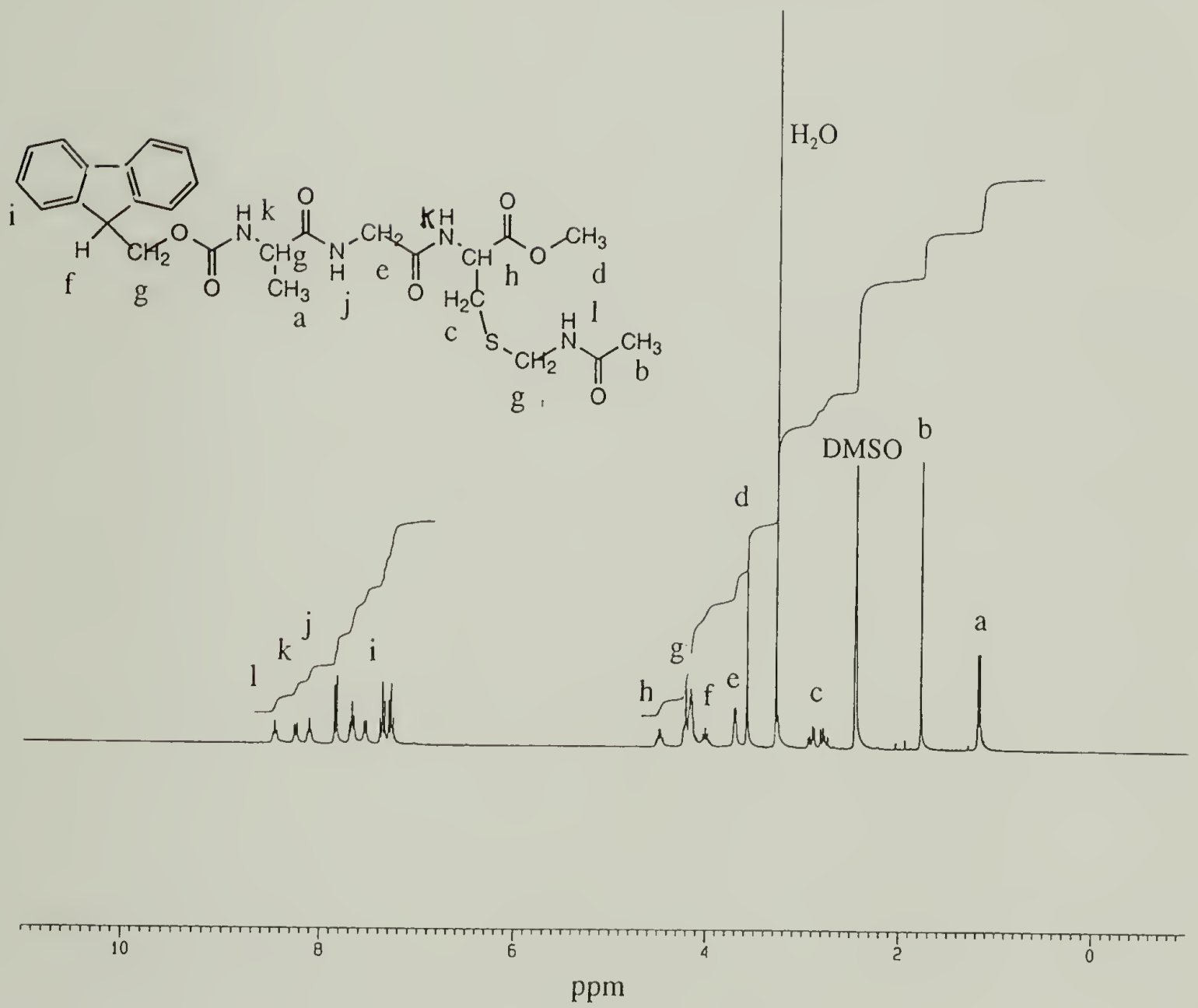


Figure B.7 300-MHz $^1$H NMR spectra in DMSO of FMOC-AlaGlyCys(acm)-OMe.

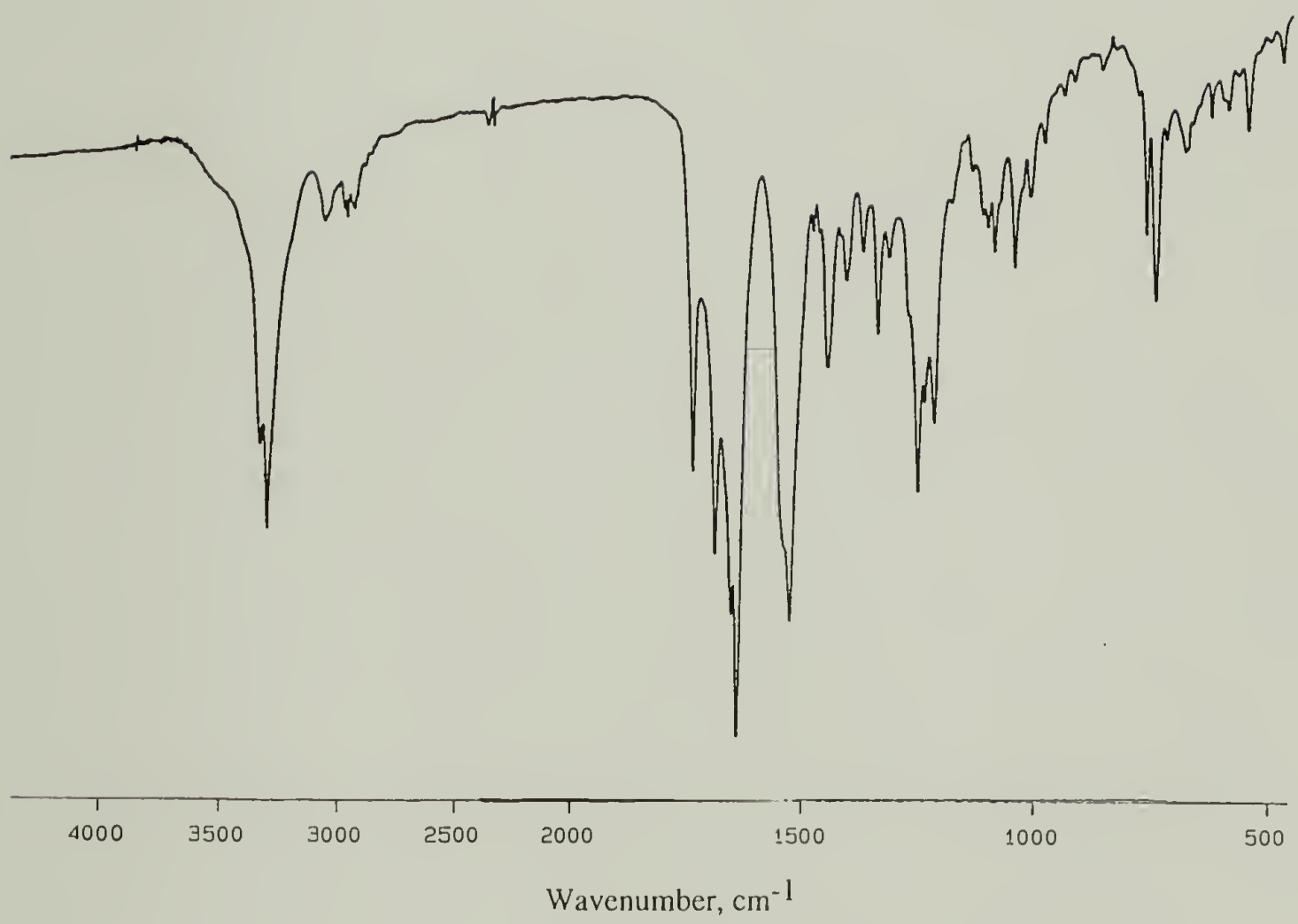


Figure B.8 Solid state IR spectra (KBr) of FMOC-AlaGlyCys(acm)-OMe.

| ELEMENT | ANALYSIS CALCULATED FOR $C_{37}H_{48}N_8O_{11}S$ | FOUND |
|---|---|---|
| C | 54.67 | 54.94 |
| H | 5.95 | 5.87 |
| N | 13.78 | 13.51 |
| S | 3.95 | 3.72 |

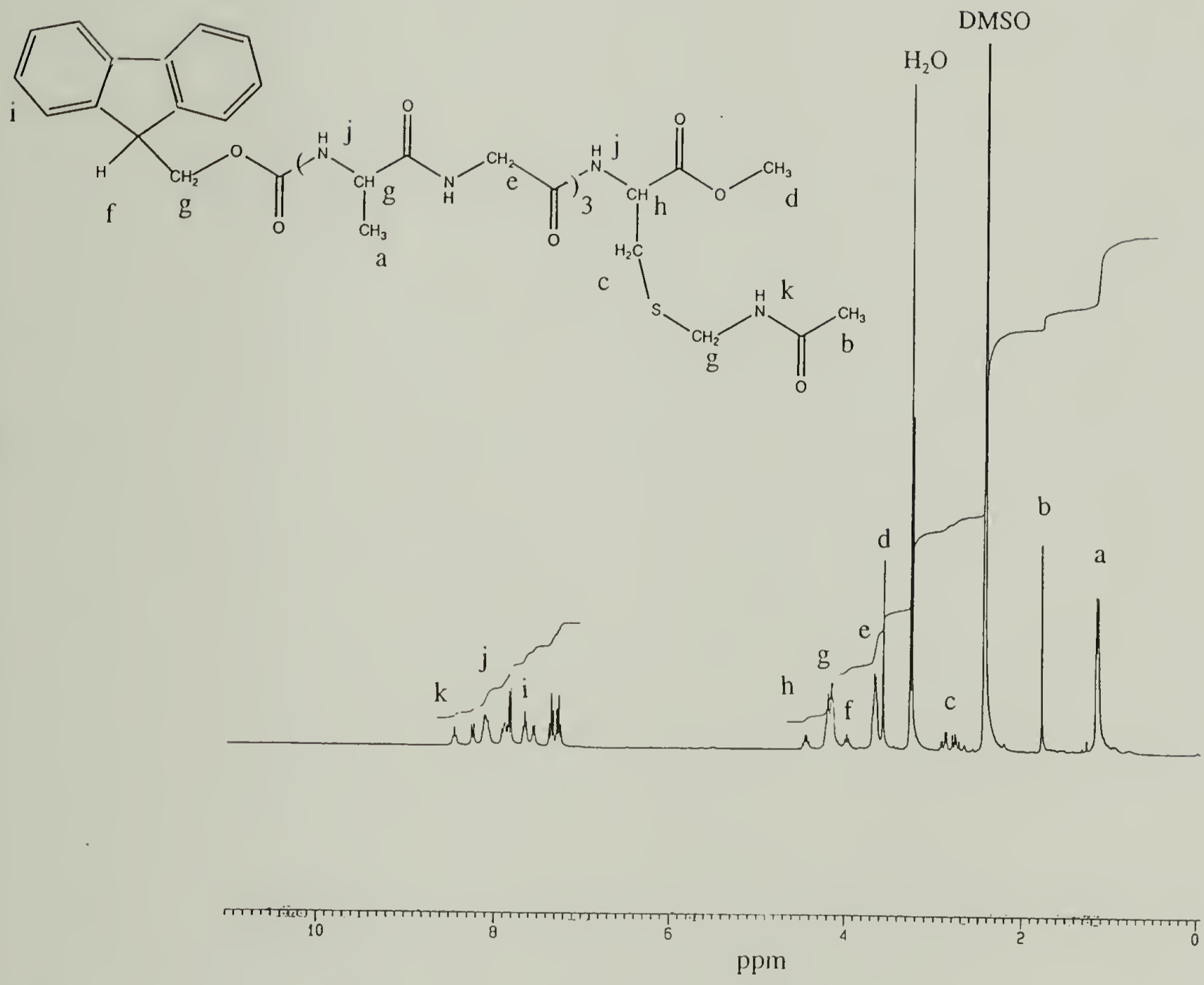


Figure B.9 300-MHz $^1$H NMR spectra in DMSO of FMOC-(AlaGly)3Cys(acm)-OMe.

| ELEMENT | ANALYSIS CALCULATED FOR $C_{24}H_{40}N_8O_{10}S$ | FOUND |
|---|---|---|
| C | 45.56 | 45.09 |
| H | 6.37 | 6.25 |
| N | 17.71 | 17.34 |
| S | 5.07 | 4.88 |

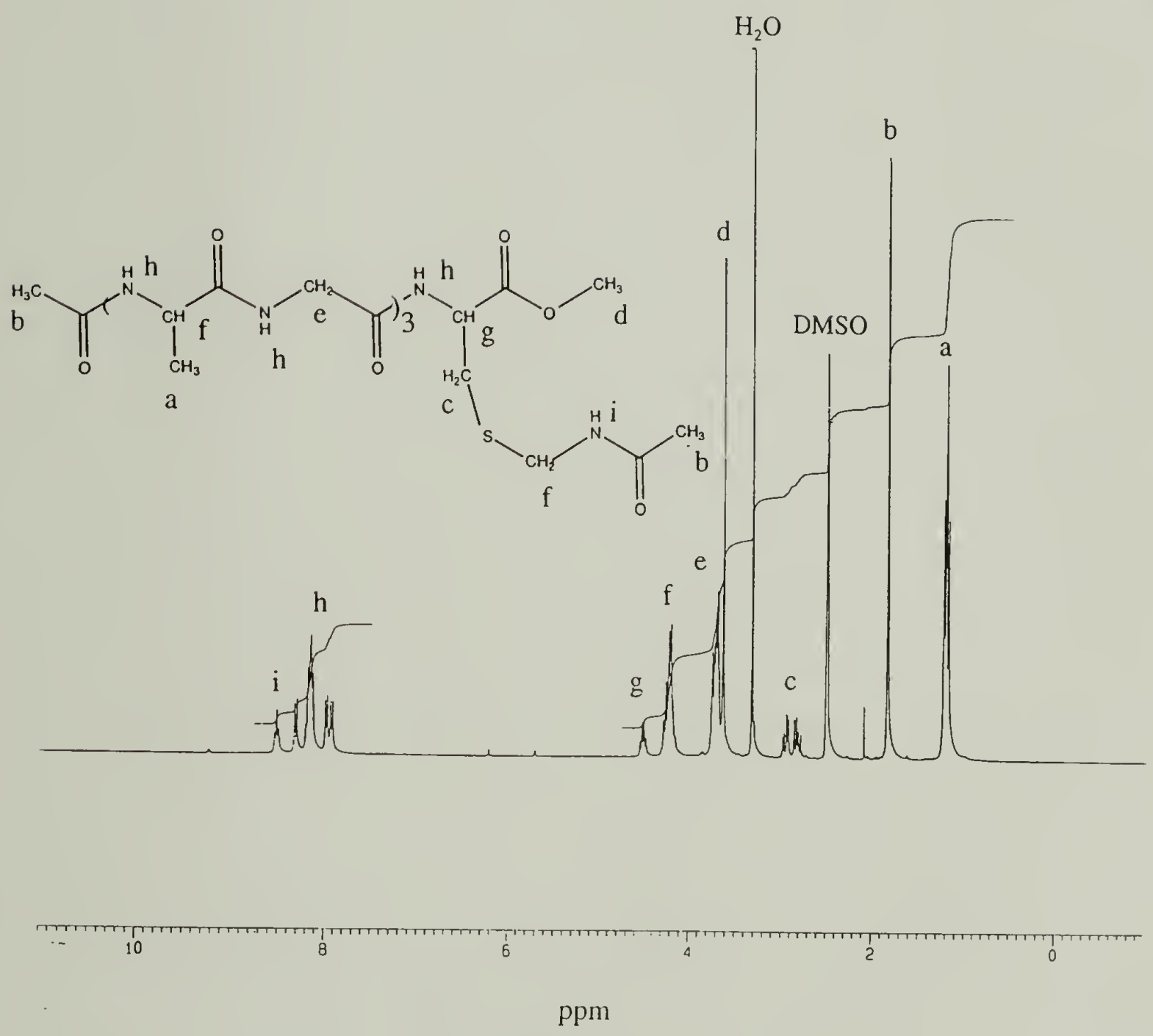


Figure B.10 300-MHz $^1$H NMR spectra in DMSO of Ac-(AlaGly)3Cys(acm)-OMe.

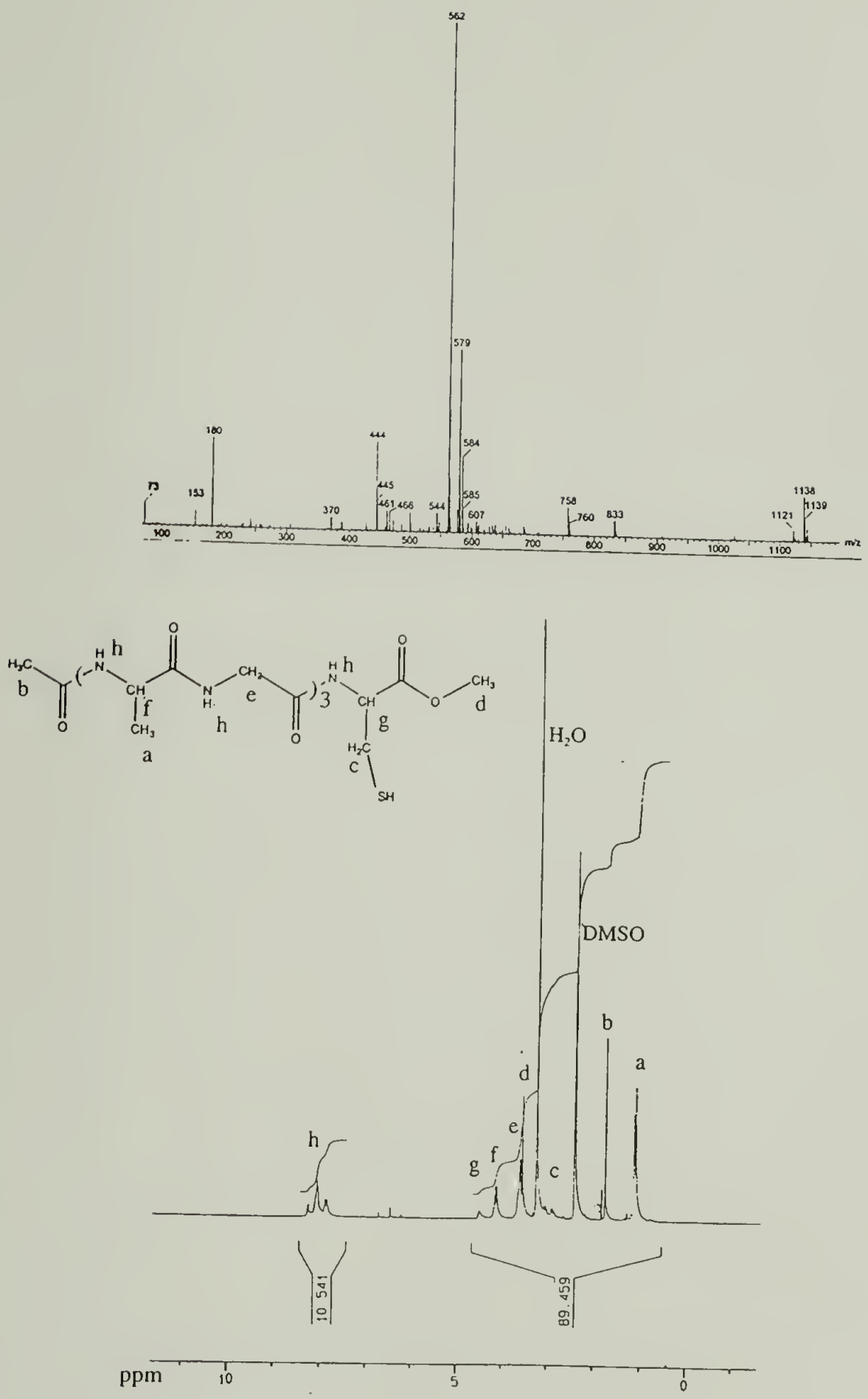


Figure B.11 300-MHz $^{1}H$ NMR spectra in DMSO of Ac-(AlaGly)3Cys-OMe.


Figure B.12 Solid state IR spectra (KBr) of Ac-(AlaGly)3Cys-OMe.

# BIBLIOGRAPHY


(1) Ahlers, M.; Muller, W.; Reichert, A.; Ringsdorf, H.; Venzmer, J. *Angew. Chem. Int. Ed. Engl.* **1990**, 29, 1269.

(2) Ahuja, R.; Caruso, P.-L.; Mobius, D.; Wolfgang, P.; Ringsdorf, H.; Wildburg, G. *Angew. Chem. Int. Ed. Engl.* **1993**, 32, 1033.

(3) Alberts, B.; Bray, D.; Lewis, J.; Raff, M.; Roberts, K.; Watson, J. D. *Molecular Biology of the Cell*, Garland: New York, **1983**; 91-98.

(4) Allara, D. L.; Nuzzo, R. G. *Langmuir* **1985**, 1, 45.

(5) Allara, D. L.; Nuzzo, R. G. *Langmuir* **1985**, 1, 52.

(6) Angle, A. K.; Yoden, T.; Sanui, K.; Ogata, N. *J. Am. Chem. Soc.* **1985**, 107, 8308.

(7) Ambrose, E. J.; Elliot, A. *Proc. Roy. Soc. Ser. A* **1951**, 205, 47.

(8) Bain, C. D.; Biebuyck, H. A.; Whitesides, G. M. *Langmuir* **1989**, 5, 723.

(9) Bain, C. D.; Troughton, E. B.; Toa, Y.-T.; Evall, J.; Whitesides, G. M.; Nuzzo, R. G. *J. Am. Chem. Soc* **1989**, *111*, 321.

(10) Bain, C. D.; Whitesides, G. M. *J. Phys. Chem.* **1989**, 93, 1670.

(11) Bandekar, J.; Krimm, S. *Biopolymers* **1988**, 27, 885.

(12) Bandekar, J.; Krimm, S. *Biopolymers* **1988**, 27, 909.

(13) Bartell, L. S.; Betts, J. *J. Phys. Chem.* **1960**, 64, 1075.

(14) Bethel, D. *Advances in Physical Organic Chemistry*; Academic Press: New York, **1993**, 28; 45-138.

(15) Bigelow, W. C.; Pickett, D. L.; Zisman, W. A. *J. Colloid Interface Sci.* **1946**, 1, 513.

(16) Bishop, A. R.; Nuzzo, R. G. *Curr. Opion. Colloid & Interface Sci.* **1996**, 1, 127.

(17) Blodgett, K. A. *J. Am. Chem. Soc.* **1935**, 57, 1007.

(18) Bradbury, E. M.; Elliot, A. *Polymer* **1963**, *4*, 47.

(19) Brown, L.; Trotter, I. F. *Trans. Farady Soc.* **1956**, 52, 537.

(20) Bryant, M. A.; Pemberton, J. E. *J. Am. Chem. Soc.* **1991**, 113, 3629.

(21) Budach, W.; Ahuja, R. C.; Mobius, D.; Schrepp, W. *Thin Solid Films* **1992**, 210/211, 434.

(22) Camillone, I. N.; Chidsey, C. E. D.; Liu, G.-Y.; Putvinski, T. M.; Scoles, G. *J. Chem. Phys.* **1991**, 94, 8493.

(23) Carpino, L.; Cohen, B. J.; Jr., K. K. S.; Sadat-Aalaee, S. Y.; Tien, J.-H.; Langridge, D. C. *J. Org. Chem.* **1986**, 51, 3732.

(24) Chaiken, I.; Chiancone, E.; Fontana, A.; Neri, P. *Macromolecular Biorecognition Principles and Methods*; Humana Press: Clifton, New Jersey, **1987**.

(25) Chailapakul, O.; Crooks, R. M. *Langmuir* **1993**, 9, 884.

(26) Chechik, V.; Schonherr, H.; Vancso, G. J.; Stirling, C. J. M. *Langmuir* **1998**, 14, 3003.

(27) Clegg, R. S.; Hutchinson, J. E. *Langmuir* **1996**, 12, 5239.

(28) Collard, D. M.; Sayre, C. N. *J. Electroannal. Chem.* **1994**, 375, 367.

(29) Colthup, N. B. et al. *Introduction to Infrared and Raman Spectroscopy;* Academic Press: Boston, **1990**; pp. 210-213.

(30) Cram, D. *J. Angew. Chem. Int. Engl.* **1988**, 27, 1009

(31) Dawson, S. L.; Elman, J.; Margevich, D. E.; McKenna, W.; Tirrell, D. A.; Ulman, A. In ACS symp. Ser. 627 Hydrogels and Biodegradable Polymers for Bioapplications; R. M. Ottenbritte, S. J. Huang and K. Park, Ed.; American Chemical Society: Washington, D. C., **1996**; pp 187-196.

(32) Dawson, S. L.; Fournier, M. J.; Mason, T. L.; Tirrell, D. A. *Polym. Prepr.* **1994**, *35*, 413.

(33) Dawson, S. L.; Tirrell, D. A. *J. Mol. Recogn.* **1997**, 10, 18.

(34) Dubois, L. H.; Nuzzo, R. G. *Annu. Rev. Phys. Chem.* **1992**, *43*, 437.

(35) Dubois, L. H.; Zegarski, B. R.; Nuzzo, R. G. *J. Am. Chem. Soc.* **1990**, *112*, 570.

(36) Elbert, R.; Laschewsky, A.; Ringsdorf, H. *J. Am. Chem. Soc.* **1985**, 107, 4134.

(37) Enriquez, E. P.; Gray, K. H.; Guarisco, V. F.; Linton, R. W.; Mar, K. D.; Samulski, E. T. *J. Vac. Sci Technol. A* **1992**, 10, 2775.

(38) Erdelen, C.; Haussling, L.; Naumann, R.; Ringsdorf, H.; Wolf, H.; Yang, J.; Liley, M.; Spinke, J.; Knoll, W. *Langmuir* **1994**, 10, 11246.

(39) Evans, S. D.; Goppert-Berarducci, K. E.; Urankar, E.; Gerenser, L. J.; Ulman, A.; Snyder, R. G. *Langmuir* **1991**, *7*, 2700.

(40) Evans, S.; Urankar, E.; Ulman, A.; Ferris, N. *J. Am. Chem. Soc.* **1991**, 113, 4121.

(41) Fawcett, J. K.; Camerman, N.; Camerman, A. *Acta Crystal B* **1975**, 31, 658.

(42) Feng, Q.; Park, T. K.; Rebek, J., Jr. *Science* **1992**, 256, 1179.

(43) Fenter, P.; Eisenberger, P.; Liang, K. S. *Phys. Rev. Lett.* **1993**, *70*, 2443.

(44) Fraser, R. D. B.; MacRae, T. P.; Stewart, F. H. C.; Suzuki, E. *J. Mol. Biol.* **1965**, 11, 706.

(45) Friggeri, A.; Veggel, F. C. J. M. v.; Reinhoudt, D. N.; Kooyman, R. P. H. *Langmuir* **1998**, 14, 5457.

(46) Fujita, K.; Kimura, S.; Imanishi, Y. *J. Am. Chem. Soc.* **1994**, 116, 2185.

(47) Greenler, R. J. *J. Chem. Phys.* **1966**, *44*, 310.

(48) Hamilton, A. D.; van Engen, D. *J. Am. Chem. Soc.* **1987**, 109, 5035.

(49) Hempel, A.; Camerman, N.; Camerman, A. *Biopolymers* **1991**, 31, 187.

(50) Holzwarth, J. F.; Whitesides, G. M. *Curr. Opion. Colloid & Interface Sci.* **1996**, 1, 61.

(51) Ikeura, Y.; Kurihara, K.; Kunitake, T. *J . Am. Chem. Soc.* **1991**, 113, 7342.

(52) Jencks, W. P. *In Design and Synthesis of Organic Molecules Based on Molecular Recognition*; Van Binst, G., Ed.; XVIIIth Solvay Conference on Chemistry; Springer-Verlag: New York, **1983**; 59.

(53) Kennard, O.; Hunter, W. *Angew. Chem. Int. Ed. Engl.* **1991**, 30, 1254.

(54) Kothakota, S.; Fournier, M. J.; Mason, T. L.; Tirrell, D. A. *J. Am. Chemical Soc.* **1995**, 117, 536.

(55) Krejchi, M. T.; Atkins, E. D. T.; Waddon, A. J.; Fournier, M. J.; Mason, T. L.; Tirrell, D. A. *Science* **1994**, *265*, 1427.

(56) Krimm, S.; Bandekar, J. *Adv. Protein Chem.* **1986**, *38*, 181.

(57) Kumar, A.; Abbott, N. L.; Kim, E.; Biebuyck, H. A.; Whitesides, G. M. *Acc. Chem. Res.* **1995**, 28, 219.

(58) Kurihara, K.; Ohto, K.; Honda, Y.; Kunitake, T. *J. Am. Chem. Soc.* **1991**, 113, 5077.

(59) Labinis, P. E.; Hickman, J. J.; Wrighton, M. S.; Whitesides, G. M. *Science* **1989**, 245, 845.

(60) Labinis, P. E.; Whitesides, G. M.; Allara, D. L.; Tao, Y.-T.; Parikh, A. N.; Nuzzo, R. G. *J. Am. Chem. Soc.* **1991**, *113*, 7152 and references therein.

(61) LaFaix, A. J.; Lebas, J. M. *Spectrochim. Acta.* **1970**, 26A, 1243.

(62) Lalitha, V.; Murali, R.; Subramanian, E. *Int. J. Peptide Protein Res.* **1986**, 27, 472.

(63) Langmuir, I. *J. Am. Chem. Soc.* **1917**, 39, 1848.

(64) Leggett, G. J.; Roberts, C. J.; Williams, P. M.; C.Davies, M.; Jackson, D. E.; Tendler, S. J. B. *Langmuir* **1993**, 9, 2356.

(65) Lehn, J.-M. *Angew. Chem. Int. Ed. Engl.* **1988**, 27, 90.

(66) Lehn, J.-M. *Angew. Chem. Int. Ed. Engl.* **1990**, 29, 1304.

(67) Lehn, J.-M.. *Pure & Appl.Chem.* **1994**, 66, 1961.

(68) Lenk, T. J. ;. V. M. H., C. L. Hoffmann, J. F. Rabolt, D. G. Castner, C. Erdelen, H. Rinsdorf *Langmuir* **1994**, *10*, 4610.

(69) Lestelius, M.; Liedberg, B.; Tengvall, P. *Langmuir* **1997**, 13, 5900.

(70) Li, T. T.-T.; Weaver, M. J. *J. Am. Chem. Soc.* **1980**, 106, 6107.

(71) Lindsey, J. S. New *J. Chem.* **1991**, 15, 153.

(72) Lopez, G. P.; Albers, M. W.; Schreiber, S. I.; Carroll, R.; Peralta, R.; Whitesides, G. M. *J. Am. Chem. Soc.* **1993**, 115, 5877.

(73) Lopez, G. P.; Biebuyck, H. A.; Kumar, R. H.; Whitesides, G. M. *J. Am. Chem. Soc.* **1993**, 115, 10774.

(74) Martensson, J.; Arwin, H. *Langmuir* **1995**, 11, 963.

(75) Matsuura, K.; Ebara, Y.; Okahata, Y. *Thin Solid Films* **1996**, 273, 61.

(76) McGrath, K. P.; Fournier, M. J.; Mason, T. L.; Tirrell, D. A. *J. Am. Chem. Soc.* **1992**, 114, 727.

(77) Miyazawa, T. In *Poly-a-Amino Acids Protein Models for Conformational Studies*; G. D. Fasman, Ed.; Marcel Dekker, Inc: New York, **1967**; Vol. 1; pp 69-103.

(78) Motesharei, K.; Myles, D. C.; *J. Am.. Chem.. Soc.* **1994**, 116, 7413.

(79) Miyazawa, T.; Blout, E. R. *J. Am. Chem. Soc.* **1961**, 83, 712.

(80) Miyazawa, T.; Shimanouchi, T.; Mizushima, S. *Journal Chemical Physics* **1956**, 24, 408.

(81) Mrksich, M.; Whitesides, G. M. In *ACS Symp. Ser, 680 (Poly(ethylene glycol));* J. M. Harris and S. Zalipsky, Ed.; American Chemical Society: Washington, D.C., **1997**; pp 361-373.

(82) Nemethy, L.; Printz, M. P. Macromolecules. **1972**, 5, 755.

(83) Netzer, L.; Sagiv, J. *J. Am. Chem. Soc.* **1983**, 105, 674.

(84) Netzer, L.; Iscovici, R.; Sagiv, J. *Thin Solid Films* **1983**, 99, 235.

(85) Nuzzo, R. G.; Allara, D. L. *J. Am. Chem. Soc.* **1983**, 105, 448.

(86) Nuzzo, R. G.; Dubois, L. H.; Allara, D. A. *J. Am. Chem. Soc.* **1990**, *112*, 55

(87) Nuzzo, R. G.; Fusco, F. A.; Allara, D. L. *J. Am. Chem. Soc.* **1987**, 109, 23

(88) Nuzzo, R. G.; Zegarski, B. R.; Dubois, L. H. *J. Am. Chem. Soc.* **1987**, 109, 733.

(89) Park, T. K.; Schroeder, J.; Rebek, J., Jr. *J. Am. Chem. Soc.* **1991**, 113, 5125.

(90) Patel, N.; Davies, M. C.; Hartshorne, M.; Heaton, R. J.; Roberts, C. J.; Tendler, S. J. B.; Williams, P. M. *Langmuir* **1997**, 13, 6485.

(91) Petka, W. A.; Harden, J. L.; McGrth, K. P.; Wirtz, D.; Tirrell, D. A. *Science* **1998**, 281, 389.

(92) Porter, M. D.; Bright, T. B.; Allara, D.; Chidsey, C. E. D. *J. Am. Chem. Soc.* **1987**, *109*, 3559.

(93) Qian, W.; Bandekar, J.; Krimm, S. *Biopolymers* **1991**, 31, 193.

(94) Quian, P.; Matsuda, M.; Miyashita, T. *J. Am. Chem. Soc.* **1993,** 115, 5624.

(95 Ringsdorf, H.; Schlarb, B.; Venzmer, *J. Angew. Chem. Int. Ed. Engl.* **1988,** 27, 113.

(96) Roberts, S. M., Ed.; *Biomolecular Recognition: Chemical and Biological Problems II; Second International Chemical and Biochemical Problems in Molecular Recognition*; Royal Society of Chemistry: Cambridge, **1992.**

(97) Rojas, M. T.; Koniger, R.; Stoddart, J. F.; Kaifer, A. E. *J. Am. Chem. Soc.* **1995**, 117, 336.

(98) Sabapathy, R. C.; Bhattacharyya, S.; Leavy, M. C.; Jr., W. E. C.; Hussey, C. L. *Langmuir* **1998**, 14, 124.

(99) Sagiv, J. *J. Am. Chem. Soc.* **1980**, 102, 92.

(100) Samuelson, L.A.; Kaplan, D. L.; Lim, J. O.; Kamath, M.; Marx, K. A.; Tripathy, S. K. *Thin Solid Films* **1994,** 242, 55.

(101) Schneider, H.-J. *Angew. Chem. Int. Ed. Engl.* **1991**, 30, 1417.

(102) Snyder, R. G.; Schachtschneider, J. H. *Spectrochim. Acta* **1963**, *19*, 85-116.

(103) Spinke, J.; Liley, M.; Schmitt, F.-J.; Guder, H.-J.; Angermaier, L.; Knoll, W. *J. Chem. Phys.* **1993**, 99, 7012.

(104) Stidham, H. D.; DiLella, D. P. *J. Raman Spectroscopy* **1979**, 8, 180.

(105) Strong, L.; Whitesides, G. M. *Langmuir* **1988**, 4, 546.

(106) Sun, F.; Grainger, D. W.; Castner, D. G. *J. Vac. Sci. Technol A.* **1994**, 12, 2499.

(107) Sun, F.; Mao, G.; W.Granger, D.; Castner, D. G. *Thin Solid Films* **1994**, 242, 106.

(108) Swalen, J. D.; Allara, D. L.; Andrade, J. D.; Chandross, E. A.; Garoff, S.; Israelachvili, J.; McCarthy, T. J.; Murray, R.; Pease, R. F.; J, F. R.; Wynne, K. J.; Yu, H. *Langmuir* **1987**, 3, 932.

(109) Takahashi, H.; Mamola, K.; Plyler, E. K. *J. Mol. Spectroscopy* **1966**, 21, 217.

(110) Tam-Chang, S.-W.; Biebuyck, H. A.; Whitesides, G. M.; Jeon, N.; Nuzzo, R. G. *Langmuir* **1995**, *11*, 4371.

(111) Tengvall, P.; Lestelius, M.; Leidberg, B.; Lundstrom, I. *Langmuir* **1992**, 8, 1236.

(112) Thompson, W. K. *J. Chem. Soc.* **1962**, 617.

(113) Tidwell, C. D.; Ertel, S. I.; Ratner, B. D.; Tarasevich, B. J.; Atre, S.; Allara, D. L. *Langmuir* **1997**, 13, 3404.

(114) Tirrell, J. G.; Fournier, M. J.; Mason, T. L.; Tirrell, D. A. *C&EN* **1994**, Dec. 19, 40.

(115) Troughton, E. B.; Bain, C. D.; Whitesides, G. M.; Nuzzo, R. G.; Allara, D.; Porter, M. D. *Langmuir* **1988**, 4, 365.

(116) Tsuruta, T.; Doyama, M.; Seno, M.; Imanishi, Y. eds *New Functional Materials: Synthesis and Function Control of Biofunctionality Materials*; Elvsevier: New York, **1993**, C; 607.

(117) Ulman, A. *An Introduction to Ultrathin Organic Films: From Langmuir-Blodgett to Self-Assembly*; Academic Press, Inc.: New York, **1991**.

(118) Uno, T.; Machida, K. *Bull. Chem. Soc.* (Japan) **1962**, 35, 276.

(119) Uvdal, K.; Bodö, P.; Liedberg, B. *J. Colloid and Interface Sci.* **1992**, *149*, 162.

(120) Van Binst, G. *Design and Synthesis of Organic Molecules Based on Molecular Recognition*; Proceedings of the Solvay Conference on Chemistry; Springer-Verlag: New York, **1986**; 2 and references within.

(121) Uvdal, K.; Bodö, P.; Liedberg, B. *J. Colloid and Interface Sci.* **1992**, 149, 162.

(122) Walczak, M. M.; Chung, C.; Stole, S. M.; Widrig, C. A.; Porter, M. D. *J. Am. Chem. Soc.* **1991**, 113, 2370.

(123) Waldman, D. A.; Kolb, B. U.; McCarthy, T. J.; Hsu, S. L. *Polym. Mater. Sci. Eng.* **1988**, 59, 326.

(124) Walton, A.; Blackwell, *J. Biopolymers*; Academic Press: New York, **1973**; p 31.

(125) Warwicker, J. O.;. *J. Mol. Biol.* **1960**, 2, 350.

(126) Wasserman, S. R.; Whitesides, G. M.; Tidswell, I. M.; Ocko, B. M.; Pershan, P. S.; Axe, J. D. *J. Am. Chem. Soc.* **1989**, 111, 5852.

(127) Whitesell, J. K.; Chang, H. K. *Science* **1993**, 261, 73.

(128) Whitesides, G. M.; Mathias, J. P.; Seto, C. T. *Science* **1991**, 254, 1312.

(129) Whitesides, G. M.; Simanek, E. E.; Mathias, J. P.; Seto, C. T.; Chin, D. N.; Mammen, M.; Gordon, D. M. *Acc. Chem. Res.* **1995**, 28, 37.

(130) Willicut, R. J.; McCarley, R. L. *J. Am. Chem. Soc.* **1994**, 116, 10823.

(131) Yoshikawa, E.; Fournier, M. J.; Mason, T. L.; Tirrell, D. A. *Macromolecules* **1994**, *27*, 5471.

(132) Zeeland, F. J.; Havinga, E. *Rec. Trav. Chim.* **1958**, *77*, 267.

(133) Zhang, G.; Fournier, M. J.; Mason, T. L.; Tirrell, D. A. *Macromolecules* **1992**, 25, 3601.